To the Graduate Council:

I am submitting herewith a dissertation written by Emran Dawoud entitled " the Multiple Convolution Integral Approach to Uncertainty Analysis In Fate and Transport Models Used in Risk Assessment". I have examined the final copy of this dissertation for form and contents and recommend that it be accepted in partial fulfiment of the requirements for the degree of Doctor of Philosophy, with a major in Nuclear Engineering.

Laurence Z Miller

Laurence Miller, Major Professor

We have read this dissertation
and recommend its acceptance:

Lawrence Townd

Dr. Lawrence Townsend

Peter J. Groet

Dr. Peter Groet

Vahid Alavian

Dr. Vahid Alavian

Accepted for the Council:

Lewminkel

Associate Vice Chancellor and
Dean of the Graduate School

THE MULTIPLE CONVOLUTION INTEGRAL APPROACH TO UNCERTAINTY ANALYSIS IN FATE AND TRANSPORT MODELS USED IN RISK ASSESSMENT

A Dissertation
Presented for the
Doctor of Philosophy
Degree
The University of Tennessee, Knoxville

Emran A. Dawoud
December 1998

DEDICATION

This dissertation is dedicated to a person that I will always miss, my father, who never stopped providing me with nourishing, caring, and spiritual support through out my life till he died on August 18, 1998. May God be pleased with him and bestow His Mercy upon him.

ACKNOWLEDGMENTS

My sincere thanks goes to Allah the almighty who provided me with enough patience to complete this work.

I would like to offer my gratitude to a very sincere and devotaed person, my Professor Dr. Bounds, who initiated the idea of this research and helped me in the basic formulation of the original problem before his death. Also, I would like to express my sincere gratitude to my advisor Dr. Larry Miller for his continuous support and persistent guidance through out the course of this work.

My thanks are extended to Dr. Townsend, Dr. Groer, and Dr. Alavian, for serving on my committee and for their helpful and productive discussions and comments that made this work better. Also, I would like to thank Dr. Dodds, the head of our department, for his valuable comments.

I would like to acknowledge that my experience in the fields of Risk Analysis and Fate and Transport Modeling used in this research was developed through five years of work as a Risk Assessor for the Risk Analysis Section of the Life Sciences Division at the Oak Ridge National Laboratory (ORNL). Therefore, I would like to thank the members of this section and the management staff for their help in acquiring such a unique opportunity. In particular, I would like to thank Mr. Robert Stewart for his discussions and helpful comments that

enhanced the quality of this work. In addition, my gratitude is extended to a person that I worked with most of the time, my friend Dr. Martin Clauberg,for the enormous productive discussions that we had and helped me in developing the professional expertise in the field of Risk Analysis. Special thanks are offered to Mr. Wison McGinn, our group leader at the risk analysis section,for giving me the opportunity to be part of his team. I am also grateful to Dr. Keith Eckerman for his substantial discussions about several issues that are related to risk analysis and valuable comments related to this work, in particular.

My thanks are due to Dr. Mark Yambert, from the groundwater group at ORNL, for his valuable comments about specific groundwater modeling aspects and problems.

My special thanks goes to Mrs.Khuloud Al-Hendi for her endless emotional support and deep understanding as my wife, and constructive discussions with respect to the theoretical aspects of this work as an electrical engineer.

Last but not the least, my deepest gratitude goes to my parents for their continuous encouragement and special attention which provided me with self steam and confidence to complete this work.

ABSTRACT

Probabilistic risk estimates are typically not obtained for time-dependent releases of radioactive contaminants to the geosphere when a series of sequentially coupled transport models are required for determining results. This is due, in part, to the geophysical complexity of the site, numerical complexity of the fate and transport models, and a lack of a practical tool for linking the transport components in a fashion that facilitates uncertainty analysis.

Using the theory of convolution integration, sequentially coupled submodels can be replaced with an independent system of impulse responses for each submodel. Uncertainties are then propagated independently through each of the submodels to significantly reduce the complexity of the calculations and computational time. The impulse responses of the submodels are then convolved to obtain a final result that is equivalent to the sequentially coupled estimates for each source distribution of interest.

In this research a multiple convolution integral (MCI) approach is developed and the decoupling of fate and transport processes into an independent system is described. A conceptual model, extracted from the Inactive Tanks project at the Oak Ridge National Laboratory (ORNL), is used to demonstrate the approach. Potential releases of ^{90}Sr from a disposal facility, WC-1 at ORNL, through the vadose zone are modeled and then transported through the groundwater to a

downgradient point at Fifth Creek. An analytical surface water model is used to transport the contaminants to a down stream potential receptor point at White Oak Creek. The probability density functions (PDFs) of the computed concentrations, and thus risks, using the MCI approach are found to be in agreement with those obtained by the traditional approach with processor time savings of, at least, a factor of two.

In this application, uncertainties in the final risk estimates resulting from the ingestion of surface water show that the range of variations of the right tail of the PDFs are over several order of magnitude. Also, sensitivity analysis shows that uncertainty in the final risk is mainly attributed to uncertainties inherent in the parameter values of the transport model and exposure duration. These results demonstrate that while the variation in the tail of time-dependent risk PDF(the region of interest to regulatory decisions) are large, the resulting confidence level that human health has been protected is only slightly increased (e.g. about 4% between the 95 and 99 fractiles). In terms of remediation cost, this slight increase yields huge costs, and might reflect poor management decisions.

The MCI approach is proven here to be a vital tool for a successful and viable application of uncertainty analysis in fate and transport processes. Ultimately, the MCI approach made uncertainty analysis a highly automated process and restored it as beneficial tool for investigators and decision makers while maintaining an effective balance between cost and level of accuracy of the model predictions.

TABLE OF CONTENTS

1. INTRODUCTION 1
1.1 DETERMINISTIC VERSUS PROBABILISTIC ESTIMATES . . 2
1.2 RESEARCH OBJECTIVE 5
1.3 SCOPE 10

2. PROBLEM FORMULATION 12

3. THE MULTIPLE CONVOLUTION INTEGRAL APPROACH 16
3.1 MATHEMATICAL DESCRIPTION 16
3.2 OVERVIEW OF THE MCI APPROACH 22
3.3 ADVANTAGES OF USING THE MCI APPROACH IN EVALUATING UNCERTAINTIES IN COUPLED SYSTEMS 25

4. UNCERTAINTY ANALYSIS TOOLS 28
4.1 RANDOM SAMPLING TECHNIQUES 30
4.3 MCI APPROACH UNCERTAINTY ALGORITHM 34

5. APPLICATION 36
5.1 CONCEPTUAL SITE MODEL 37
5.2 CHARACTERIZATION OF EXPOSURE SETTING 38
5.2.1 Site Physical Characteristics 41
5.2.2 Site Surface Hydrology 41
5.2.3 Site Hydrogeology 44
5.2.4 Tank WC-1 Description 50
5.2.5 Toxicity of Strontium-90 50
5.3 DISPOSAL UNIT SOURCE TERM (DUST) 51
5.3.1 Applicability 52
5.3.2 Model Components and Equations 54
5.3.3 Finite Difference (FD) Model 60

5.3.4 Uncertainties in DUST Parameters 63
5.3.5 Limitations Of DUST Code 65
5.4 FTWORK MODEL 66
5.4.1 Applicability 67
5.4.2 Conceptual Uses and Limitations 68
5.4.3 Mathematical Model 73
5.4.4 Numerical Techniques 79
5.4.5 Uncertainties in Critical Model Inputs . 80
5.5 ANALYTICAL SURFACE WATER MODEL 84
5.6 WATER INGESTION RISK MODEL 86
5.7 UNCERTAINTY ANALYSIS 87

6. CONCLUSIONS 124

REFERENCES 128

APPENDICES 133
APPENDIX 1 A Matlab Program Propagating The DUST Estimates Through to The FTWORK . . 135
APPENDIX 2 A Matlab Program Convolving the DUST Estimates With the FTWORK Estimates 143
APPENDIX 3 A Matlab Program Convolving the Analytical Surface Water Model Estimates with DUST-FTWORK Convolved Estimates 151
APPENDIX 4 Matlab Functions Called by Main Programs 155
APPENDIX 5 A Mathematical Demonstration of The Accuracy Of the MCI Approach . . . 159

VITA 161

LIST OF TABLES

5.1 Critical input parameters for FTWORK 81
5.2 Uncertain parameters, references, and their corresponding PDFs used in the different models 90
5.3 Statistical description of the estimated concentrations of ^{90}Sr in groundwater (pCi/cm^3) using the traditional approach of propagating uncertainty for different time intervals 99
5.4 Statistical description of the estimated concentrations of ^{90}Sr in groundwater (pCi/cm^3) using the convolution approach of propagating uncertainty for different time intervals 106
5.5 Statistical description of the estimated concentrations of ^{90}Sr in surface water (pCi/cm^3) using the Multiple Convolution Integral approach of propagating uncertainty for different time intervals 113
5.6 Statistical description of the estimated risks from the ingestion of ^{90}Sr in surface water using the Multiple Convolution Integral approach estimates of the concentration for different time intervals 119

LIST OF FIGURES

Figure Page

1.1 A block diagram showing standard propagation of uncertainties through sequentially coupled transport submodels used to estimate uncertainty in the final risk predictions 6

2.1 Conceptual model for assessing risk from exposure to released and transported contamination from a particular source to potential receptor points 13

3.1 A block diagram showing a system of two sequentially coupled submodels. 19

3.2 A block diagram demonstrating the convolution of the impulse responses of the decoupled submodels 19

3.3 A block diagram showing propagation of uncertainties through decoupled transport submodels using the Multiple Convolution Integral approach to estimate uncertainty in the final risk predictions 24

5.1 Solid Waste Management Units at WAG 1 39

5.2 Map of water table under high base conditions at WAG 1, April 1991. 47

5.3 Map of water table under low base conditions at WAG 1, September 1991. 48

5.4 The convolution integral of the DUST and FTWORK results versus the traditional step-by-step predictions as a function of time 93

5.5 Frequency and cumulative distributions of the propagated concentrations through the DUST and FTWORK after 30 years from the release time 94

Figure Page

5.6 Frequency and cumulative distributions of the propagated concentrations through the DUST and FTWORK after 50 years from the release time 95

5.7 Frequency and cumulative distributions of the propagated concentrations through the DUST and FTWORK after 100 years from the release time 96

5.8 Frequency and cumulative distributions of the propagated concentrations through the DUST and FTWORK after 200 years from the release time 97

5.9 Frequency and cumulative distributions of the propagated concentrations through the DUST and FTWORK after 300 years from the release time 98

5.10 Frequency and cumulative distributions of the convolved concentrations of the DUST and FTWORK predictions after 30 years from the release time 101

5.11 Frequency and cumulative distributions of the convolved concentrations of the DUST and FTWORK predictions after 50 years from the release time 102

5.12 Frequency and cumulative distributions of the convolved concentrations of the DUST and FTWORK predictions after 100 years from the release time 103

5.13 Frequency and cumulative distributions of the convolved concentrations of the DUST and FTWORK predictions after 200 years from the release time 104

5.14 Frequency and cumulative distributions of the convolved concentrations of the DUST and FTWORK predictions after 300 years from the release time 105

5.15 Groundwater and surface water predictions on two different scales versus time for the same scenario 107

Figure Page
5.16 Frequency and cumulative distributions of the Multiple Convolution Integral of the DUST, FTWORK, and surface water responses after 30 years from the release time108
5.17 Frequency and cumulative distributions of the Multiple Convolution Integral of the DUST, FTWORK, and surface water responses after 50 years from the release time109
5.18 Frequency and cumulative distributions of the Multiple Convolution Integral of the DUST, FTWORK, and surface water responses after 100 years from the release time110
5.19 Frequency and cumulative distributions of the Multiple Convolution Integral of the DUST, FTWORK, and surface water responses after 200 years from the release time111
5.20 Frequency and cumulative distributions of the Multiple Convolution Integral of the DUST, FTWORK, and surface water responses after 300 years from the release time112
5.21 Frequency and cumulative distributions of the estimated risk from the ingestion of the modeled surface water concentrations after 30 years from the release time 114
5.22 Frequency and cumulative distributions of the estimated risk from the ingestion of the modeled surface water concentrations after 50 years from the release time 115
5.23 Frequency and cumulative distributions of the estimated risk from the ingestion of the modeled surface water concentrations after 100 years from the release time116
5.24 Frequency and cumulative distributions of the estimated risk from the ingestion of the modeled surface water concentrations after 200 years from the release time117
5.25 Frequency and cumulative distributions of the estimated risk from the ingestion of the modeled surface water concentrations after 300 years from the release time118

CHAPTER 1

INTRODUCTION

Human health risk assessment plays an important role in environmental remediation activities across the Department of Energy (DOE) complex. Costs of remediation are directly related and often very sensitive to the findings in the risk assessment phase. Protection of human health is a priority in any environmental restoration project and therefore, risks to exposed individuals are often conservatively estimated. These conservative estimates while protecting human health can significantly drive up the cost of the project.

A typical human health risk assessment is performed in a deterministic manner. This means that for each parameter in the risk model, single highly conservative values are used, resulting in ultra conservative time-independent risk estimates. It can be demonstrated that while these risk estimates are high in magnitude, the resulting level of confidence that human health has been protected (a driving factor in decision making) is only slightly increased over a conservative probabilistic approach that produces a lower risk estimate and therefore, a reduced remedial cost.

The scope of this work is to develop a practical tool to facilitate probabilistic time-dependent risk estimates

resulting from a sequence of release, transport, and exposure mechanisms of radioactive contamination in the geosphere.

1.1 DETERMINISTIC VERSUS PROBABILISTIC ESTIMATES

In a typical deterministic approach to risk assessment, a conservative value is taken from the Probability Density Function (PDF) for each term in the risk model. For example, it is common to select the upper 95% confidence limit on the mean concentration value from the PDF. This is considered a conservative estimate of the concentration term because while the true value is unknown, there is 95% chance that it is actually less than this selected value (EPA 1991). This general approach is used to determine the exposure and toxicity values as well. The multiplication of these three terms produces a single value for the estimate of risk.

In a probabilistic approach, the actual PDF for each term is used rather than the single point value. The three PDFs for concentration, exposure, and toxicity are multiplied together producing a PDF for the resultant risk. The investigator can then select a conservative value from the resulting PDF as the final risk estimate. For example selecting the 95% value from the risk PDF implies that while the true risk is unknown there is a 95% chance that the true risk to an exposed individual is less than this value.

The deterministic multiplication of conservative single point values taken from the PDF of each term can result in risk value with an extremely high value in the modeled Risk PDF (e.g. upper 99%) with only a small increase in confidence (e.g. 4%). The following demonstrates how probabilistic analysis works and how deterministic risk assessment leads to overly conservative point values.

In a cost benefit analysis, the point estimate may yield only an incremental change in the confidence limit, while significantly increasing the total cost to the project. For example, if choosing a confidence level of 95% in the Risk PDF, then at most the Point estimate can only increase confidence by 5%. The relationship between cost and incremental risk is often exponential.

Such cost saving results have been demonstrated in the field. In the example of East Fork Poplar Creek in Oak Ridge (DOE 1994), findings from the estimates made by deterministic methods suggested that the risk based cleanup goal for mercury levels should be 50 mg/kg. A subsequent probabilistic estimate of risk was made resulting in a suggested cleanup goal of 180 mg/kg with a projected savings of $82 million dollars. Through a series of extensive meetings with investigators, regulators, and the community, the probabilistic estimate was understood and accepted.

Although a probabilistic approach can produce a more realistic risk assessment without loss of the conservatism

necessary to protect human health, investigators have avoided application of these methods. This is due, in part, to the geophysical complexity of the site, numerical complexity of the fate and transport models, and a lack of a practical tool for linking fate and transport components together in a fashion that easily facilitates uncertainty analysis. However, armed with high quality tools and information that is tractable, defendable, and accepted by the scientific community, investigators can feel more confident in applying probabilistic methods to individual projects with potentially enormous cost savings to stakeholders and without compromising human health protection.

In the absence of groundwater or surface water sampled concentrations, fate and transport models are used to estimates water concentration at potential receptor points. These point estimates of the modeled concentration in the geosphere are used to determine potential risk from the ingestion of released contaminants from an identified source term. Risk from exposure to the fate and transport predictions of contaminants released from a low-level waste disposal facility can be an important component in environmental analysis with significant implications for the final remedial decision that concerns decision makers in the environmental field. Unfortunately, the geophysical complexity of sites in combination with technical issues surrounding fate and transport codes, make single deterministic point predictions

of the fate of a released and transported contaminant a lengthy and involved analysis. Moreover, the modeling process is actually a series of inter-dependent submodels (see Fig.1). Usually, more than one code is used to perform each substep, each producing results that must be post-processed before they can be passed to the software performing the next step.

In addition, software may require different configurations which depend on the results of the previous step. Therefore, these prevailing circumstances make multiple simulations (i.e, propagated uncertainty analysis) of the transport process untractable and exclude traditional uncertainty analysis as viable analysis tool.

1.2 RESEARCH OBJECTIVE

The objective of this work is to develop a tool, the Multiple Convolution Integral (MCI) approach, that allows coupling of the seperated components of a tedious, sequential, inter-dependent, string of environmental submodels. The MCI facilitates the coupling of the self contained units, so that uncertainty analysis can be propagated independently through these units. Note that the convolution integral theory is a commonly used theory in other engineering fields (e.g., in signal processing) utilized to determine the response of a system for an arbitrary input from the corresponding impulse

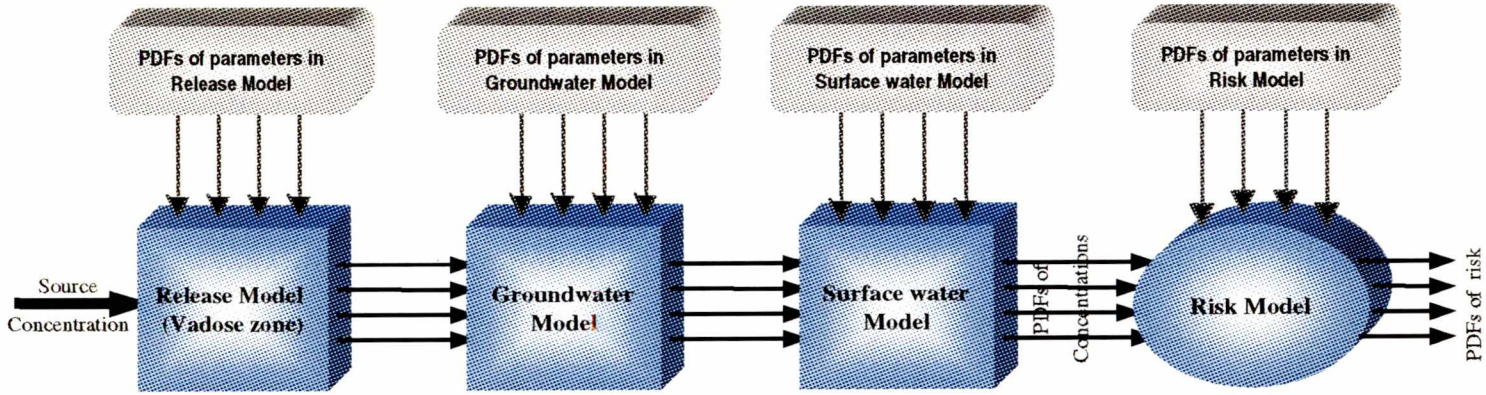


Figure 1.1 A block diagram showing standard propagation of uncertainties through sequentially coupled transport submodels used to estimate uncertainty in the final risk predictions

response of that system. In Environmental Engineering, several researchers (e.g., Codell et al. 1982; Yeh 1981; Van Genuchten and Alves 1982; and Whelan et al. 1987) used the convolution integral to generalize solutions for the advective-dispersive equations for the saturated zone of an instantaneous contaminant release (i.e. impulse response).

In this study, the multiple convolution integral is used to generalize the solution for arbitrary time-varying releases through a multi-stage sequentially coupled system to calculate risk from exposure to potential source releases. The use of the multiple convolution integral will facilitate the coupling of the impulse responses of the separated submodels so that uncertainties in each individual submodel can be propagated within itself, independently. The propagated impulse responses of the individual submodels will be coupled with the time-varying releases to determine the uncertainty in the final model prediction of the sequentially coupled system. Figure 1, is a block diagram that demonstrates the propagation of uncertainty through a sequentially coupled system using standard step-by-step approach. The use of the multiple convolution integral to solve for the time-varying responses of a sequentially coupled system will make uncertainty analysis a tractable, defendable, accurate, and efficient process.

The inter-dependent submodels used in this work are run independently, with results that can be reassimilated or

convolved into the final result using the MCI approach. Therefore, tasks associated with stepwise post-processing of submodel results or the configuration of software are minimized or removed altogether. Ultimately, the objective is to make uncertainty analysis a highly automated process and to restore it as a tractable and beneficial tool for investigators and decision makers while maintaining an effective balance between cost and the level of accuracy of the model predictions.

Following a full characterization of the site containing the waste disposal facility, fate and transport codes are calibrated, potential exposure pathways are determined, and potential receptor points are identified. Several codes are available to simulate the release of contaminants from waste sites and transport through the unsaturated zone underneath it (e.g., the MOC code, DUST code, etc.). Also, various codes are available to simulate the transport mechanism of the released contaminants to potential receptors (e.g., FTWORK, MODFLOW, PORFLOW, etc.). However, none of the available codes can perform a comprehensive simulation of potential releases from the storage site (constrained to the site specification, contaminant characteristics, and failure analysis) to the receptor point. The release rates are either analytically calculated or estimated using structural integrity information to simulate current or potential failure of the waste container. Once the contaminant releases are simulated, other

codes can be used to model and simulate transport through the subsequent environmental media components (i.e., unsaturated layer, groundwater, and surface water).

The Multiple Convolution Integral approach is tested on the function of a waste release and transport model through the vadose zone with the function of a numerical groundwater lateral fate and transport model, with the function of a surface water model at a down stream receptor location. In this work, the DUST code is used to simulate the contaminant release rate from a waste facility due to a potential failure scenario and transported via the vadose zone by an advective/diffusion model, the FTWORK code is used to simulate the contaminant concentration at a specified confluence point with a downgradient surface water stream, and an analytical one dimensional surface water model, Till et. al 1983, is used to estimate the contaminant concentration at a down stream receptor point.

Monte Carlo analysis techniques are used to propagate uncertainties within each model component. The MCI approach is used to couple the propagated uncertainties across the decoupled component to determine statistical distributions for the water concentration at potential receptor points for a particular remedial alternative as a function of time.

The final contaminant concentration in the surface water at the receptor point of interest is used to estimate the risk from the ingestion of the contaminated groundwater or surface

water using United States Environmental Protection Agency (EPA) approved *Risk Assessment Guidance for Superfund* model, EPA 1991. Uncertainties in the risk predictions using the MCI approach are tested against the corresponding predictions of the traditional step-by-step approach that propagates the released concentration from the waste form through the inter-dependent model components to the down stream potential receptor location. The uncertainty results are compared, the time investments are evaluated, and advantages of using the MCI approach to perform uncertainty analysis for sequentially coupled systems are demonstrated.

1.3 SCOPE

This document provides an overview of fate and transport conceptual model used in this study (Chapter 2); describes the convolution integral theory, presents a mathematical description of the Multiple Convolution Integral approach, and advantages of this approach(Chapter 3); presents alternative random sampling technique and alternative uncertainty analysis algorithms, and (Chapter 4); and demonstrates the application of the MCI approach in performing a tractable uncertainty assessment in the final risk estimate (Chapter 5). The application used in this study is extracted from the Inactive tanks project at the Oak Ridge Reservation. For the purpose of

illustration, the actual groundwater system of this application is simplified and the actual fate and transport models of the in Inactive tanks project are used in this study. This exercise demonstrates the capability of the MCI approach in performing a tractable, and efficient uncertainty analysis as demonstrated in the results and discussions sections of this chapter. Chapter 6 presents conclusions emphasizing the significance of using uncertainty analysis, in general, and the MCI approach in particular as a useful tool in decision making. Also, recommendations are made regarding when to use the MCI approach in the process of uncertainty evaluation are presented in this chapter.

CHAPTER 2

PROBLEM FORMULATION

Fate and transport models are commonly used to predict potential releases of contamination from a point source at a particular receptor point. Given complexities in both the site geohydrology and the required numerical models, this can be a lengthy and involved process. In practice, this process is comprised of a series of inter-dependent submodels that rely on the predictions of previous models. For example, the first submodel may determine the portion of the radioactive source released if infiltrating water contacts the waste form, the second submodel may predict contaminant releases from the waste site through the vadose zone. The third submodel implements the results from step two to predict transport through the saturated zone and probably to potentially exposed receptors. A fourth submodel may be used to model contaminant movement in surface water. This example relationship is depicted in Figure 2.1.

A comprehensive site conceptual model that can fully evaluate the fate and transport mechanism of contaminants released from a waste disposal facility is usually accomplished by employing the following main diffusion-convective submodels:

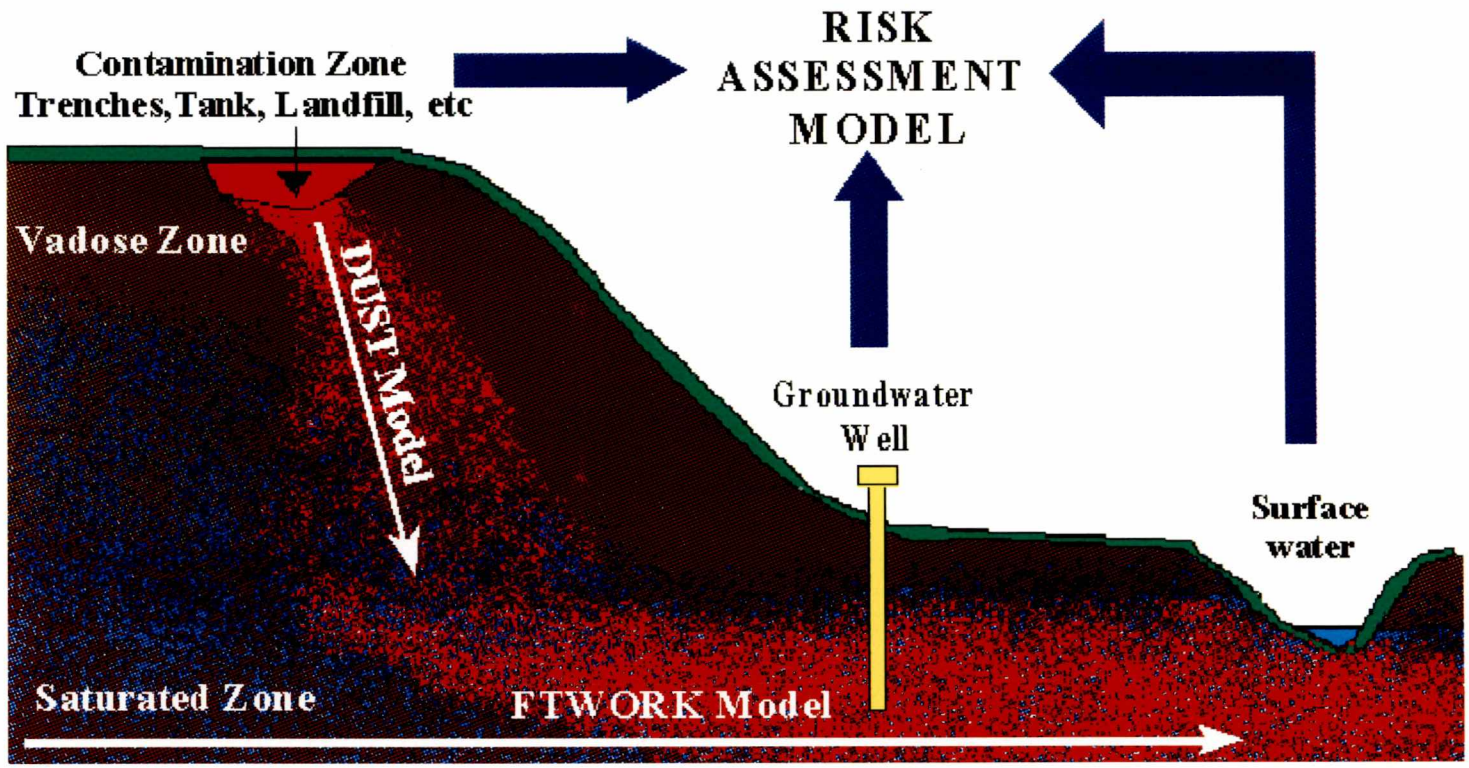


Figure 2.1 Conceptual model for assessing risk from exposure to released and transported contamination from a particular source to potential receptor points

- Leaching contaminants from waste packages, trenches, and pits through the waste barrier due to infiltration.
- Short range transport of contaminants from the burial site through the vadose zone to the saturated zone
- Transport of contaminants in the groundwater to potential receptors down gradient or to the surface water
- Transport of contaminants in the surface water to potential receptor down stream.

The site conceptual model forms the framework within which the environmental pathways of concern for contaminant release from the waste facility are identified and evaluated. The mechanism of contaminant release is initiated by the failure of the waste facility and results in potential migration of contaminants from the storage area into the intermediate environment (i.e., the unsaturated zone). Contaminants are then released into the groundwater and then transported into the surface water. During release and transport, the radioactive contaminants in the source area and in the environment are subject to radioactive decay. The environmental components of the release and transport processes are discussed in Sec. 5.

Given the site specific nature of environmental analysis, and the complexity of the geophysical characteristics of the site, it is rare that a single software package contains the various submodels required to perform rigor analysis. For example, in fate and transport modeling, the DUST code can be

used to model transport through the vadose. FTWORK then uses the DUST results to model transport through the saturated zone. An analytical surface water model then uses the results of the FTWORK to model transport through surface water to a potential receptor. There are several practical implications for combining submodel codes in a sequential fashion. These include:

Compatibility: Since available software packages are not necessarily compatible, results from each software must be postprocessed into an acceptable input format for the next submodel.

Configuration: Since the input of each component is the output of the preceding system component, configurations (often set manually) for software are dependent on or restrained to the previous model results.

Reproduction: Since the system is sequentially inter-dependent, reproducing results could require repetition of the entire sequential process.

Under these conditions, traditional uncertainty analysis is not usually tractable. This dissertation outlines specific goals that facilitates probabilistic risk assessment through computational tools, and a standardized approach for inter-dependent environmental models that can be used to direct and support timely, cost efficient analyses.

CHAPTER 3

THE MULTIPLE CONVOLUTION INTEGRAL APPROACH

3.1 MATHEMATICAL DESCRIPTION

In simple mathematical terms, suppose that a continuous time system is specified by a transfer function h(t). The system differential equations can be written directly from the that function. Therefore, the transfer function is a complete description of the system, regardless of the input function. For this reason, the impulse response of a continuous time system (i.e., the transfer or Greens's function, in this case) can be represented as a block diagram with the system transfer function given inside the block.

It is a common engineering practice to specify a continuous-time system in this manner, where h(t) is continuous at t=τ , the impulse response of the system can be defined by the integral,

$$\int_{-\infty}^{\infty} h(\tau)\ \delta(t - \tau)\ d\tau = h(t) \qquad (1)$$

where δ is the Dirac delta function (i.e.,δ = 1 at t = τ, and

δ = 0 otherwise). The system response to any input x(t) is expressed as an integral involving only the input function and the system response to an impulse function, h(t), yielding the following convolution integral

$$y(t) = \int_{-\infty}^{\infty} x(\tau)\, h(t - \tau)\, d\tau \qquad (2)$$

The theory of the convolution integral is used in this work to couple time dependent solutions of second order differential equations such as the diffusion-convective equations used in the modeling of the fate and transport of released contaminants from disposal facilities or landfill sites through soil, subsoil, and surface water layers. This approach requires the decoupling of the system components and the identification of the impulse responses of each of the decoupled components. Impulse responses from the decoupled components are then convolved with arbitrary inputs using the Multiple Convolution Integral.

The impulse solution can be used to assess uncertainty in the modeling predictions assuming various time-dependent input sources. Variance propagation is performed for each component, independently, to obtain corresponding frequency distributions. Therefore, the main requirement to perform uncertainty analysis using the MCI approach for an n-coupled components is to produce sets of impulse response functions for every time-dependent component of the coupled system. Once these sets of functions are produced the uncertainty in the

final estimate is determined by performing an n+1 multiple convolution integrals for the size of the sample set yielding time-dependent PDFs of the system solution.

Figure 3.1 illustrates the convolution integral for a mathematical model which consists of two coupled components where h(t) and g(t) are the impulse response functions of the coupled components, and z(t) is the final output of the coupled system. Figure 3.2 demonstrates the decoupling of the subject system.

For an impulse input, $x(t) = \delta(t)$, the analytical impulse response of the coupled system might be easy to calculate. The final solution will be equivalent to the convolution of the impulse responses of the decoupled components. However, for an arbitrary input function x(t), the analytical solution of the coupled system might be hard to calculate.

For realistic models the analytical solution might be impossible to calculate. However, a numerical evaluation of the convolution integral can be always used to determine the final output of the coupled system. In general, the impulse response of a two subsystem model can be written using a single convolution for a continuous function :

$$z_1(t) = \int_0^t h(\tau)\, g(t-\tau)\, d\tau \qquad (3)$$

or for a discrete function:

$$z_1(m) = \sum_{n=0}^{m} h(n) \cdot g(m-n) \qquad (5)$$

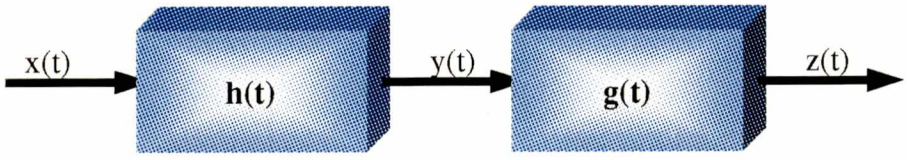


Figure 3.1 A block diagram showing a system of two sequentially coupled submodels

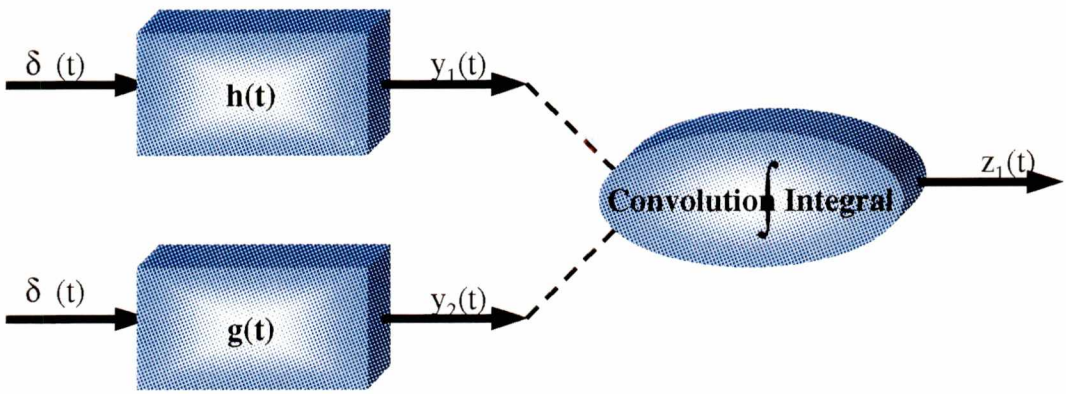


Figure 3.2 A block diagram demonstrating the convolution of the impulse responses of the decoupled submodels

where h and g are the impulse responses of the decoupled components, $y_1(t)$ and $y_2(t)$, respectively.

In general, using the convolution notation, z_1 can be written as,

$$z_1(t) = h(t) * g(t) \tag{5}$$

where (*) denotes a convolution integration or summation. To perform uncertainty analysis, h(t) and g(t), sets of impulse response functions, with the number of elements equivalent to the sample size are calculated as a function of time. The sampled data from the PDFs of h(t) and g(t) are convolved to determine the PDF of $z_1(t)$, a time-dependent set function with the same number of sample data as h and g. Therefore, In sets notation, equation 5 can be written as:

$$\{z_1(t)\} = \{h(t)\} * \{g(t)\} \tag{6}$$

The final output of the two inter-dependent coupled system for an arbitrary input function can be written using a Multiple Convolution Integral as follows, for a continuous function:

$$z(t) = \int_0^t h(t - t_1)\, dt_1 \int_0^{t_1} g(t_1 - \tau)\, x(\tau)\, d\tau \tag{7}$$

or for a discrete function:

$$z(k) = \sum_{m=0}^{k} h(k-m) \sum_{n=0}^{m} g(m-n) \cdot x(n) \qquad (8)$$

In general, using the convolution notation, z can be written as:

$$z(t) = h(t) * g(t) * x(t) \qquad (9)$$

To perform uncertainty analysis, h(t), g(t), and x(t), sets of impulse response functions, with number of elements equivalent to the sample size are calculated as a function of time. The sampled data from the PDFs of h(t), g(t), and x(t) are convolved using the MCI to determine the PDF of z(t), a time-dependent set function with the same number of sample data as h, g, or x. Therefore, In sets notation, equation 9 can be written as:

$$\{z(t)\} = \{h(t)\} * \{g(t)\} * \{x(t)\} \qquad (10)$$

For real environmental transport models, uncertainties in the parameters of each submodel are propagated, independently, through the impulse response solutions of the individual submodels. A set of functions are created for each model as a function of time. The sets of the impulse response functions are convolved. The resulting set of functions is convolved with the arbitrary time-dependent input function to determine a time dependent PDFs of the final output at the point of

interest. The coupling process is not limited to two or three submodels, actually it can extend to as many time-dependent submodels as available. The implications of coupling a few components are limited to the mass storage requirements , and the speed of the mathematical processor used to perform the couplings. Appendix 5 presents a simple mathematical case study that demonstrates the validity and efficiency of the MCI Approach in propagating uncertainty through inter-dependent models.

3.2 OVERVIEW OF THE MCI APPROACH

Commonly, fate and transport modelers avoid the evaluation of uncertainties in the final model predictions resulting from the propagation of parameter uncertainty through sequentially inter-dependent submodels because of limitations inherent in the traditional uncertainty analysis approach. The Convolution Integral approach is used to determine system responses for an arbitrary input function from the impulse responses of that system. Codell et al. 1982; Yeh 1981; Van Genuchten and Alves 1982; and Whelan et al. 1987 used the convolution integral to generalize solutions for the advective-dispersive equations for the saturated zone of an instantaneous contaminant release (i.e. impulse response). In this study, the Multiple Convolution Integral approach is used to facilitate the

processing of uncertainty analysis through coupled fate and transport systems in an efficient, tractable, and accurate manner.

To perform uncertainty analysis using the MCI approach, the inter-dependent submodels must be first decoupled (separated from the entire system). The decoupling allows independent evaluation of the submodels, with submodel results that can be reassimilated or *convolved* into the final result using the MCI approach. Figure 3.3 demonstrates the process of uncertainty propagation through the decoupled submodels and the coupling of the results using the MCI to estimate uncertainty in the final concentration at a specific downstream receptor point. The predicted time-dependent probability density functions of the final concentration, and uncertainties in other sensitive exposure parameters are propagated through the risk model to estimate uncertainty in the final risk predictions. Therefore, tasks associated with stepwise post-processing of submodel results or the configuration of software are minimized or removed altogether. For investigators, the MCI approach automates uncertainty analysis and restores it as an efficient, practical, and beneficial tool. For decision makers, this approach strengthens uncertainty analysis and makes it an attractive tool to use for remediation of complex sites.

Therefore, the emphasis is to integrate the function of a waste release model that can simulate the contaminant release

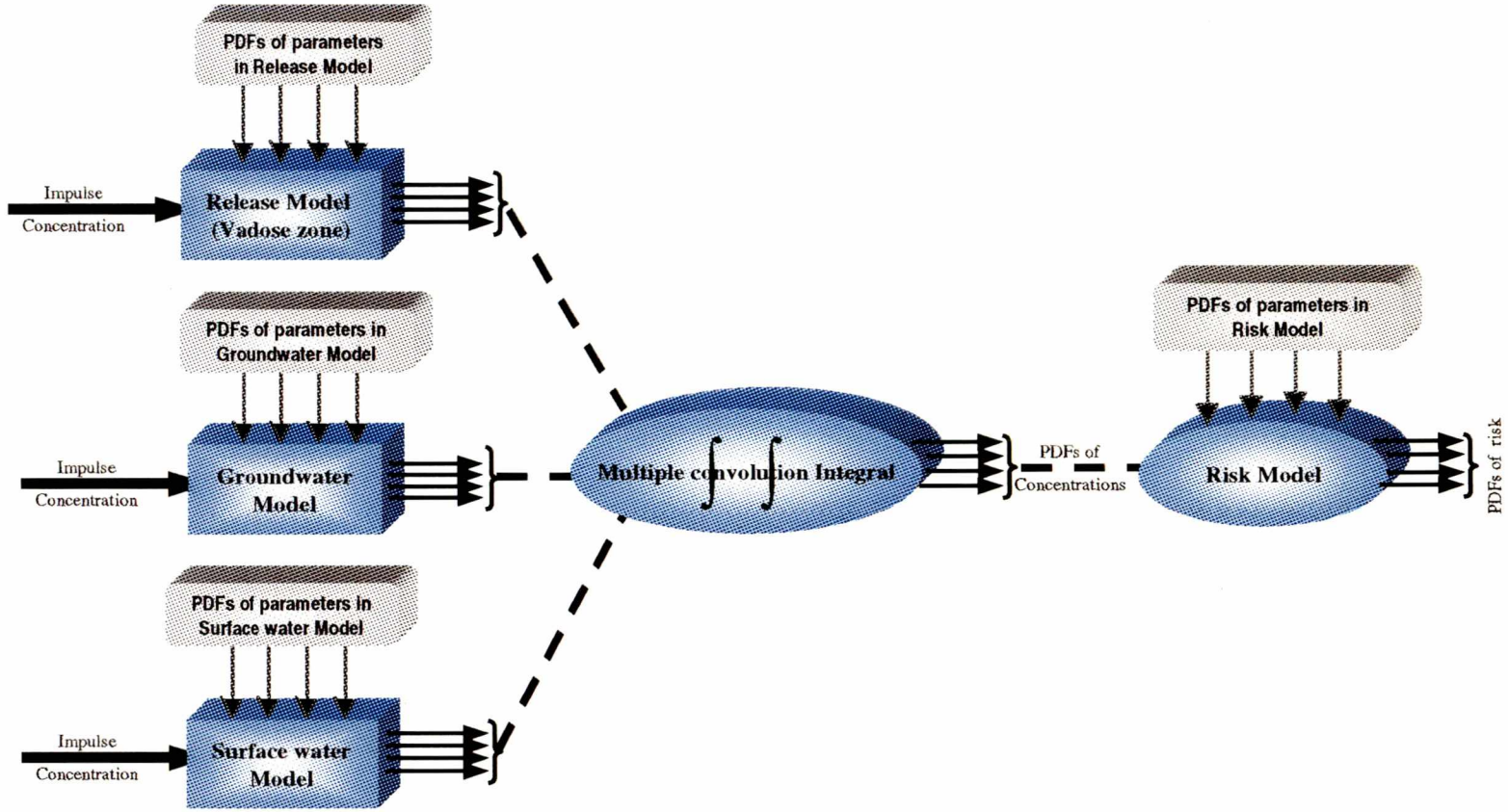


Figure 3.3 A block diagram showing propagation of uncertainties through decoupled transport submodels using the Multiple Convolution Integral approach to estimate uncertainty in the final risk predictions

rate from a waste facility due to a potential failure scenario with the function of an analytical or numerical transport code through groundwater and/or surface water that can simulate the contaminant concentration at a specified receptor location using the MCI approach.

3.3 ADVANTAGES OF USING THE MCI APPROACH IN EVALUATING UNCERTAINTIES IN COUPLED SYSTEMS

The potential benefits of using the MCI approach in propagating uncertainties through inter-dependent fate and transport models are notable for the following reasons:

- Submodels are now separated or decoupled and can be executed independently.
- Submodel input/output manipulation and soft configuration efforts are significantly reduced
- Simulations attributed to updates or errors in the final result are repeated, only, for the affected submodel rather than the entire process.
- Uncertainty analysis becomes a viable option for risk-based remedial decisions.

The major requirements for performing uncertainty analysis for inter-dependent submodels using the Multiple Convolution Integral Approach is to save the results of each decoupled component(a set of impulse response functions) for the selected sample size of the uncertain parameters. Saving

the intermediate simulation results implies that, in case the source term is updated or more statistical data are made available, only, the affected submodel is reassimilated and not the entire system. For Problems involving rigorous groundwater modeling, processing time is a very critical factor in performing quantitative uncertainty analysis. This is because such models are time consuming or require several expertise for each decoupled submodel. For such problems, the MCI can be used to enhance the chances of using uncertainty analysis as a practical decision tool in the remediation process.

In general, the convolution approach might be a viable tool to facilitate the use of uncertainty with the minimum repetition of the modeling efforts necessary to account for any updates or alterations in the submodels. Therefore, the uncertainty analysis can be used independently as a black box with defined boundaries of knowledge about the individual specifications or details of the professional submodels.

In addition, assuming compatibility, configuration, and reproduction implications are eliminated in the traditional approach, the processing time of uncertainty analysis is still, at least, two to three times greater than the time needed in the MCI Approach (as presented in Section 5.9). This is attributed to the fact that standard step-by-step propagation of information through sequentially coupled submodels requires the simulation of transient systems for

each time step of the numerical solution. Instead, for the decoupled submodels, steady state systems are processed, only, which require at most half of the processing time of the corresponding transient system (refer to Section 5.9).

CHAPTER 4

UNCERTAINTY ANALYSIS TOOLS

In a modeling process, a set of input parameters is required. The exact value of any given parameter is rarely known but rather estimated from a data set. Uncertainty of such parameter is quantified by a PDF. When performing an uncertainty analysis, the PDF, rather than a single representative value, is passed to the model. The result is a PDF of possible outcomes.

In practice, this is achieved through *simulation*. A single simulation is performed by drawing one value at random from each distribution and passing it as an input value to the model. The model (or series of submodels) produce the corresponding result. This process may be repeated a number of times to numerically produce the distribution of outcomes. The implication for fate and transport modeling is that for each simulated value, results are processed through the entire chain of submodels to produce a single output. If the sample size of the simulated input is 1000, then the submodels must be used 1000 times including any associated operations required to make input/output compatible and to configure software. For this reason traditional uncertainty analyses can be untractable. By using the MCI Approach, it is possible

separate sequentially inter-dependent transport (or similar) submodels into a series of decoupled submodels producing results that can be reassembled or convolved immediately into the final result. For the purpose of illustration, the fate and transport predictions of the released contamination from a disposal facility can be broken into three main components:

1. a given source term that determines the initial contaminant inventory released and transported through the vadose zone maintaining an equilibrium condition between the decayed source terms and leaching contaminant.
2. a ground water transport component that carries the leachate laterally through the ground water table to a potential receptor while maintaining the same equilibrium conditions over the life time of the decay, release, and transport processes, and
3. A surface water component which dilutes the transported concentrations through the groundwater to a potential receptor down stream.

Parameter uncertainties within each submodel are either sequentially propagated through the entire system or independently propagated through the decoupled impulse responses of each submodel and then coupled using the convolution integral. In either way, the final result (i.e., the concentration PDF at the point of interest) is used to determine uncertainties in the output of the coupled system.

The first step towards performing uncertainty analysis is to identify the most sensitive parameters and their associated PDFs in each submodel. The PDFs are used to establish random sample data sets that preserves the statistical properties of the evaluated uncertain parameters. This is achieved by using random sampling techniques such as Monte Carlo analysis. Section 4.1 describes alternative sampling techniques.

The second step in performing uncertainty analysis for coupled systems is to propagate the sampled data of the uncertain parameters through the system components. The traditional approach of uncertainty analysis is to propagate information in a sequential manner to determine the uncertainty in the final outcome as depicted in Fig. 1.1 using the algorithm presented in Section 4.2. The alternative approach is to couple uncertainties within each model component using the MCI approach to determine the uncertainty in the final outcome at the point of interest as depicted in Fig. 3.3. The alternative uncertainty algorithm is presented in Section 4.3.

4.1 RANDOM SAMPLING TECHNIQUES

Sampling techniques such as Monte Carlo analysis can be used to construct model input data sets by randomly sampling these input parameters to obtain distributions of the desired

output of each component. The accuracy of probabilities obtained from such distributions is proportional to the number of random samples. For example, if the random sample size is 1000 and the number of time steps is 1000 then the total number of values that need to be saved is 1,000,000 for each subsystems. Also, the number of convolution multiplication should be equivalent to the size of the sample, and even with the power of modern and fast computers, for complicated numerical models, this can lead to significant amount of computational time and mass storage requirements. Therefore, a more desirable sampling approach is to use systematic sampling techniques such as Latin Hypercube Sampling (LHS) technique. The LHS is similar to Monte Carlo but rather than randomly sampling from the input parameter distributions, the distributions are first divided into equal probability intervals. This design ensures that the entire range of each parameter is evenly sampled and results in the same output accuracy as simple random sampling techniques while requiring approximately 10 times fewer samples to obtain the same distribution of the output (Gardner et al., 1983).

The output of an LHS simulation is referred to as a design matrix of the uncertain parameters. Specifically, if N computer runs are made for a computer code that has K parameters under study, the design matrix will be N x K. Each row of the matrix contains the input settings for each of the K parameters being studied. Latin Hypercube Sampling has

several potential advantages over other sampling techniques (McKay et al, 1997) in that it covers the range of each input parameter reserving its statistical properties in a fewer number of samples. Typically, for an N x K design matrix, each of the k parameters divided into N equi-probable intervals. Then random sample is chosen from each interval in a manner that preserves the individual probability density function. In this manner, K N-tuples of input settings are determined. If the parameters are all assumed to be independent, then these N-tuples are randomly joined to gather to form the N x K design matrix. If independence of these parameters are is not a reasonable assumption, then the desired rank correlation matrix is used to match the N-tuples in a such a manner that approximates this correlation structure. It should be emphasized that LHS strictly ends with the development of the design matrix.

The design matrix for N computer runs is used as input to the computer code of interest and the desired outputs are recorded for each of these N runs.

4.2 TRADITIONAL UNCERTAINTY ALGORITHM

The traditional approach of propagation of uncertainty between sequentially coupled submodels using Monte Carlo analysis requires implementation of the following algorithm:

1. determine uncertain parameters and corresponding PDFs in the each submodel,
2. Create a matrix design for for all identified uncertain parameter using LHS procedure,
3. use the first sample set to solve for the output of the release model at the vadose zone-groundwater interface,
4. use the output of the release model to solve for the output of the groundwater model at the point of interest,
5. Save the output of the resulting simulation as a function of time for that sample set,
6. use the output of the groundwater model to solve for the output of the surface water model at the second point of interest,
7. Save the final output of the resulting simulation as a function of time for that sample set,
8. choose the next following sample set and repeat steps 3 through 7 until the end of the sample size.
9. Use the statistical properties of the resulting sample to obtain the PDF of the estimated concentration at the point of interest,
10. Create a matrix design for the exposure parameters used to evaluate risk,
11. Use the concentration sample data and the exposure sample set data to estimate the uncertainty in the final risk.

According to this algorithm, future alteration of the source term requires that the entire process be repeated and

thus, impact the uncertainty in the model prediction. Also, changes in the model predictions of any intermediate step affects the out come of the following steps. Therefore, the entire uncertainty analysis has to be repeated, if the source term is updated, or if any intermediate step is altered.

4.3 MCI APPROACH UNCERTAINTY ALGORITHM

Performing uncertainty analysis using the MCI approach eliminates the need for repetitive modeling simulations if the impulse responses of the decoupled components are initially determined. Uncertainty analysis using the MCI for the decoupled impulse responses using Monte Carlo analysis requires the implementation of the following alternative algorithm:

1. determine uncertain parameters and corresponding PDFs in the each submodel,
2. Create a matrix design for all identified uncertain parameter using LHS procedure,
3. solve for the output of the decoupled release model (i.e.,the impulse response of the first submodel)for the size of the sample , and save that output as a function of time,
4. solve for the output of the decoupled groundwater model (i.e.,the impulse response of the second submodel)for the

size of the sample , and save that output as a function of time,

5. solve for the output of the decoupled surface model (i.e.,the impulse response of the third submodel)for the size of the sample , and save that output as a function of time,
6. couple the results of each sample set obtained from steps 3, 4, and 5 using the convolution integration twice
7. Save the convolved result as a function of time for each sample set,
8. Use the statistical properties of the resulting sample to obtain the PDF of the estimated concentration at the point of interest,
9. Create a matrix design for the exposure parameters used to evaluate risk,
10. Use the concentration sample data and the exposure sample data to estimate the uncertainty in the final risk.

CHAPTER 5

APPLICATION

The following section presents an example application taken from the Oak Ridge Reservation Inactive Tanks project. This example demonstrates a typical complexity surrounding the hydrolgeological characteristics of the site. The modeling efforts involved in fully characterizing the site and potential releases to identified receptor point are presented. Also, a description of the calibrated codes used to simulate the fate and transport process is presented.

This example demonstrates how to perform an uncertainty analysis in the final risk predictions using both the traditional and the MCI approaches, in spite of the complexity of the site characteristics. In addition, this case study demonstrates the advantages of using the MCI approach in evaluating uncertainties in the fate and transport predictions including time savings and processing speed without loss of accuracy.

Section 5.1 demonstrates the conceptual site model that will be studies to propagate uncertainty through its components or submodels. Sections 5.2 presents characterization of the exposure settings of the selected application. Section 5.3 presents the function and theory of the DUST release and transport model through the vadose zone.

Section 5.4 summarizes the groundwater fate and transport model (i.e., the FTWORK)used in this assessment. Section 5.5 presents the analytical model used to evaluate surface water concentrations at the receptor point of interest. Section 5.6 presents the risk model used to quantify risk of ingestion contaminated water at Fifth Creek or WOC. Section 5.7 presents the uncertain parameters and their corresponding statistical distributions used in this study to estimate risk at the points of interest. Section 5.8 presents results of the standard approach versus the MCI approach. Section 5.9 discusses the findings of the results and demonstrates the efficiency and time savings of the MCI approach.

5.1 CONCEPTUAL SITE MODEL

The modeling efforts for this task are divided into four major parts. The first part involves a full site characterization of the exposure settings of WAG 1 and WC-1 Inactive tank. The second part involves the failure analysis of carbon steel containers and estimated releases from Wc-1 through the vadose zone over time using the DUST code. The third part involves the evaluation of the fate and transport of contaminant in the subsurface soil, specifically in the groundwater regime using FTWORK. The fourth part involves the transport of contaminants through an analytical surface water

model to a down stream potential receptor. Surface water concentrations from the modeling results are used to calculate risk estimates over time at identified receptor points of interest. The conceptual model was depicted in Figure 1.1.

Several sources of uncertainty were identified in this study , such as the uncertainty in the source term, the site characteristics, the modeling assumptions and parameters, and the exposure assumptions.

5.2 CHARACTERIZATION OF EXPOSURE SETTING

Waste Area Grouping 1 (WAG 1) at the Oak Ridge national Laboratory, an area of approximately 150 acres, contains most of ORNL's original research and development facilities and their associated waste management units (refer to Figure 5.1). Seventy-three waste storage tanks within WAG 1 are listed as solid waste management units (SWMUs). These tanks and their associated buried piping systems were put in place during the early 1950s (Binford and Orfi 1979). Of the 73 tanks, 23 are active (receiving programmatic wastes from continuing operations at ORNL), two are in active use for waste oil collection and 48 are inactive, Category D tanks (physically or administratively isolated from low-level liquid waste program sources but still may be collecting non-programmatic wastes such as in-leakage from vault seals, wastes from floor

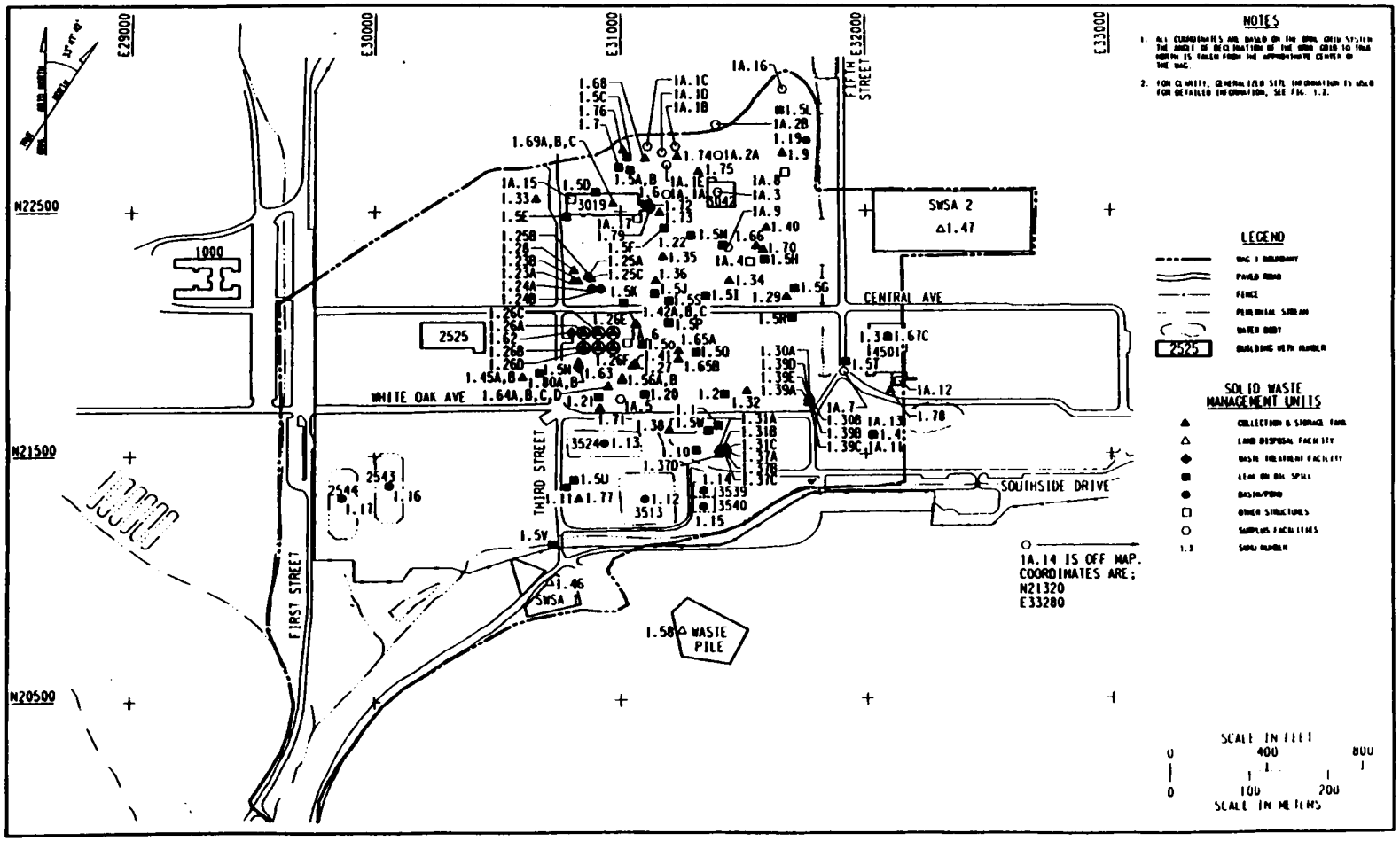


Figure 5.1 Solid Waste Management Units at WAG 1

drains and sumps and/or condensate collected in the gaseous ventilation systems) (Robinson et al. 1991).

A set of tanks, identified as Batch I tanks (WC-1, T-30, W-19, W-20, 3001-B, 3004-B, 3013 and H-209) has been assembled to address remediation alternatives. Tank WC-1 elected in this study to determine uncertainty in the risk predictions posed by the ingestion of contaminated water from potential releases of this tank. The radionuclide contaminant of potential concern which is evaluated in this study is strontium-90 with a concentration obtained from the *Waste Characterization Data Manual for the Inactive Liquid Low-Level Waste Tank Systems at Oak Ridge National Laboratory, Oak Ridge, Tennessee* (DOE 1993).

Ingestion of water is the only exposure pathway that is evaluated for the future residential exposure scenario. Because leached contaminants in groundwater are assumed to be at 100% concentrations in drinking groundwater, this pathway should reflect the most conservative risk evaluation as compared to other potential residential exposure pathways (i.e., inhalation or dermal contact). Risk from the ingestion of surface will be evaluated for future residents in near proximity to contaminated surface water in Fifth Creek and White Oak Creek (WOC).

5.2.1 Site Physical Characteristics

Information regarding site physical characteristics has been extracted from DOE (1992). WAG 1 is located in Bethel Valley between Chestnut Ridge (elevation >1200 ft) to the northwest and Haw Ridge (elevation >1040 ft) to the southeast. The topographic high at the northern boundary of WAG 1 is just over 900 ft. The topographic high within WAG 1 has slopes on the order of 18 to 25%. Stockdale (1951) describes Bethel Valley as a 7.5 mi long portion of an elongated northeast-southwest trending trough with a valley floor averaging 100 ft wide. The valley floor slopes southward at 4%.

WAG 1 is approximately 150 acres in size and includes the main laboratory area at ORNL; consequently it has been highly developed. Based on estimates made from available site maps, an estimated 40% of the WAG is overlain by impervious cover (buildings, roads, parking lots or sidewalks).

5.2.2 Site Surface Hydrology

The natural drainage system includes three perennial streams: First Creek, Fifth Creek and WOC. White Oak Creek has its headwaters to the northeast on Chestnut Ridge and flows southwest along the southeastern boundary of WAG 1 through the water gap in Haw Ridge into and through Melton Valley after which it joins Melton Branch and ultimately discharges into White Oak Lake. Its average gradient is just

under 10%, but it is <1% inside WAG 1 boundaries. The WOC drainage area is 2.1 mile^2.

First Creek originates from a spring on Chestnut Ridge and flows southeast to its confluence with the Northwest Tributary which then enters WOC about 650 ft upstream of the 7500 bridge. Fifth Creek also originates on Chestnut Ridge and flows southeast to its confluence with WOC near the southeast corner of WAG 1. Both First and Fifth Creeks have 4 - 5% gradients at their headwaters and 1 - 2% gradients through the WAG 1 area. The natural drainage of the main plant area is augmented by a system of storm drains in roads and parking lots that discharge into the streams.

The lengths of Fifth Creek, First Creek and the Northwest Tributary are approximately 1.0, 0.6 and 1.25 miles, respectively. The channels of the tributaries are narrow and shallow. The WOC channel at the 7500 bridge is about 15 ft wide and average water depth is about 18 in. In the main plant area, the channels of First and Fifth Creeks pass through many culverts under roads and sidewalks. Approximately 500 ft of the Fifth Creek channel just before its confluence with WOC is an underground concrete pipe-arch 72 in wide and 44 in high.

The flows of WOC and its tributaries within WAG 1 include surface runoff from pervious areas, runoff from impervious areas (mainly from the main plant area), interflow (stormflow), baseflow (groundwater discharge) and imported

water brought to the plant from the DOE water supply treatment plant. WOC and its tributaries are also fed by springs along the southwest slopes of Chestnut Ridge and in the valleys. These springs are believed to have large recharge areas beyond the surface water drainage divide on Chestnut Ridge.

Dry weather flow measurements performed by ORNL during April 1992 at upstream stations showed that the flow of the downstream station was only 20% of that at the upstream station, indicating loss of flow due to infiltration from the stream bed (Borders 1992).The baseflow increases in the downstream reaches, consistent with the observation that WOC is a discharge location for groundwater in WAG 1. In addition the flow duration curves at the 7500 bridge and the WOC flume are flatter, indicating that effluent discharges and groundwater contributions sustain dry weather flow at higher levels all year round.

In WAG 1 streams waters are of the calcium-bicarbonate type, are moderately hard to very hard and have low sodium, potassium and chloride content (McMaster 1967). During October 1990 and March 1991 surface water grab samples were collected from WOC and its tributaries during both low and high baseflow conditions, as well as during storms that occurred during low and high baseflow conditions. No apparent differences were found in the quality of the surface waters among tributaries. Water temperatures ranged between 11.4 and 14.1°C during the high baseflow events (March 1991) and

between 11.1 and 16.6°C during the low baseflow events (October 1990). The pH of the surface waters ranged from 6.89 to 8.08, indicating neutral waters. In general conductivity and chloride, nitrate/nitrite and sulfate concentrations appear to be inversely correlated with the flow rate (*i.e.*, the higher the flow rate, the lower the concentration due to dilution).

5.2.3 Site Hydrogeology

Much of the groundwater movement at WAG 1 occurs in secondary porosity features in the bedrock and is strongly influenced by structural and stratigraphic controls. Structural and stratigraphic control of groundwater flow directions is well documented elsewhere on the Oak Ridge Reservation (ORR) and to some extent has been observed in tracer tests at WAG 1 (Stueber et al. 1981).

The water table surface mimics site topography with highs occurring north of WAG 1 and sloping southward toward WOC. Many undulations occur in the water table surface at WAG 1 as a result of local influences. One such feature is a depression in the water table surface near Building 3042. This depression is probably the result of sumps operating in the building and extracting an estimated 8 gallons per minute (gpm) of groundwater that enters the building through pipeline trenches and as leakage through the walls. The connection

between sumps and groundwater was demonstrated by Huff (1985) and Melroy (1986). During both the April and September 1991 monitoring events, a small groundwater divide was present directly west of Third Street. The divide indicates that flow lines originating from the north diverge towards the southeast and southwest.

Surface impoundments 3542, 3539 and 3540 appear to exert a localized impact on groundwater levels. Mounding in association with the 3500 series impoundments has appeared in some shape or form on most water table maps for WAG 1 as far back as Stockdale (1951). Mounding in the vicinity of the impoundments is evidence of leakage and suggests that the impoundments are actively recharging the water table. Ashwood et al. (1986) conducted a study of leakage from the equalization basin and found flow pathways associated with abandoned stormwater and sanitary sewer lines underlying a portion of the basin. The extent to which similar mechanisms exist for the other impoundments is not known.

The principal influence on groundwater levels at WAG 1 is precipitation recharge. Groundwater increased in elevation from June 1990 through April 1991, followed by a decline until July when water levels rose in response to short-duration summer storms. After July water levels again fell until December 1991. In December there was a 2-day rainfall event of approximately 1.5 in, which strongly affected the groundwater levels. Single storm events did not cause a lasting effect on

groundwater levels. Significant changes in groundwater baseflow occurred during storm clusters when water levels could not decline fully after one storm event before the next storm started. Figures 5.2 and 5.3 are maps of the groundwater table conditions under high base and low base elevations for the years of 1990/1991.

Twice-daily fluctuations of less than 0.2 ft were seen in some wells, most notably deeper wells. These are likely earth tidal effects caused by lunar gravitational forces. This type of fluctuation is not seen in strictly water table aquifers, indicating that some of the deeper areas in the aquifer underlying WAG 1 are at least partially confined.

The complex pattern of groundwater fluctuation observed at WAG 1 reflects variations in site geology, recharge rates and the influences from pipeline networks and building sumps. Fluctuations within the WAG 1 boundary were generally <6 ft and most were <3 ft. These results reflect generally low recharge rates within the WAG due to the high density of paved areas, buildings and surface drainage controls.

Perched water tables have been encountered at WAG 1, generally at depths ranging from 2 to 10 ft BGS (below ground surface). These zones are believed to result from localized variations in permeability within the vadose zone and are apparently transient in most areas.

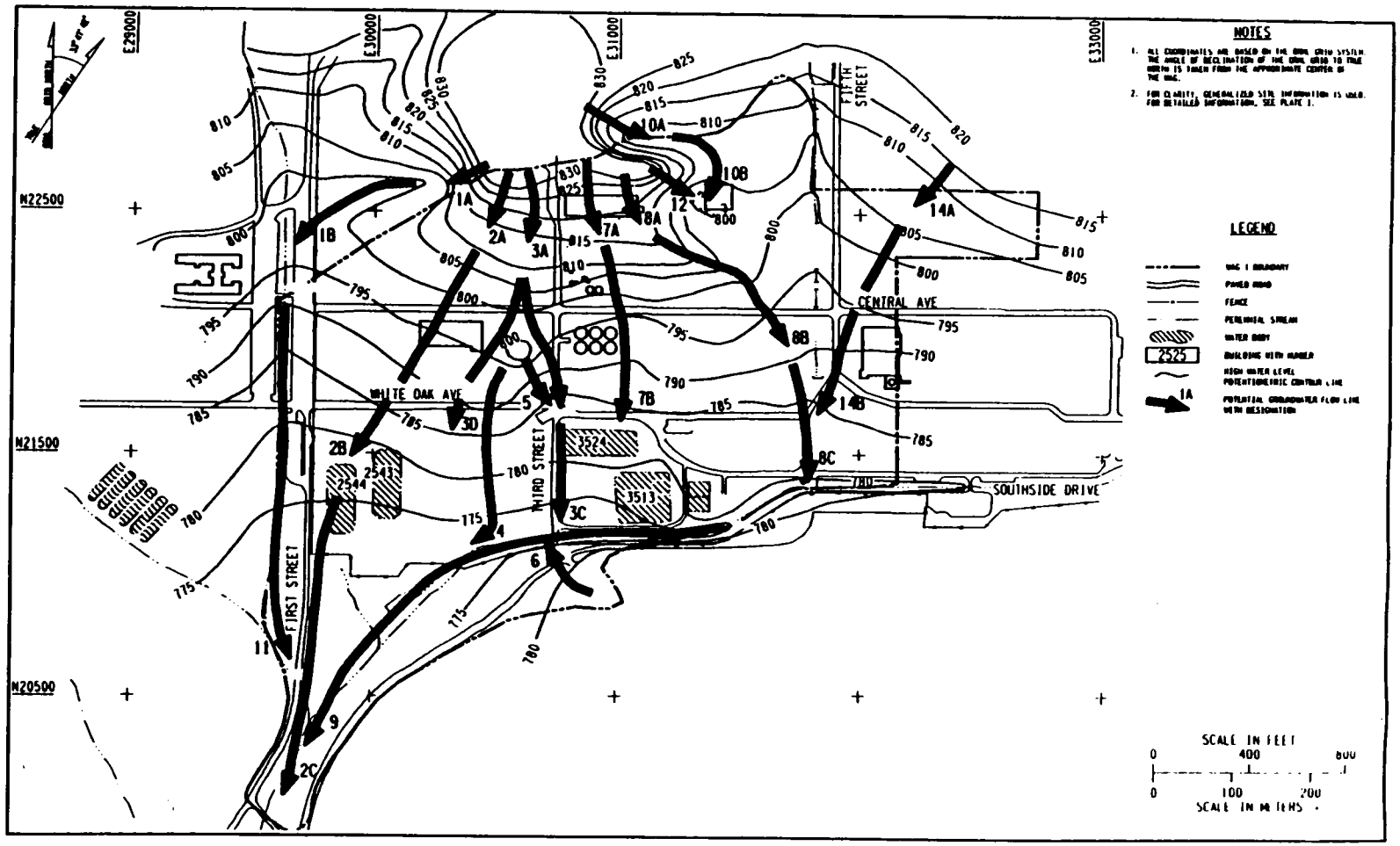


Figure 5.2 Map of water table under high base conditions at WAG 1, April 1991

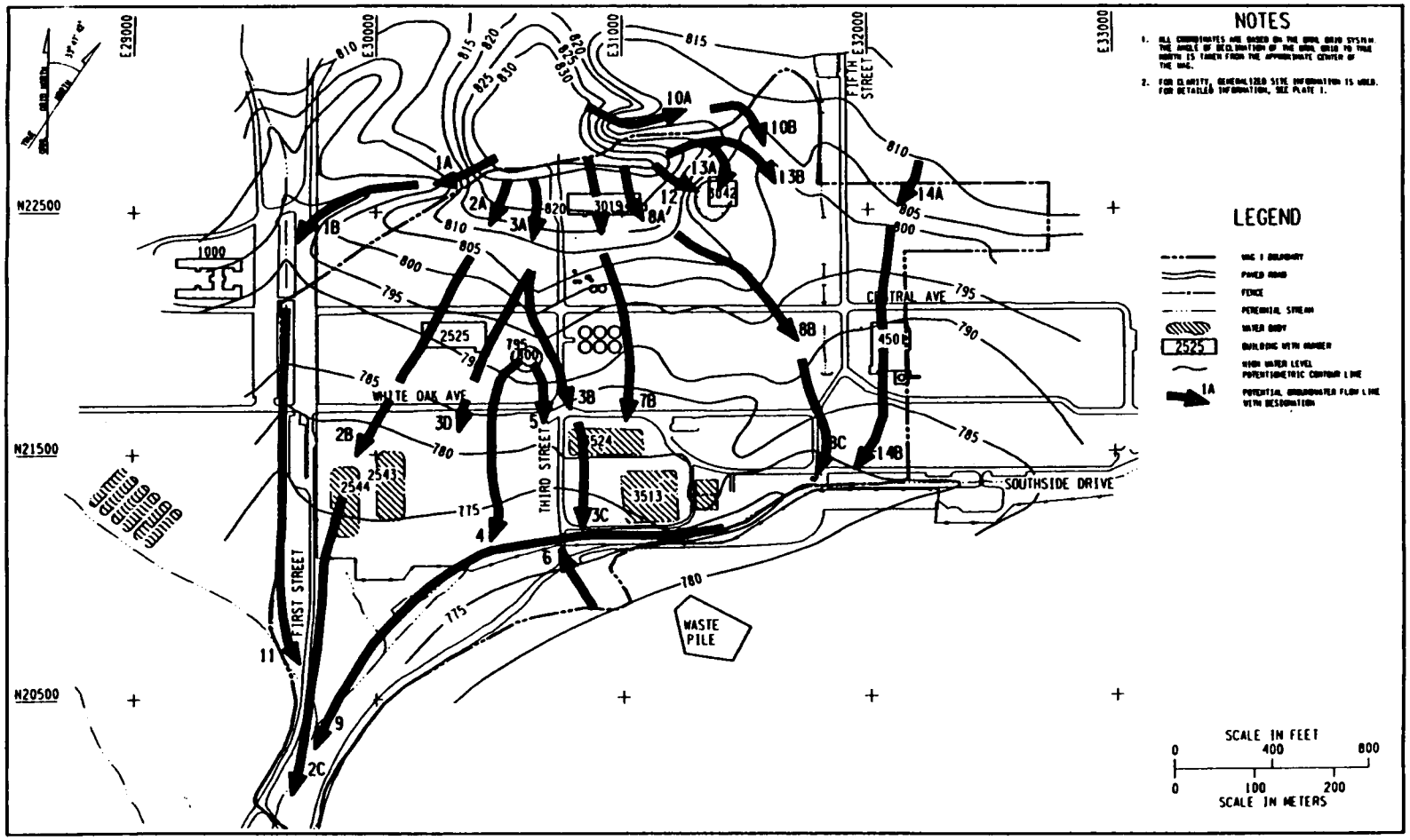


Figure 5.3 Map of water table under low base conditions at WAG 1, September 1991

Groundwater recharge and discharge areas. WAG 1 is predominantly a groundwater discharge area, and recharge occurs only in the northern-most portion of the WAG and locally at the impoundments and leaking pipelines and tanks. In general groundwater recharge areas correspond to higher ground, and discharge areas are along the WOC drainage system. The area directly to the north of WAG 1 near Building 2000 is a major recharge area, as indicated by the groundwater mound and by the high fluctuations in water levels in this area. It is also likely that the topographic high north of Solid Waste Storage Area 2 (SWSA 2) provides recharge to the WAG, as indicated by the direction of groundwater flow from that area. Groundwater recharge is also received from areas east of the WAG between WOC and SWSA 2. Based on limited head data from areas south of WAG 1, it is believed that Haw Ridge is contributing recharge to WOC and the southern portion of WAG1.

Groundwater contours suggest that groundwater exits WAG 1 through the WOC water gap that passes through Haw Ridge. Locally, flow directions vary widely due to influences from local recharge and discharge areas. For example, flow lines originating at the major recharge area north of the WAG radiate in directions ranging from east to west. In addition some seepage of groundwater probably occurs locally into First and Fifth Creeks. However the flow lines eventually converge at the WOC water gap at the southwestern boundary of WAG 1.

5.2.4 Tank WC-1 Description

Tank WC-1 is a 2150 gal stainless steel tank located in the Isotopes Circle area of the Bethel Valley main laboratory area. The tank was installed in 1950 to collect Liquid Low Level Waste from isotope production and development. Sampling of the tank contents indicated that there are 2-7/8 inches of sludge in the tank. The tank has a diameter of 8.66 ft and has a height of 6 ft. The density of the sludge in tank WC-1 was not determined by the sampling analysis. Examination of sample analyses from other tanks indicate typical sludge densities of 1.2 to 2.0 g/cm^3. The average mass of the sludge in the tank is estimated to be 640 Kg. The sampled concentration of strontium in the sludge is found to be 3.03E5 Bq/g, ORNL 1992 (ORNL/ER80).

5.2.5 Toxicity of Strontium-90

Strontium-90 is a beta-emitting radionuclide with a half-life of 28.6 years and a maximum energy of 0.546 MeV (Kocher 1981). It decays to yttrium-90 which is also a beta emitter with a half-life of 64 hours and a maximum energy of 2.27 MeV (Turner 1986). Beta particles from yttrium-90 and strontium-90 must be considered when assessing the potential effects of strontium-90. Concentrations of strontium-90 in the environment are related to nuclear weapons testing and

production with more strontium deposited in the northern hemisphere than the southern.

Atmospheric deposition of strontium-90 on land and its transfer to humans by ingestion is the most important pathway of human exposure. Concentrations in milk and grain products decline rapidly following deposition, while concentrations in fruits and vegetables decline more slowly because soil concentrations continue to contribute to uptake. Once strontium-90 enters waterways, the most important pathway of human exposure is ingestion of water and fish. It is assumed that approximately 30% of ingested strontium-90 is absorbed through the gastrointestinal tract (ICRP 1991).

Strontium-90 resembles calcium and accumulates in the bones causing continuous beta radiation exposures. Strontium-90 causes a prolonged exposure to the bone marrow and impacts blood cell formation, which can result in leukemia, other blood disorders or bone cancers. Strontium ingestion or inhalation exposes the large intestine to beta radiation.

5.3 DISPOSAL UNIT SOURCE TERM (DUST)

The Disposal Unit Source Term (DUST) prepared for the United States Nuclear Regulatory Commission is a one-dimensional finite difference numerical code, Sullivan 1993. This DUST code was developed to predict the rate of release

of radionuclides from a shallow land disposal facility (i.e., the source term). The inventory of the tanks is treated as a known quantity. The DUST model incorporates the different processes that influence release rates. These include: water flow, container degradation, waste form release and transport within the facility. These processes are in turn influenced by the design of the disposal facility, precipitation, hydrology, geochemistry and waste form/container characteristics. The detailed equations pertaining to these processes are presented in the following subsections.

The DUST code provides two alternative methods to model transport within the disposal facility. The multi-cell mixing cascade (MCMC) model and the one-dimensional finite difference (FD) model. The FD model is more general since it provides numerical solution rather than analytical solution that requires additional simplification of the actual problem. For this assessment, the FD model might be a better and more general alternative. Therefore, for the purpose of this demonstration, only the FD model, limitations, and pertaining parameters are presented.

5.3.1 Applicability

Aqueous release of contaminants from the waste disposal unit will be controlled by water flow, access of the water to the wasteform, and transport to the disposal unit boundary.

These processes are influenced by the design of the disposal unit, precipitation, hydrology, and wasteform/waste characteristics. The DUST code is designated to simulate current or future releases due to failure of waste containers. Releases are a function of container performance (time to failure) and wasteform performance (release rate). The code is intended for steel containers where time to failure is easily determined from historical data for both general and local failures. For other structures, the time of failure has to be analytically determined or professionally estimated. Precipitation causes infiltration of water into the soil layers covering the waste disposal unit. Interactions of infiltrated water with the container contents causes container degradation and thus potential release of contaminants to the environment that commences upon container failure. Once the leachate is generated, percolation down through the unsaturated zone will facilitate the transport of contaminants to the groundwater underneath the disposal unit. Different release mechanisms that could be modeled include: diffusion, dissolution, surface rinse with partitioning, and releases associated with limited solubility.

The DUST computer code is used to simulate the different release mechanisms and transport through the vadose zone that follows the failure scenario. This will help in well defining the actual contained source term and thus simulate accurate contaminants potential releases as a function of time.

5.3.2 Model Components and Equations

The DUST framework includes the models for water flow, container degradation, wasteform release, and transport. The following subsections contain the definitions and the basic equations that governs these processes which will influence modeled releases.

Water flow. Infiltration of water into a facility involves precipitation, evapotranspiration and surface run off. For the FD transport model, water infiltration is calculated as a function of time through tabular input (i.e. $V_d = F(t)$) where,

V_d = the volumetric flow velocity (Darcy velocity) of the water and

$F(t)$ = value defined in an input table

This flow rate should be yearly average based on expected conditions. For advection driven transport it has been shown that the average rate of contaminant transport depends on the average flow rate (Sullivan, 1988).

Container degradation. The degradation models are semi-empirical and rely on the existing corrosion in soil data base. In the DUST code, two types of failure were modeled: general and localized failures. General failure is based on the assumption that at the time of failure the container no longer provides a barrier to water flow. For localized failure, contaminants are assumed to be released before the general corrosion allowance is reached. The following

paragraphs outline conditions, assumptions and variables pertaining to both types of failure.

In the DUST code, general failure is modeled through a user-specified time of failure at which point the container is assumed to no longer provide a barrier to water flow. The time of failure is estimated to be the thickness of the container divided by the time averaged corrosion rate. The estimated failure time is then input for each container in units of years.

The FD transport model also evaluates localized failure prior to general failure. If such a failure is assumed, groundwater will contact the waste form, thereby causing the release of contaminants before general corrosion occurs. If the solute is not released immediately after local failure (i.e., is still contained in the container) for any reason, a large pulse release will occur when general failure allowance is reached. For metallic containers, localized failure can occur due to pitting or stress corrosion cracking. In these scenarios, only a small portion of the container will permit water access to the waste form. Under localized failure, the possible breached area in the container can be estimated from the following equation:

$$A_b = N_p \times A_c \times \pi \times (h^2 - T^2) \qquad (11)$$

where,

T = the thickness of the metal wall of the container in cm.

A_c = $\pi R^2 + 2\pi RL$, the total cylindrical container area in cm^2 where, R and L are the container radius and height, respectively

N_p = $N A_t$, the number of localized failures per unit area of the container, where N is a pitting parameter with a mean value of 0.05 pits/cm^2 for carbon steel

h = $k t^n$, the penetration depth where k and n are determined for carbon steel to be 0.074 cm/y^n and 0.39, respectively, and t is time in years.

It is important to note that internal corrosion is not included in the previous empirical model. However, the DUST code accounts for the inclusion of this type of corrosion if sufficient data are provided.

Waste Form Release. Release of contaminants from the waste form commences upon container failure. The major waste streams are categorized as activated metals, dry active wastes, resins and filter media. The distribution of the contaminants between the different waste forms is radionuclide dependent (e.g., 80% of the Th-232 is disposed with sorbents, while over 50% of the C-14 is in cement, etc.). Therefore, different release mechanisms (i.e., solubility limited, surface wash-off subject to partitioning, diffusion and uniform releases) were modeled based on the previously

mentioned categories. A detailed description of these mechanisms is presented in the DUST User's Manual. In general, a waste form may release radionuclides by more than one mechanism.

Uniform Release. The uniform release model assumes that the waste form release rate decreases in time due to radioactive decay and solubility constraints only. The release rate as function of time, Q(t) , can be calculated as follows:

$$Q(t) = Q_f \times M_{wf} \times e^{-\lambda t} \left(1 - \frac{C(t)}{C_{sat}} \right) \qquad (12)$$

where,

Q_f = fractional release rate

C(t) = solution concentration at time t

C_{sat} = saturated concentration of solution

M_{wf} = initial mass of the contaminant in the waste form (i.e., container inventory)

λ = radioactive decay constant

The total mass released in a time step, t, is obtained by analytically integrating Eq. 2 over that time step. The DUST code will perform this integration provided that the parameters in Eq. 2 are loaded properly. The fractional release rate is the fraction of the initial mass in the waste form that is released per unit time.

Solubility-limited Release. Modeling of this release is performed by allowing an instantaneous release of radionuclides into solution until the limit is reached or the entire inventory is released. If a solubility limit is specified and other release mechanisms are used to predict release, the amount released will be constrained such that the solubility limit is not exceeded. Obtaining reliable solubility limits in this environment is a difficult task because it must be justified as conservative under all of the potential conditions. For this reason , the default solubility limit is arbitrarily set to 10 g/cm^3 which is high enough to insure that the release is not affected.

Surface Rinse with Partitioning. The surface rinse model assumes that the radionuclides in the wasteforms are available for release as soon as water contact occurs. Prior to container failure, the contaminants may be held on the wastes by adsorption, chemisorption, adhesion, and ion exchange among other factors. To account for those factors a partition factor, which is an equilibrium ratio relating the amount on the waste form to that in solution, can be used. This partition factor depends on the properties of the wasteform and the local chemistry. The partition factor is a lumped parameter that covers many physical processes. Therefore, obtaining reliable estimate may be difficult.

Diffusion-Controlled Release. Diffusion release is characterized by relatively high leach rates at early times which continually decrease over time. Although, analytically, the release rate is integrable, it approaches infinity as time approaches zero. Therefore, a release model based on a constant release rate is difficult to justify for diffusion - controlled release. Choosing a constant release rate based on short term releases may be overly conservative while choosing some average value may underpredict early releases. The diffusion model will consider cylindrical and rectangular geometries of the disposal facilities. To simplify the situation, it will be assumed that the concentration in the contacting solution is zero which will lead to the highest predicted release rates.

Selection of release models. Several studies that discuss the distribution of contaminant releases by waste class, waste stream, and wasteform (Cowgill, 1992a; Sullivan, 1991; Cowgill, 1992) were used to provide a selection process of the appropriate leaching model. It was found that, limited data on releases from most LLW streams or wasteforms are available. Due to lack of data, the following recommendations suggest the use of:

- Surface rinse model for all dry active wastes and dewatered resins. If partitioning coefficient is available and can be justified, it should be used.

- Diffusion -controlled release for cement solidified wastes where release is geometry dependent. The choice of diffusion coefficient should be supported by data. If data does not exist, a conservative estimate of 10^{-6} should be used.
- Uniform release model for activated metals. A fractional release rate based on typical dissolution rates of the metals may be possible to justify.
- Solubility-limit of 10 g/cm^3 to insure that releases are not influenced by the solubility limit. Representative ranges of solubility are presented in Looney, 1987.

5.3.3 Finite Difference (FD) Model

The FD model is a one-dimensional finite difference model that is used to estimate the release of contaminants from a disposal facility into the unsaturated zone. The model begins with a one-dimensional advection-dispersion transport equation:

$$\frac{\partial}{\partial t}(R\theta C) = \frac{\partial}{\partial x}\left(\theta D\frac{\partial C}{\partial x}\right) - \frac{\partial}{\partial x}(V_D C) - \lambda\theta RC + q \qquad (13)$$

where,

$$D = D_{eff} + \frac{a_t|V_D|}{\theta} \qquad (14)$$

and

$$R = 1 + \frac{\rho K_d}{\theta} \tag{15}$$

where,

θ = volumetric moisture content of the region

D = diffusion-dispersion coefficient

D_{eff} = effective diffusion coefficient

a_t = dispersivity coefficient

ρ = bulk density of the solid

q = source/sink term used to model release from the waste form and external sources (e.g., production due to radioactive decay)

R = retardation coefficient

K_d = distribution coefficient

The FD model transforms Eq. 3 into a set of coupled algebraic equations using a control volume approach, where the modeled domain is divided into control volumes. A mass balance is performed for each control volume through approximation of the derivative terms in Eq. 3 using finite differences. The time derivative is estimated using a backward difference procedure. The diffusion/dispersion term is estimated using central differences, and the advection term is modeled using an upward difference.

To perform the mass balance using the control volume approach, different parameters must be provided. These include

the parameters listed in Eqs. 3, 4 and 5 as well as the number of positions at which the concentration is calculated (NNP) and the locations which are used to determine the control volumes, X(I), where I ranges from 1 to NNP. The average concentration can be viewed as the concentration at the midpoint of the control volume. The FD model will determine the first concentration value as the average for the region X(1) and X(1) + (½)(X(2) - X(1)); the second concentration value is for the region X(1) + (½)(X(2) - X(1) and X(2) + (½)(X(3) - X(2)); and so on. If uniform spacing is assumed, the first concentration value represents the concentration at X(1) + (1/4)(X(2) - X(1)), the second concentration at X(2), the third at X(3), etc. This pattern continues until the last control volume, where the concentration at the last computational point is approximately the concentration at the point given by X(NNP) - (1/4)(X(NNP) - X(NNP-1)). The FD model calculates the flux of contaminants as a function of time at the base of the vadose zone following both failure scenarios provided that the top and bottom boundary conditions are defined. In this regard, special consideration is given to the first and last control volumes. These control volumes are modified to reflect the boundary conditions imposed on the problem. Typical boundary conditions are that the concentration or the flux is specified as a function of time. The details of how the FD model handles the boundary conditions are presented in Appendix A of the DUST manual.

5.3.4 Uncertainties in DUST Parameters

After defining the actual contained source term (from sampled data), the assumptions made to simulate potential release of contamination becomes the major source of uncertainty in determining releases to groundwater and therefore to potential receptors. Those assumptions are inherent in the choice of two main options: 1) the selection of the failure scenario (local versus general failure scenarios), 2) and the selection of the release mechanism (uniform, surface rinse, diffusion, and/or dispersion). For general failure, the container type and thickness will determine the corrosion rate and thus when should the container fail. For local corrosion, an assumption of the penetration depth should be made based on professional judgment. Literature information indicate that vertically downward dispersion of 10% the actual thickness to the groundwater table is a reasonable estimate. The selection of a suitable release model is based on information presented in Section. 5.3.2. Selection of the suitable release model are based an available data and professional judgment, and therefore uncertainties in the DUST predictions resulting from the selection of a specific release model are not quantified. Other source of uncertainties are in the selection of the input parameters which include:

- uncertainties in the partitioning factor, K_d, for the different contaminants (site and contaminant specific) the K_d value is the main source of uncertainty since it is very site specific that varies over several orders of magnitude. Therefore, the level of accuracy in the model predictions greatly depends on the method used to select the proper K_dI.
- uncertainty in the V_D which is assumed constant over time.
- uncertainty in the waste density.
- and the penetration depth, h, for carbon steel which is estimated from the K and n constants. The K was found to range from 0.03-0.15 cm/y^n with a mean value of 0.74 cm/y^n . A quantitative sensitivity assessment of the K parameter showed a strong dependence of the model predictions of the flow rate (a variation of almost one order of magnitude) closer to the upper bound of this parameter. Negligible variation was observed closer to the other end of this parameter. The n parameter was found to range from 0- 0.92 with a mean value of 0.39.Sensitivity analysis of this parameter on the model predictions showed similar behavior to that of the K parameter.
- uncertainty in the moisture contents in the unsaturated zone (a default value is 25%). This assumption often based on professional judgment.

- uncertainty in the area scaling factor. The area scaling factor ranged from 0.08 - 0.32 with a mean value of 0.149 and standard deviation of 0.042. Sensitivity analysis of this parameter on the model predictions showed that its impact is similar to that of the K and n parameters.
- uncertainty in the assumption of the infiltration rate.

It is important to note that site specific data greatly reduces the uncertainty in the release prediction. Therefore, the level of accuracy needed depends on the availability of the site-specific information. The importance of accurate designation of site-specific parameters are determined by the scope of the work. However, justification of the choice of input parameters is always a critical aspect in developing confidence in DUST predications.

5.3.5 Limitations Of DUST Code

A number of assumptions were invoked in the process of developing the DUST code due to lack of data and in order to limit the problem size. The implications of some of these assumption inherent in the code led to the following limitations:

- The code simulates only one spatial dimension releases.
- The code models flow through porous medium. Fracture flow is not considered.

- Water flow and container failure time are not calculated from first principles in Dust. They are determined through input.
- The diffusion release is independent of the concentration in solution and solubility limits.
- The code does not consider variations in the partitioning coefficient (provided by the user) due to change in Ph, Eh , or competition with other ions for sorption sites.

5.4 FTWORK MODEL

Flow of contaminants through the saturated zone (groundwater medium) is performed using FTWORK. This model is a three dimensional numerical code that is used to simulate groundwater flow and solute transport processes under confined and unconfined conditions. The flow and the transport equations are solved separately using finite-difference method. Transport mechanisms that the code can simulate include advection, dispersion, adsorption, and radioactive decay. Also, solutions to transient and steady state flow conditions with source and sink terms can be found. The model uses a block-centered grid that allows variable spacing and the approximation of irregular geometry. In addition, the code is capable of simulating heterogeneous and anisotropic conditions. Furthermore, the code has the

capability to provide for parameter estimation of the steady-state flow equation. The FTWORK was developed for the Savannah River Laboratory, to simulate the groundwater flow through large, complex, multilayered, fully saturated, porous hydrogeologic systems. The model is being calibrated by Energy Systems staff to simulate groundwater flow underlying the Oak Ridge National Laboratory waste disposal facilities.

5.4.1 Applicability

FTWORK is designed for use in the simulation of saturated groundwater flow systems. It is not capable of modeling unsaturated flow in the vadose zone. It may be run in either *flow only* or *flow and transport* mode. In the *flow only* mode, it can be used to solve both steady-state and transient groundwater flow problems for either confined or unconfined aquifers. It can be applied to problems ranging in complexity from simple, one-dimensional analyses of homogeneous systems to full, three-dimensional analyses of extremely heterogeneous systems. The code can be used to model aquifers that have variable thicknesses and can simulate the effects of aquitards between aquifers. FTWORK is formulated on the assumption that groundwater density is constant. Therefore, the code should not be used to simulate the interaction between two fluids (i.e., groundwater/brine infiltration or groundwater/fuel oil spill).

In the *flow and transport* mode, FTWORK may be used to simulate the transport of a single, dissolved contaminant at low concentrations through the saturated groundwater system. The effects of convection, hydrodynamic dispersion, first-order decay, as well as linear adsorption can be simulated. As with the *flow only* model, the code has the ability to model systems that are highly heterogeneous with regard to transport properties.

FTWORK is capable of simulating numerous physical boundary conditions. These include prescribed head conditions (rivers, lakes, etc.), specified flux boundaries (recharge), head-dependent flux conditions (drains and seeps), and fluid sources/sinks (pumping wells). Chemical sources and sinks may also be modeled.

5.4.2 Conceptual Uses and Limitations

A groundwater model that is capable of representing every possible conceptual model of a groundwater flow system does not exist. In general, specific assumptions and simplifications are made to achieve a usable product. Consequently, even for the simplest conceptual model of a site, care should be taken in selecting an appropriate tool for use in an analysis. Furthermore, the user should be well aware of the limitations associated with the particular model that is selected.

FTWORK is formulated on the assumption that an aquifer behaves as an ideal porous medium in which flow is governed by Darcy's Law, which states that flow occurs from regions of high potential (hydraulic head) to areas of low potential (Freeze and Cherry 1979). In addition, the aquifer can be characterized by a set of properties: the density, viscosity, and compressibility of water and the porosity, permeability, and compressibility of the geologic media (Freeze and Cherry 1979). FTWORK may be used to simulate flow for sites which can be directly conceptualized in this manner. Common examples of such systems include nearly homogeneous aquifers which consist primarily of sand, gravel, or other similar material.

However, in reality, most sites are considerably more geologically complex than a simple, homogeneous porous medium. These sites include aquifers that exhibit a high degree of heterogeneity such as those containing localized *pockets* of different material or are intersected by multiple geological formations, as well as sites with multiple aquifers separated by confining aquitards. Again, provided that the location of various subsurface formations can be identified, and that the aquifer can be assumed to behave as a porous medium, FTWORK may be used for analysis. One particularly important example of such a system is that of a fractured rock aquifer. In cases where the rock is highly and uniformly fractured, hydraulic behavior is similar to that of a porous medium. Therefore, FTWORK may be used. While such an approach cannot be used to

estimate localized flow within individual fractures, in general it should provide reasonable head and water balance estimates for the regional system. However, as fracturing becomes increasingly non-uniform or where flow is known to be governed by a few highly-conductive, irregular conduits, use of FTWORK is discouraged. Such would be the case in most karst aquifers where caves and other highly-conductive flow channels are likely to occur.

The transport portion of FTWORK may be used to simulate movement of a single, dissolved contaminant at a low concentration through the groundwater. As with the flow portion of FTWORK, the transport section of the code is based on a porous media formulation which assumes that the migration of contaminants in the groundwater is primarily governed by the effects of advection and hydrodynamic dispersion. This assumption is reasonable for most simple aquifer systems but becomes less valid with increasing aquifer complexity (Gorelick et al. 1993). In particular, extreme caution should be used when considering FTWORK for use in modeling contaminant transport in fractured rock aquifers. Similar to its applicability for groundwater flow calculations in highly fractured aquifers, FTWORK can provide reasonable estimates of solute mass balance over a broad area. However, if detailed knowledge of localized transport though discrete fractures is needed, FTWORK should not be used since movement of solute through fractured aquifer systems may be dominated by

individual fractures or controlled by molecular diffusion into the rock matrix (Gorelick et al. 1993). FTWORK does not contain provisions for handling these processes and should not be used when they are thought to play a significant part in overall contaminant transport. In addition to advection and dispersion, other secondary processes may affect the movement of contaminants in groundwater. Most notable of these is the process of adsorption, through which solute particles become attached to the solid matrix material of the aquifer. This results in a contaminant velocity that is retarded relative to the actual groundwater velocity. FTWORK incorporates the effects of adsorption through the use of a linear isotherm relationship (i.e., the solute is assumed to be at sufficiently low concentrations such that the rock matrix is assumed to have an infinite capacity for sorption of solute, and the rate at which this sorption occurs is independent of solute concentration). Therefore, FTWORK should only be used to model contaminant transport under conditions where the solute concentration is significantly lower (preferably orders of magnitude lower) than the contaminant's solubility limit in water. FTWORK may also be used to model contaminants subject to first order loss processes such as radioactive decay. It is not capable of simulating more complicated physical, chemical, or biological processes.

FTWORK uses finite difference techniques to simultaneously solve equations for groundwater flow and

contaminant transport (Faust et al. 1990). Such techniques require extensive numerical operations and are most practical when used in conjunction with the most powerful computer processor available. The actual amount of computer resources required is dependent on the size and complexity of the problem being addressed. For many one and two-dimensional, and even some three-dimensional steady-state flow/contaminant transport problems, satisfactory results may be obtainable using a *fast* PC such as those based on the Pentium processor technology. However, for problems requiring transient flow/transport solutions, as well as those which require large, complicated three-dimensional grids, it is recommended that the analysis be performed on a UNIX-based workstation or other mainframe-type of comparable computing power.

The user should also be aware of the potentially enormous amount of output information FTWORK is capable of producing. In addition to processor speed, a large amount of disk storage space is vital toward achieving practical use of the code. Finally, it is strongly recommended that some type of graphical pre/post-processing system be used as an aid in generating model input files and viewing/interpreting model results.

5.4.3 Mathematical Model

This section introduces the general mathematical basis for FTWORK. This description includes the governing equations, important auxiliary relationships, initial conditions and boundary conditions. The conservation equations of mass and momentum of water and dissolved species are combined to yield two coupled nonlinear partial differential equations. The spatial and temporal options included in the model are:

1. one-, two-, and three-dimensional Cartesian coordinate,
2. deformed coordinate approximation for variable thickness layers, and
3. Steady or unsteady groundwater flow with unsteady transport.

Governing equations.

Flow and transport equations are posed in terms of hydraulic head (h) and concentration (C). This formulation is based on the following assumptions:

1. changes in density do not depend on concentration
2. changes in density and porosity due to changes in hydraulic head have negligible effects on transport of solute

The governing equations of the flow and transport mechanisms are:

$$\frac{\partial}{\partial x_i}\left(K_{ij}\,\frac{\partial h}{\partial x_j}\right) = S_s\,\frac{\partial h}{\partial t} - W(x,y,z,t) \qquad \textbf{(16)}$$

and

$$\frac{\partial}{\partial x_i}\left(K_{ij}\frac{\partial h}{\partial x_j}\right) + \frac{\partial}{\partial x_i}\left(\phi D_{ij}\frac{\partial C}{\partial x_i}\right) = \frac{\partial}{\partial t}(\phi CR) - C'W^{+} - CW^{-} + \lambda R\phi C \quad (17)$$

where,

x_i = Cartesian space coordinates (m), I = 1, 2, 3

t = time (years)

h = hydraulic head (m)

C = concentration (kg/m^3)

K_{ij} = hydraulic conductivity tensor (m/year)

S_s = specific storage (1/m)

W^+ = volume flux per unit volume in (1/year)

W^- = volume flux per unit volume out (1/year)

W = $W^+ + W^-$; net volume flux per unit volume (1/year)

D_{ij} = dispersion tensor (m^2/year)

ϕ = effective porosity (dimensionless)

R = retardation coefficient (dimensionless)

λ = radioactive decay constant (1/year)

C′ = concentration of fluid in flux (kg/m^3)

Auxiliary Relationships.

Hydraulic conductivity. If it is assumed that the principal components of the hydraulic conductivity tensor are aligned with the coordinate axes, then

$$K_{ij} = \begin{pmatrix} K_{11} & 0 & 0 \\ 0 & K_{22} & 0 \\ 0 & 0 & K_{33} \end{pmatrix} \quad (18)$$

Hydrodynamic dispersion. Hydrodynamic dispersion depends on velocity which is defined using Darcy's equation,

$$v_i = - K_{ij} \frac{\partial h}{\partial x_j}$$

and

$$|v| = \sqrt{(v_1)^2 + (v_2)^2 + (v_3)^2} \quad (20)$$

The dispersion tensor coefficients are given by the following :

$$D_{ij} = \alpha_T |v| \delta_{ij} + (\alpha_L - \alpha_T) \frac{v_i v_j}{|v|} \quad (21)$$

where

δ_{ij} = Kronecker delta; δ_j = 1 for I = j and $_{ij}\delta$ = 0 otherwise,

α_L = longitudinal dispersivity (m), and

α_T = transverse dispersivity (m)

Adsorption. The retardation coefficient (R) includes a linear equilibrium adsorption isotherm. The R can be determined by

$$R = 1 + K_d \frac{(1-\phi)\rho_r}{\phi} \quad (22)$$

where

ρ_r = density of aquifer grains (kg/m^3)

K_d = distribution coefficient (m^3/kg)

ϕ = effective porosity

Radioactive decay. Radionuclides activities decay according to the following mathematical law:

$$\frac{dC}{dt} = -\lambda C \quad (23)$$

where C is the mass concentration (kg/m^3) of the material as a function of time and λ is the decay constant (1/year) which is calculated from the radionuclide half-life time, $t_{1/2}$ (years), (i.e., $\lambda = 0.693/t_{1/2}$). The negative sign is needed because C decreases as time increases.

Initial Conditions

The initial conditions for Eqs. 6 and 7 consist of the distribution of heads and concentration within the volume of considerations. These conditions are stated as follows:

$$h = h^{\circ}(\underline{x}), \quad in\ v \quad (24)$$

$$C = C^{\circ}(\underline{x}), \quad in\ v \quad (25)$$

where $\underline{x}$ is the vector position (m), v is the simulated

domain, and h^o and C^o are the initial dependent variable distribution.

Boundary Conditions

Three types of boundary conditions of the simulated domain can be developed for the governing equations 6 and 7. These include the following prescribed conditions:

Heads and concentrations

The mathematical representation of the boundary conditions of prescribed heads or concentrations which are known as the Drichlet boundary conditions are:

$$h = h^b(x), \quad on \; S_1^h \tag{26}$$

$$C = C^b(x), \quad on \; S_1^c \tag{27}$$

where h^b and C^b are the head and concentration specified along the boundaries S_1^h and S_1^c, respectively. It is important to note that, the prescribed concentration may be physically unrealistic and should be applied with care. For example, the solute concentration at the boundary of groundwater outflow will be controlled by the concentration of the fluid crossing the boundary.

Flux conditions

For flow and solute transport application, several

combinations of flux boundary conditions may be specified. The mathematical formulation of the flux conditions is:

$$Q_n^w = Q_n^w(x) \quad for\ x\ on\ S_2^h \tag{28}$$

$$Q_n^s = Q_n^s(x) \quad for\ x\ on\ S_2^c \tag{29}$$

where Q_n^w and Q_n^s are the normal flux(m^3/year) and solute normal mass flux (kg/year) into the boundaries along S_2^h and S_2^c, respectively. A special boundary condition would be the zero flux condition which represents an impermeable boundary. A prescribed non-zero flux may describe an inflow or an outflow from an adjacent aquifer . However, these fluxes are incorporated into the generalized source term (W) in Eqs. 28 and 29.

For the transport equation , a non-zero solute mass flux is usually associated with groundwater crossing the boundary. It is assumed that advective flux dominates over dispersive flux. Therefore, concentration should be specified for groundwater inflow boundaries. For outflow boundaries, solute flux should not specified since it is determined by the concentration and the groundwater flux at the boundary.

Head dependent flux

The mathematical formulation of this boundary condition is as follows:

$$\frac{\partial h}{\partial n} + g(x)\, h = f(x) \quad for\ (x)\ on\ S_3^h \tag{30}$$

where the partial derivative is the normal derivative of head across the boundary S_3^h and g(x) and f(x) are functions of position. The head condition describes flow across a semi-pervious boundary such as a streambed or aquitard. It also can be used to simulate flow to a drain or seep.

5.4.4 Numerical Techniques

For the general case of inhomogeneous hydraulic properties and a non-uniform flow field presented by Eqs. 6 and 7, numerical solutions are necessary. The major elements of this numerical model include the finite difference approximation, the solution scheme used to solve each governing equation, and the procedure for coupling the solution of the two equations. The three-dimensional model presented here is based on a finite difference scheme using a block centered grid that allows variable spacing and the approximation of irregular geometry. The model also allows for the approximation of layers that have irregular thickness and/or that are not horizontal. Details about the constituting elements of the numerical model are presented in the FTWORK computer work documentation (FTWORK Version 2.4, 1990).

5.4.5 Uncertainties in Critical Model Inputs

Flow and transport solutions calculated by FTWORK are highly sensitive to a number of critical input parameters. These are listed in Table 5.1. In the case of the flow portion of the model, probably the most critical input parameter is hydraulic conductivity. While default values for conductivity can be found in literature for various types of geologic systems, such values can vary by as much as 10 orders of magnitude (Freeze and Cherry 1979).

Use of these default data in the absence of site-specific measurements is highly discouraged. It is strongly recommended that, whenever possible, site-specific hydraulic conductivity data be obtained. Just how much site-specific information is required is a rather difficult question to answer. While one local measurement is better than none, two are better than one, etc. Ideally, measurements should be taken at multiple spatial locations that extend throughout the entire domain to be modeled. Obviously, this is not always practical since each additional measurement also means additional cost. Furthermore, one must realize that even if hundreds or thousands of measurements are taken, uncertainties in conductivity values still exist at those locations not measured. One method of determining whether additional conductivity measurements are needed is to ask the question of whether a reasonably well calibrated model can be obtained

Table 5.1 Critical input parameters for FTWORK

Parameter	Flow	Transport
Hydraulic conductivity	x	
Recharge	x	
Effective porosity	x	x
Storage term	x	
Boundary conditions	x	x
Initial conditions	x	x
Decay coefficient		x
Retardation factor		x
Dispersivity		x

using the existing range of known conductivity values. If not, additional measurements may be necessary. If a detailed analysis is required for a local region of the modeled area for which no conductivity data exist, additional measurements would probably be beneficial.

As with hydraulic conductivity, site-specific values for recharge, the amount of water due to precipitation that reaches the water table, are necessary for effective simulations using FTWORK. Storage terms (storativity for confined aquifers and specific yield for unconfined aquifers) are used to quantify the amount of water released from an aquifer due to changes in hydraulic head. They are applicable only to transient flow analysis problems. Generally, values of storativity for confined aquifers are small, as is the associated water flux. For unconfined aquifers, specific yield values vary in range over about an order of magnitude. While site-specific values can be determined from pumping tests, often reasonable default values can be used, provided that they result in a satisfactory transient model calibration. Effective porosity represents the fraction of a given aquifer volume that is actually available to water infiltration. As with all model parameters, site-specific values obtained from measurements should be used if available. However, in their absence, satisfactory results can be obtained using default values that generally range from 1 to 20%.

For contaminant transport calculations, one of the most sensitive model input parameters is the retardation factor. Like hydraulic conductivity, default literature values as well as formulas for estimating the retardation factor exist for many contaminants. However, the retardation factor is highly dependent on soil type and the amount of organic material present in the soil. Therefore, use of site-specific retardation values is advised.

A second, critical input parameter for transport simulation of solute subject to first-order decay processes such as radioactive decay is the decay coefficient. In general, standard values from literature suffice for this parameter. Dispersivity is a parameter used by FTWORK to represent the effects of mechanical dispersion. Since, in general, dispersion effects are dominated by those of advection, and because it is difficult to obtain accurate measurements for dispersivity, default dispersivity values are generally sufficient for transport modeling using FTWORK.

The final, and perhaps most critical, information required by FTWORK is that which describes the model's boundary conditions. Such information is inherently site-specific. The location of all relevant fluid sources and sinks, constant head boundaries, contaminant sources, etc., must be specified accurately to obtain meaningful results. In addition, detailed maps of initial head and contaminant concentration are required, respectively, for transient flow

analyses and some contaminant transport analyses. Furthermore, even for steady-state flow analyses, knowledge of the site hydrology (i.e., hydraulic head distribution, discharge to seeps, etc.) is a useful, if not mandatory, prerequisite for achieving a well-calibrated model.

5.5 ANALYTICAL SURFACE WATER MODEL

Once the groundwater effluent is laterally mixed at the confluence point with the surface water, it is further transported under steady state conditions mostly by simple advection of the river flows according to Fick's second law.

$$\frac{dC}{dt} = D \frac{d^2C}{dx^2} \qquad (31)$$

C = concentration of contaminant in surface water (Ci/cm^3)

D = Longitudinal dispersion coefficient in the x direction in(cm^2/y)

t = time of travel (y)

x = Longitudinal distance (cm)

This is simply an expression of equating the rate of change of the concentration profile with respect to distance. If the effluent is highly unsteady conditions due to the velocity of the stream, the following equation also applies

$$\frac{dC}{dt} = -U \frac{dC}{dx} \qquad (32)$$

where U is the velocity of a stream (cm/y). This expression equate the rate of change of concentration with time to a combination of differential shear flow nonuniform river velocity distribution) and cross-sectional turbulent mixing. If the effluent concentration is radioactively decaying, then combining these two equations with the decay rate contribution, the well known dispersion equation in one direction is derived

$$\frac{dC}{dt} + U \frac{dC}{dx} = D \frac{d^2C}{dx^2} - \lambda t \qquad (33)$$

where λ is the radioactive decay coefficient in (1/y).

For an instantaneous accidental release of radionuclide mass, M_0, the time and space dependent concentration distribution is given by,

$$C(x,t) = \frac{M_0}{WH\sqrt{4\pi Dt}} \exp[-\frac{(x - Ut)^2}{4Dt} - \lambda t] \qquad (34)$$

where, W and H are the stream width and depth in cm. This equation expresses the down stream motion of a radionuclide pulse at velocity U and its simultaneous longitudinal spread. This equation is useful in estimating exposure levels downstream from accidental releases. Note that dilution and

dispersion effects at the confluence point of the groundwater plume with the surface water is not considered in this model. Therefore, the initial surface water concentrations are assumed to be equivalent to the instantaneous groundwater releases that would arrive at the point of interest.

Liu 1977 has derived an accurate method for predicting the dispersion coefficient.

$$D = 0.18 \left(\frac{V}{U}\right)^{3/2} \frac{Q^2}{V H^3} \qquad (35)$$

Where,

Q = the volumetric rate of flow (cm^3/y),

V = Shear velocity $(gHs)^{½}$, (cm/y)

g = gravitational acceleration (cm^2/y)

s = slope of river

In examining several rivers using this model, the largest error between the observed and predicted dispersion coefficient was only a factor of 6 as compared to 700 by other models.

5.6 WATER INGESTION RISK MODEL

In this study, the only evaluated pathway is the water ingestion pathway for the residential scenario. The model and corresponding parameters are approved by EPA and presented in

the *Risk Assessment Guidance for Superfund, 1992* document.

$$\text{Ingestion risk} = C_w \times IR_w \times EF \times ED \times SF_o \quad (36)$$

where

C_w = Modeled radionuclide concentration in water (pCi/L)

ED = exposure duration (yr)

EF = exposure frequency (day/yr)

IR_w = water ingestion rate (L/day)

SF_o = oral slope factor (risk/pCi)

5.7 UNCERTAINTY ANALYSIS

Uncertainties in the input parameters of each submodel constituting the sequentially coupled system presented in Figure 1 are propagated through the inter-dependent components to determine uncertainties in the final risk prediction at the receptor point using the traditional approach. Alternatively, the uncertainty in the final risk prediction is performed independently using the MCI-based algorithm presented in Section 4.3. In this approach parameter uncertainties within each submodel are performed independently. The resulting predictions of the first two submodels (i.e, two sets of impulse response functions) are convolved. The yielding result is then convolved, again, with the predictions of the third submodel (i.e, the third set of

impulse response functions). The outcome of the second convolution is the set of final time-dependent concentrations at the receptor point of interest (i.e., confluence point of Fifth creek and WOC) that should be used in the risk model.

Two main Matlab functions are written to propagate uncertainties through an environmental system using both the traditional and the MCI approach for the size of the sample of the uncertain parameters. These Matlab codes call other functions written specifically to read/write DUST and FTWORK output files. The main programs and called functions are presented in Appendices 1, 2, 3, and 4.

The final concentration estimates for each sample set are then used to establish a PDF of the risk prediction at the point of interest.

The focus of this study is to demonstrate the advantages of using the MCI approach over the traditional approach in evaluating uncertainty analysis in the risk predictions. This study is not intended to identify or quantify the sensitivity of the different parameters in each code. Therefore, although we tried to use actual data and referenced PDFs of the most sensitive parameters, values and corresponding distributions of certain parameters are assumed based on professional judgement. Hence, the findings of this study should not be used to establish risk-based clean up decisions subject to the estimated uncertainty in the final risk predictions.

The following is a list of uncertain parameters considered in the course of this evaluation:

- In the vadose zone, the distribution coefficient K_d , moisture contents, density, vertical Hydraulic conductivity, and effective porosity in the vadose zone;
- In the groundwater, distribution coefficient K_d , porosity, recharge rate, effective porosity, density, and dispersion coefficients. Note that although the hydraulic conductivity is a very critical parameter in the ground model, constant spatial site-specific values are used. Therefore, their uncertainties are not considered in this study because of complexity of the problem and lack of probabilistic information;
- In the surface water, the river width, water elevation, river flow rate, and channel slope.
- In the risk model, the water concentration, exposure frequency, exposure duration, and intake rate.

Table 5.2 summarizes the Statistical properties and the corresponding literature references, if available, of the uncertain parameters used in the current application.

This study concentrates on the fate and transport of ^{90}Sr from Tank Wc-1 through the vadose, saturated groundwater, and surface water to a potential receptor at Fifth Creek or WOC.

The probability density functions of the 16 selected uncertain parameters in each transport model will be sampled creating a 16 x 100 design matrix using LHS technique.

Table 5.2 Uncertain parameters , references, and their corresponding PDFs used in the different models

Uncertain Parameters	Units	Distribution	Distribution parameters*			References
DUST Parameters						
Distribution Coefficient	cm^3/g	Lognormal	Mean=3.6	S.D=1.6		Baes 1984
Soil Density	g/cm^3	Normal	Mean=1.3	S.D=0.15		DOE1997
Vertical hydraulic conductivity	cm/s	Lognormal	Mean=5.0E-5	S.D. =4.9E-5		DOE 1992
Effective porosity		Triangular	Min=2.5E-3	Max=6.0E-3	Mode=4.2E-3	Moore 1989
Moisture Contents		Uniform	Min=0.3	Max=0.5		Moore 1988
FTWORK Parameters						
Distribution Coefficient	cm^3/g	Lognormal	Mean=3.6	S.D=1.6		Baes 1984
Soil Density	g/cm^3	Normal	Mean=1.3	S.D=0.15		DOE1997
Effective Porosity in soil		Triangular	Min =0.001	Max=0.1	Mode=3.5E-2	Moore 1989
Effective porosity in Bedrock		Triangular	Min =0.1	Max=1.0	Mode=0.15	BNI 1991
Recharge rate	ft/d	Uniform	Min=6.9E-4	Max=1.4E-3		DOE 1992
Longitudinal Dispersion	ft	Lognormal	Mean=0.47	S.D.=1		Lee 1989
Transverse Dispersion	ft	Lognormal	Mean=0.25	S.D. =1		Lee 1989
Surface Water Parameters						
River width	ft	Uniform	Min =1	Max =6		Assumed
Water Elevation	ft	Normal	Mean=815.4	S.D. =9.0E-2		DOE 1992
River Flow Rate	cfs	Custom	Min =0.02	Max =20	Mean=1.5	DOE 1992
River Slope		Uniform	Min = 2%	Max = 5%		DOE 1992
Risk Model Parameters						
Exposure Duration	y	Lognormal	Mean=11.36	S.D. = 13.7		Israeli 1992
Exposure Frequency	d/y	Triangular	Min = 180	Max = 365	Mode= 345	Smith 1994
Ingestion rate	L/d	Lognormal	Mean = 1.26	S.D. = 0.66		Smith 1994

*Mean = mean value
S.D. = Standard deviation
Min = minimum value
Max= maximum value

The developed design matrix (i.e, the 16 100-tuples)is propagated through the entire process to determine the uncertainty of the final concentration at the receptor point. Also, the design matrix is propagated independently through the individual submodels. The sets of decoupled results are convolved using the MCI approach to estimate the PDF of the resultant concentration at the point of interest.

Probability density functions of the exposure parameters are sampled using LHS. The resulting sample data sets of the uncertain exposure parameters, in addition to the distributions of the propagated concentrations are used to determine uncertainties in the final risk estimates.

The sensitivities of final risk estimates are calculated by computing the rank correlation coefficients between every parameter and every risk distribution using Crystal Ball decisioneering software. These coefficients provide a meaningful measure of the degree to which input assumptions and output predictions change together.

5.8 RESULTS

The analysis are performed for 300 years from the initial time of release (i.e., at t = 0). An electronic data is available for every year during the 300 years of simulation. For the purpose of demonstration, the statistical

distributions(i.e, frequency and cumulative distributions) of the predicted concentrations at the points of interest are presented in this report for selected time intervals (i.e., 30, 50, 100, 200, and 300 years), only.

Two exposure points of interest are identified. These points will be referred to as the first and second points of interest. The first point occurs at the confluence of the groundwater with the surface water at Fifth Oak Creek. The second point is 700 ft down stream of the Creek at the confluence of Fifth Oak Creek with WOC.

The statistical descriptions of the different predictions are expressed in terms of the mean, median, standard deviation, variance, kurtosis, skewness, minimum, maximum, and the 10% right tail fractiles (i.e., 90, 95, 97.5, and 99%-tiles).

Figure 5.4 demonstrates a comparison of the predictions of the convolution integral of the impulse responses of the first two submodels (i.e, the DUST and the FTWORK predictions) with the standard step-by-step approach predictions for a particular set of random numbers as a function of time.

Figures 5.5 through 5.9 demonstrates the statistical distributions of the standard approach to estimate the concentration at the first point of interest for the selected time intervals. Table 5.3 summarizes the statistical information of the standard approach at the first point of interest for the selected time intervals.

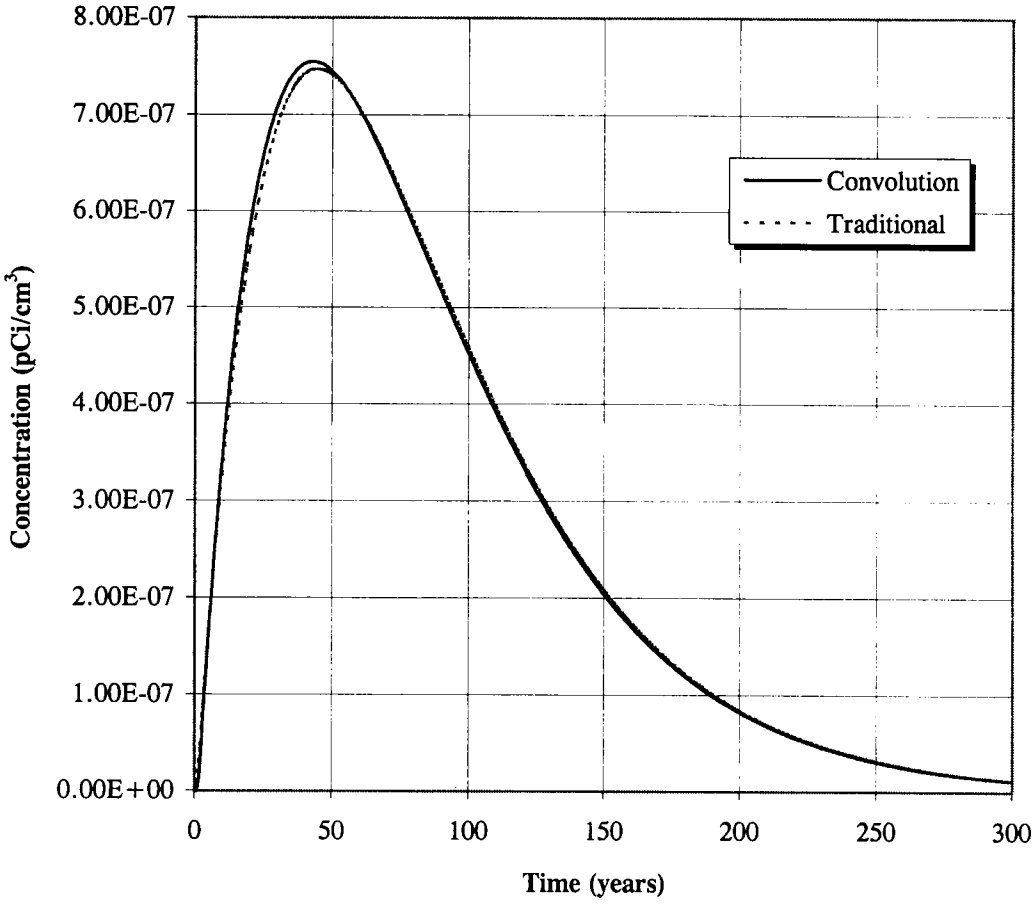


Figure 5.4 The convolution integral of the DUST and FTWORK results versus the traditional step-by-step predictions as a function of time

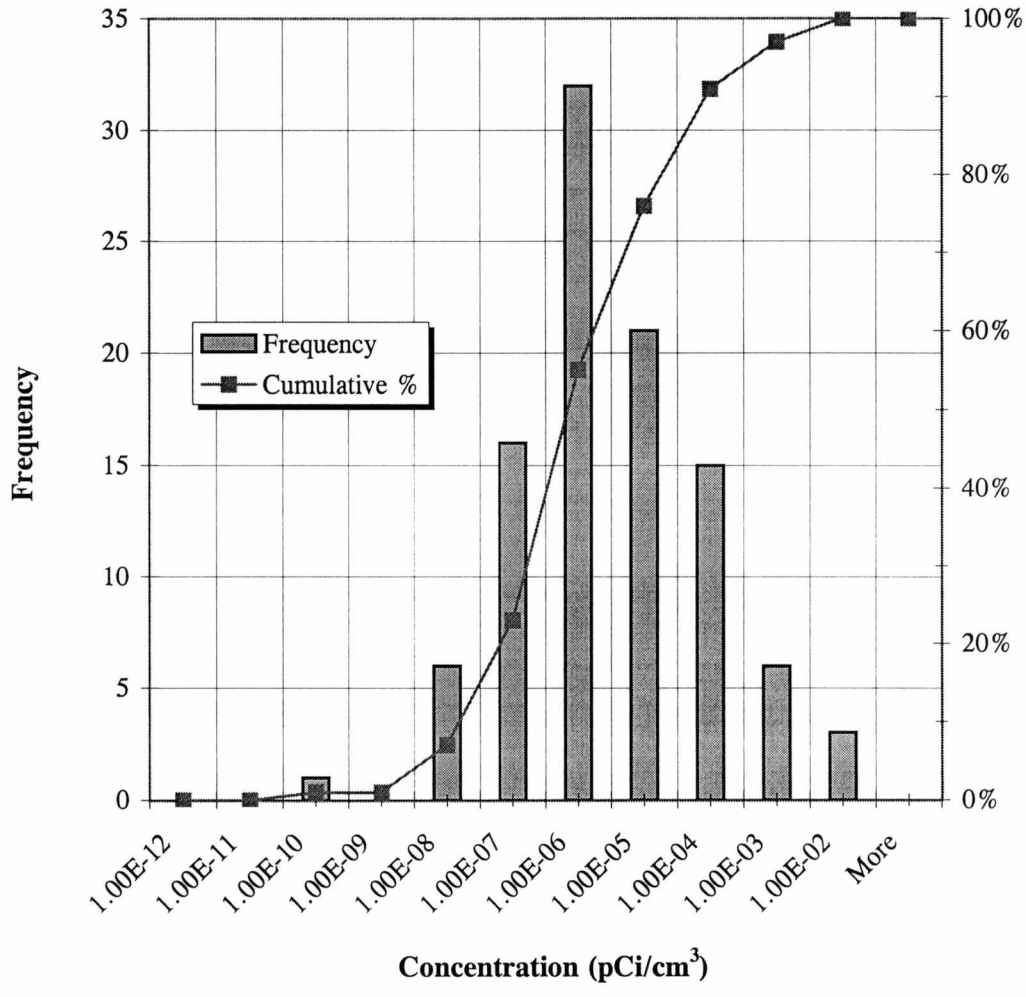


Figure 5.5 Frequency and cumulative distributions of the propagated concentrations through the DUST and FTWORK after 30 years from the release time

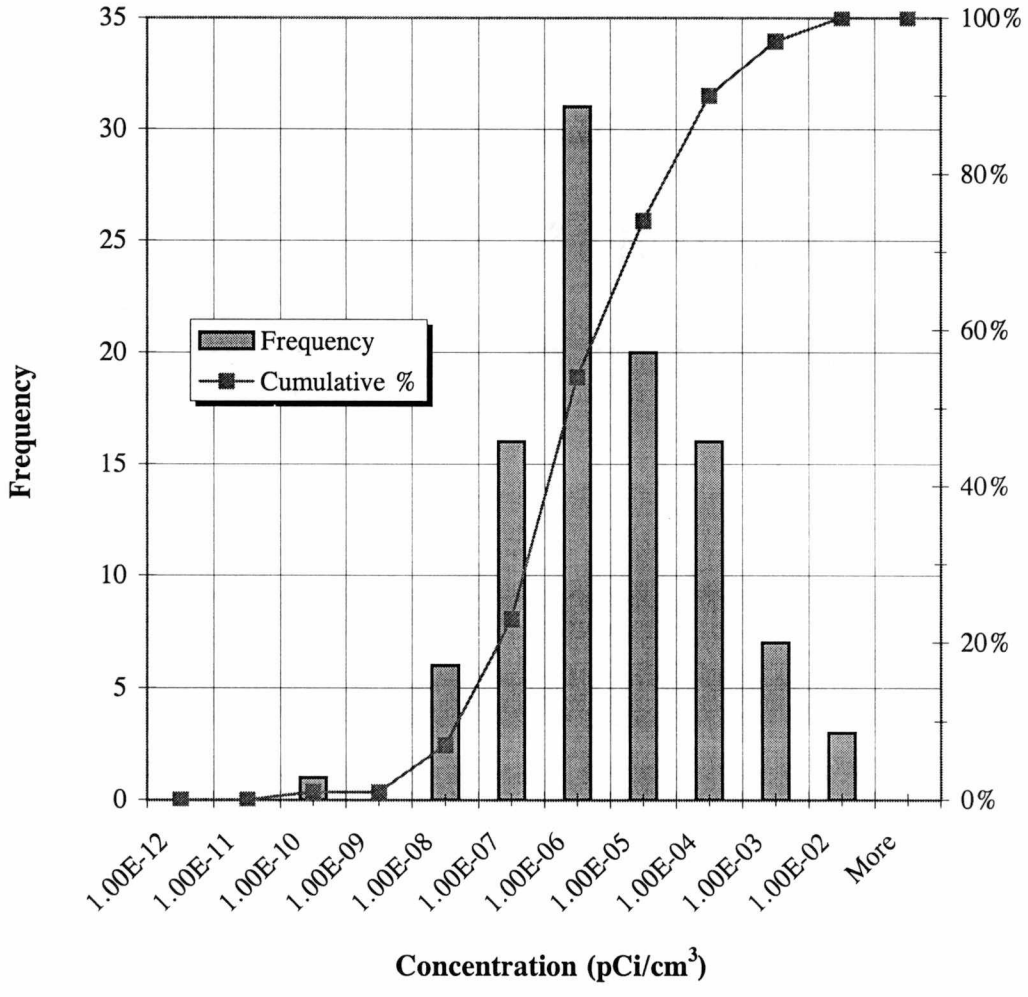


Figure 5.6 Frequency and cumulative distributions of the propagated concentrations through the DUST and FTWORK after 50 years from the release time

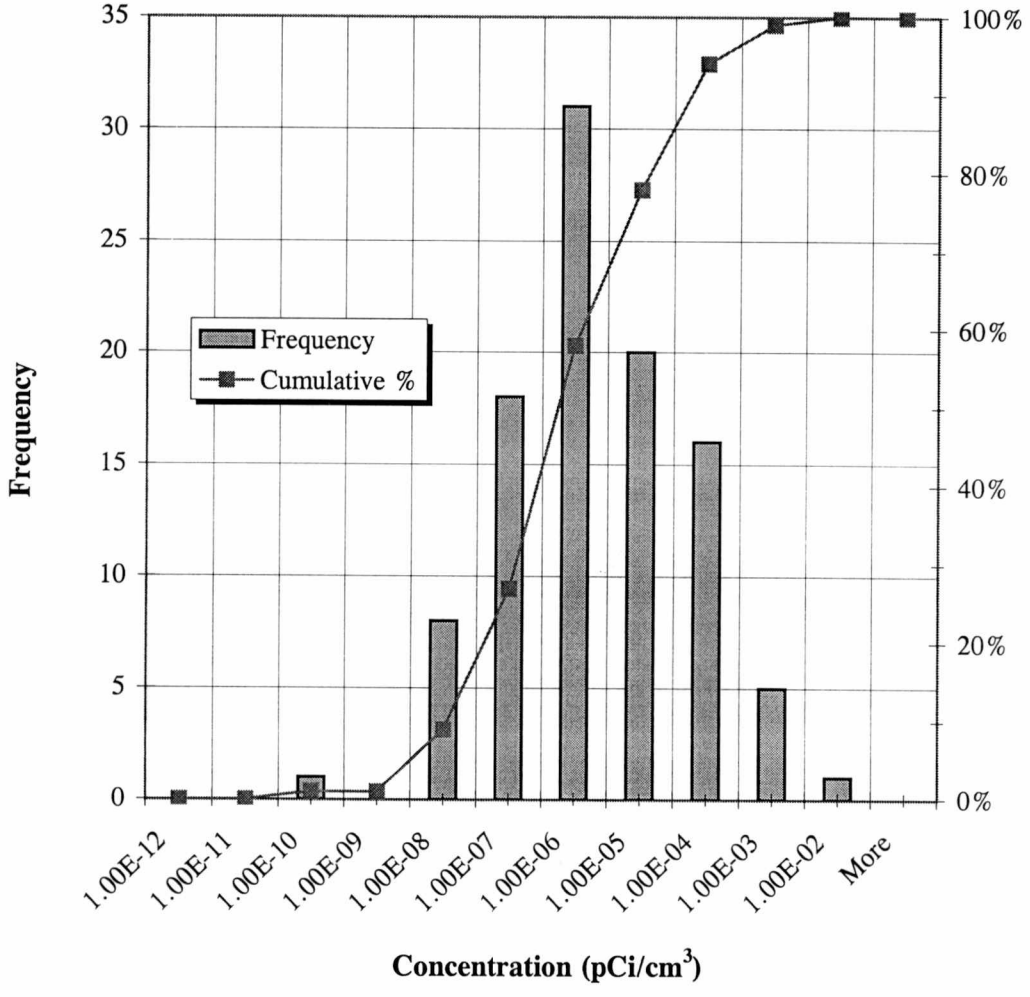


Figure 5.7 Frequency and cumulative distributions of the propagated concentrations through the DUST and FTWORK after 100 years from the release time

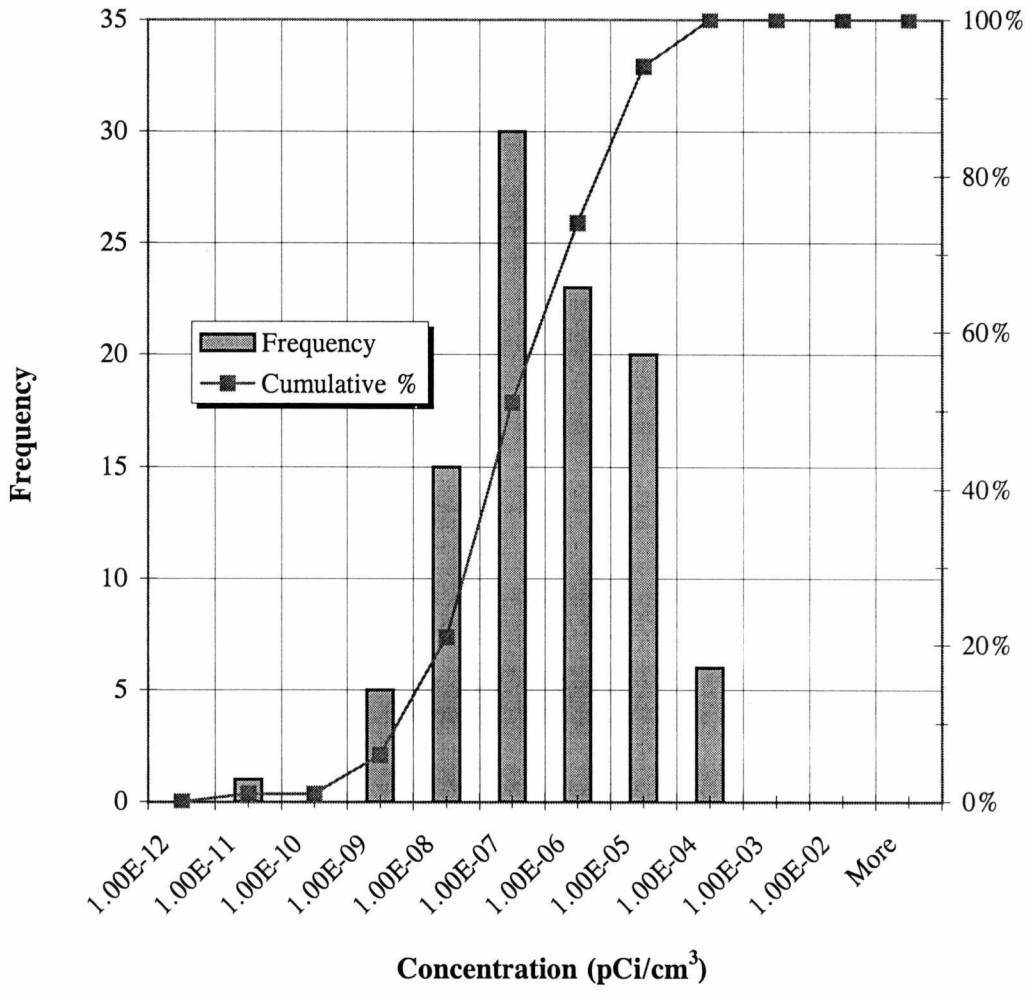


Figure 5.8 Frequency and cumulative distributions of the propagated concentrations through the DUST and FTWORK after 200 years from the release time

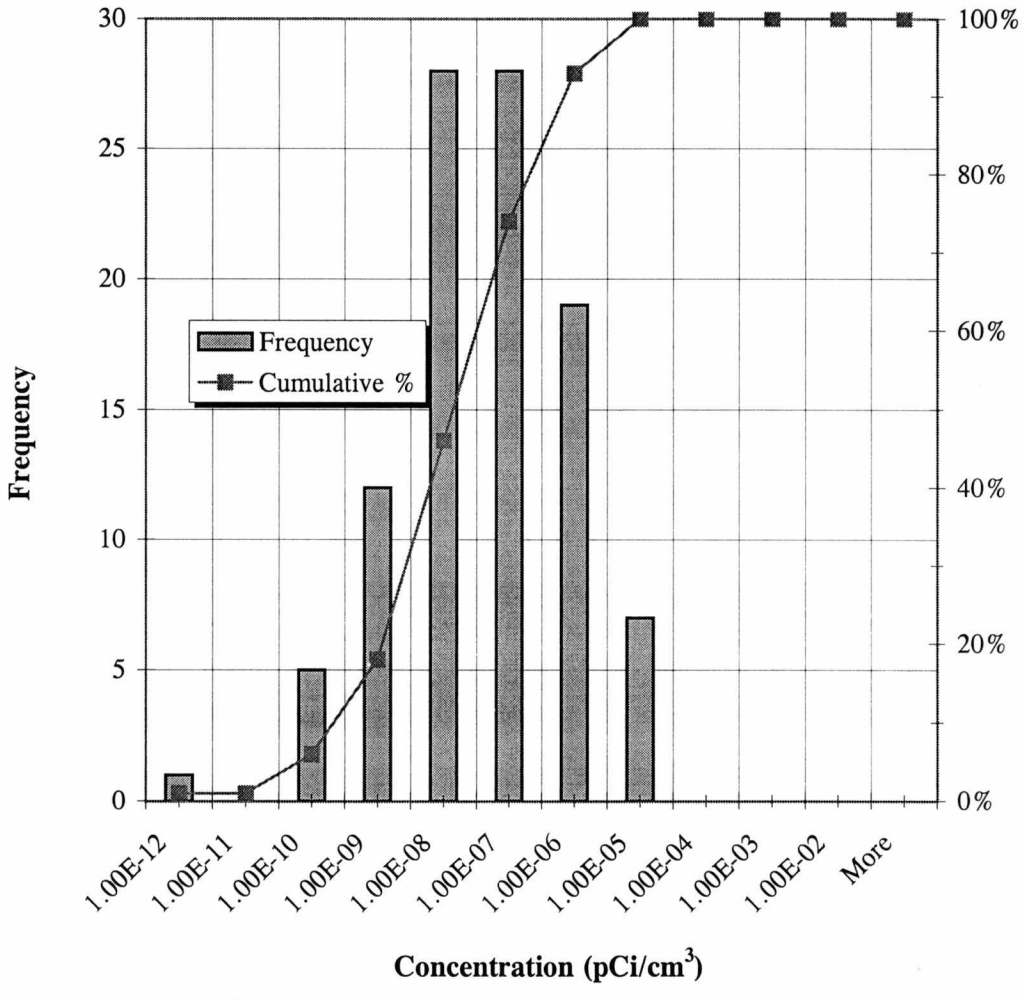


Figure 5.9 Frequency and cumulative distributions of the propagated concentrations through the DUST and FTWORK after 300 years from the release time

Table 5.3 Statistical description of the estimated concentrations of ^{90}Sr in groundwater (pCi/cm^3) using the traditional approach of propagating uncertainty for different time intervals

Time (Years)	*30*	*50*	*100*	*200*	*300*
Mean	1.21E-04	9.37E-05	3.42E-05	3.27E-06	2.72E-07
Median	7.05E-07	7.77E-07	4.89E-07	8.90E-08	1.19E-08
Standard Deviation	6.29E-04	4.30E-04	1.44E-04	1.19E-05	8.98E-07
Sample Variance	3.96E-07	1.85E-07	2.09E-08	1.42E-10	8.07E-13
Kurtosis	4.99E+01	3.59E+01	4.56E+01	3.91E+01	3.53E+01
Skewness	6.86E+00	5.93E+00	6.41E+00	5.95E+00	5.66E+00
Minimum	5.24E-11	5.67E-11	3.55E-11	6.61E-12	9.11E-13
Maximum	5.22E-03	3.01E-03	1.19E-03	9.28E-05	6.72E-06
90.0%-tile	8.03E-05	8.20E-05	4.25E-05	5.34E-06	5.50E-07
95.0%-tile	2.90E-04	2.80E-04	1.32E-04	1.42E-05	1.10E-06
97.5%-tile	9.95E-04	9.52E-04	3.37E-04	2.45E-05	2.02E-06
99.0%-tile	3.23E-03	2.73E-03	6.57E-04	6.46E-05	5.19E-06

Figures 5.10 through 5.14 demonstrates the statistical distributions of the convolution approach to estimate the concentration at the first point of interest for the selected time intervals. Table 5.4 summarizes the statistical information of the convolution integral predictions at the first point of interest for the selected time intervals.

Figure 5.15 demonstrates the groundwater and surface water predictions for the same release scenario on two different scales. The groundwater at the first point and the surface water at the second point peaked at the same time(i.e., after 50 years from the release time).

Figures 5.16 through 5.20 demonstrates the statistical distributions of the convolution approach to estimate the concentration at the second point of interest for the same time intervals. Table 5.5 summarizes the statistical information of the Multiple Convolution Integral predictions at the second point of interest for the same time intervals.

Figures 5.21 through 5.25 demonstrates the statistical distributions of the risk estimate from the ingestion of surface water at the second point of interest for the same selected time intervals. Table 5.6 summarizes the statistical information of risk predictions at the second point of interest for the selected time intervals. Also, table 5.6 presents the sensitivities of the risk model parameters for all times of interest.

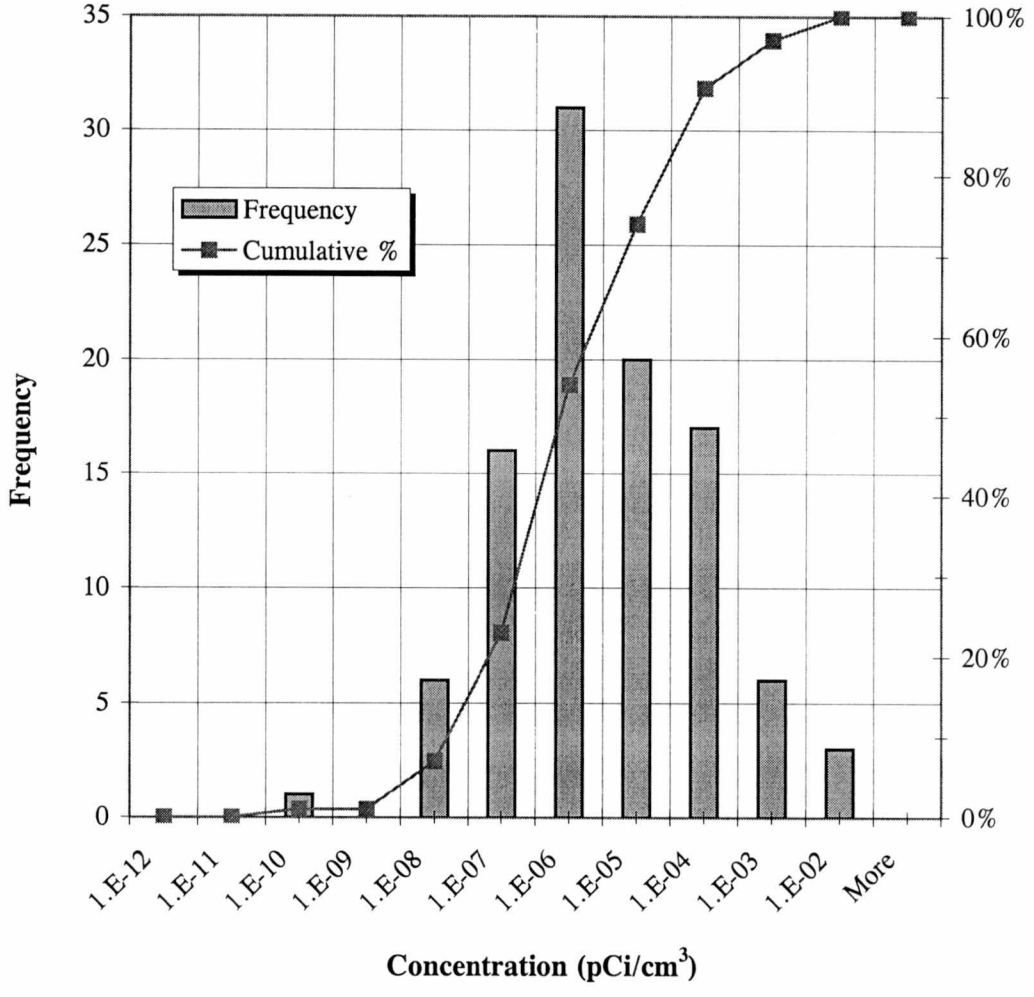


Figure 5.10 Frequency and cumulative distributions of the convoluted concentrations of the DUST and FTWORK predictions after 30 years from the release time

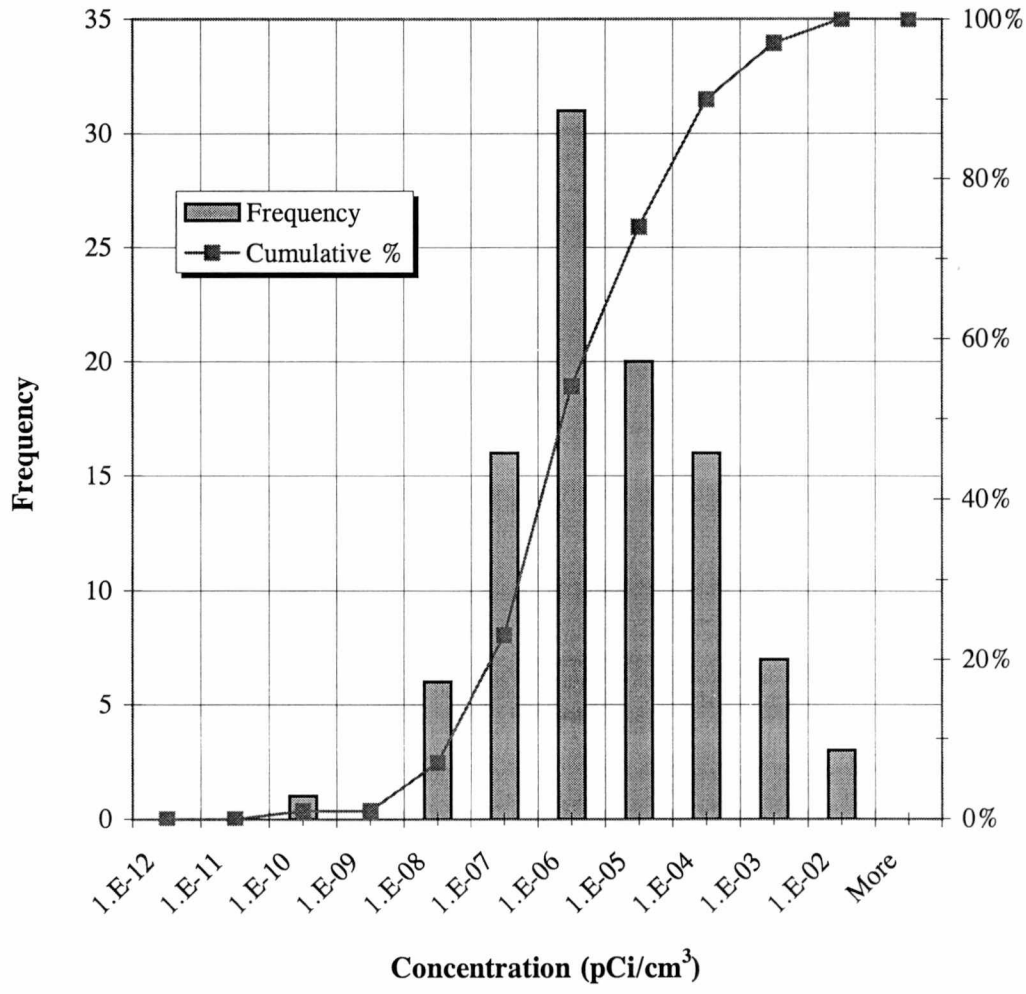


Figure 5.11 Frequency and cumulative distributions of the convoluted concentrations of the DUST and FTWORK predictions after 50 years from the release time

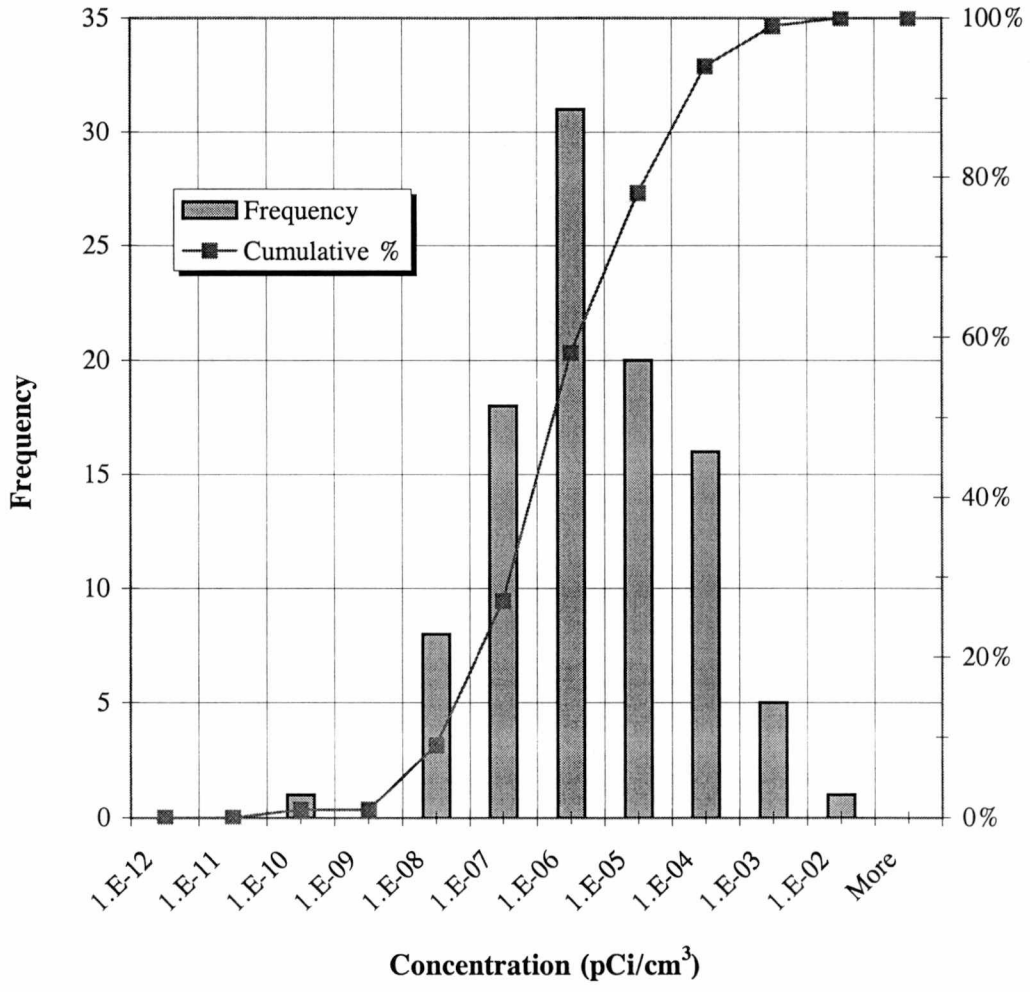


Figure 5.12 Frequency and cumulative distributions of the convoluted concentrations of the DUST and FTWORK predictions after 100 years from the release time

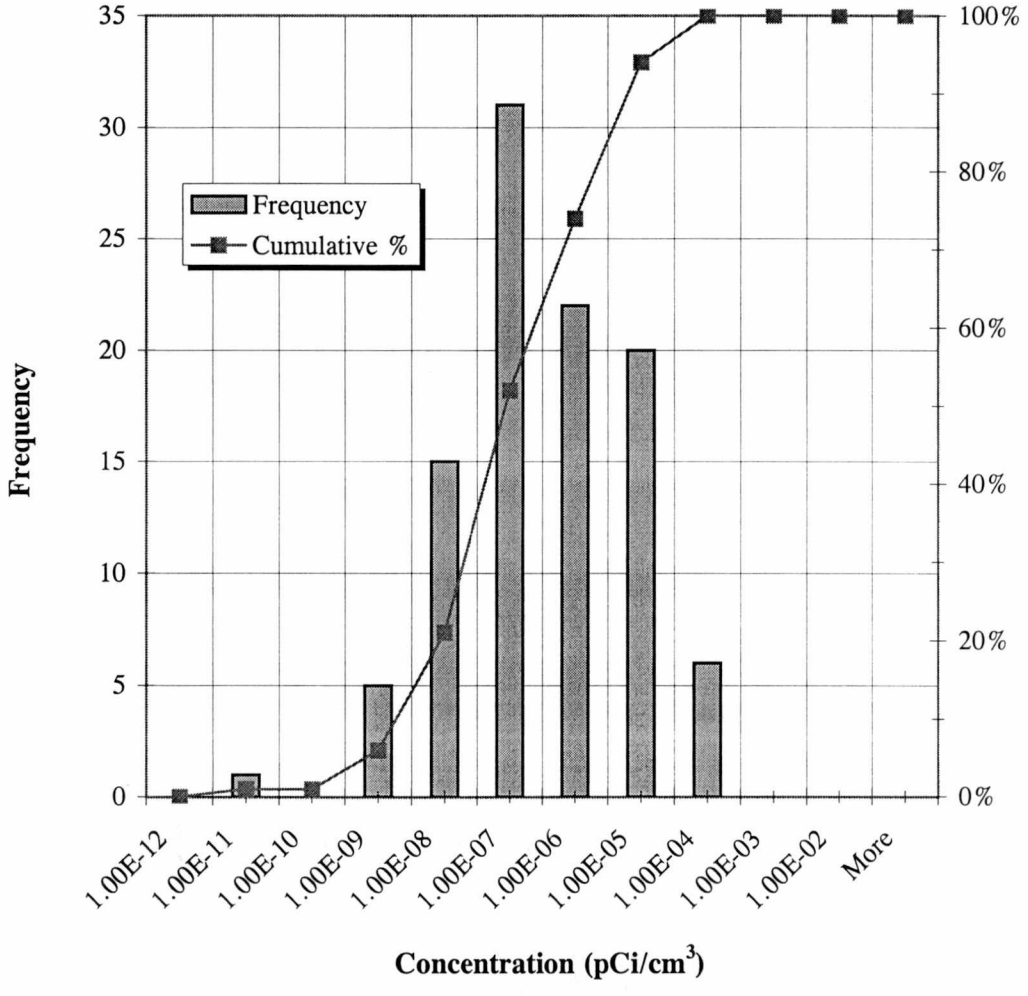


Figure 5.13 Frequency and cumulative distributions of the convoluted concentrations of the DUST and FTWORK predictions after 200 years from the release time

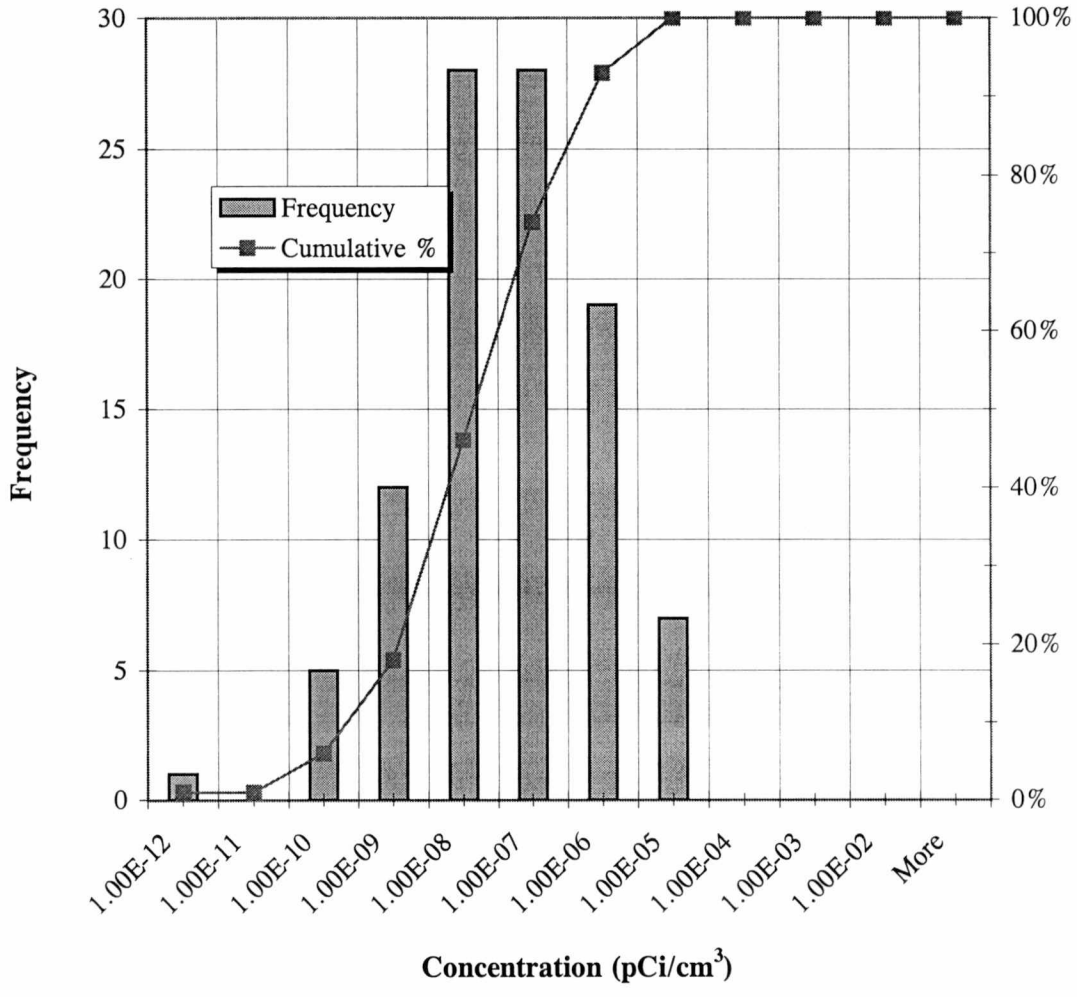


Figure 5.14 Frequency and cumulative distributions of the convoluted concentrations of the DUST and FTWORK predictions after 300 years from the release time

Table 5.4 Statistical description of the estimated concentrations of ^{90}Sr in groundwater (pCi/cm^3) using the convolution approach of propagating uncertainty for different time intervals

Time (Years)	*30*	*50*	*100*	*200*	*300*
Mean	1.25E-04	9.37E-05	3.34E-05	3.09E-06	2.57E-07
Median	7.56E-07	7.92E-07	4.78E-07	8.52E-08	1.13E-08
Standard Deviation	6.42E-04	4.30E-04	1.41E-04	1.13E-05	8.24E-07
Sample Variance	4.13E-07	1.85E-07	1.98E-08	1.27E-10	6.79E-13
Kurtosis	4.69E+01	3.63E+01	4.54E+01	3.95E+01	3.24E+01
Skewness	6.68E+00	5.96E+00	6.39E+00	5.99E+00	5.43E+00
Minimum	5.41E-11	5.71E-11	3.50E-11	6.43E-12	8.81E-13
Maximum	5.18E-03	3.06E-03	1.16E-03	8.77E-05	5.91E-06
90.0%-tile	8.48E-05	8.24E-05	4.13E-05	5.14E-06	5.34E-07
95.0%-tile	2.97E-04	2.82E-04	1.32E-04	1.43E-05	1.07E-06
97.5%-tile	1.03E-03	9.50E-04	3.28E-04	2.22E-05	1.97E-06
99.0%-tile	3.52E-03	2.67E-03	6.40E-04	6.25E-05	4.95E-06

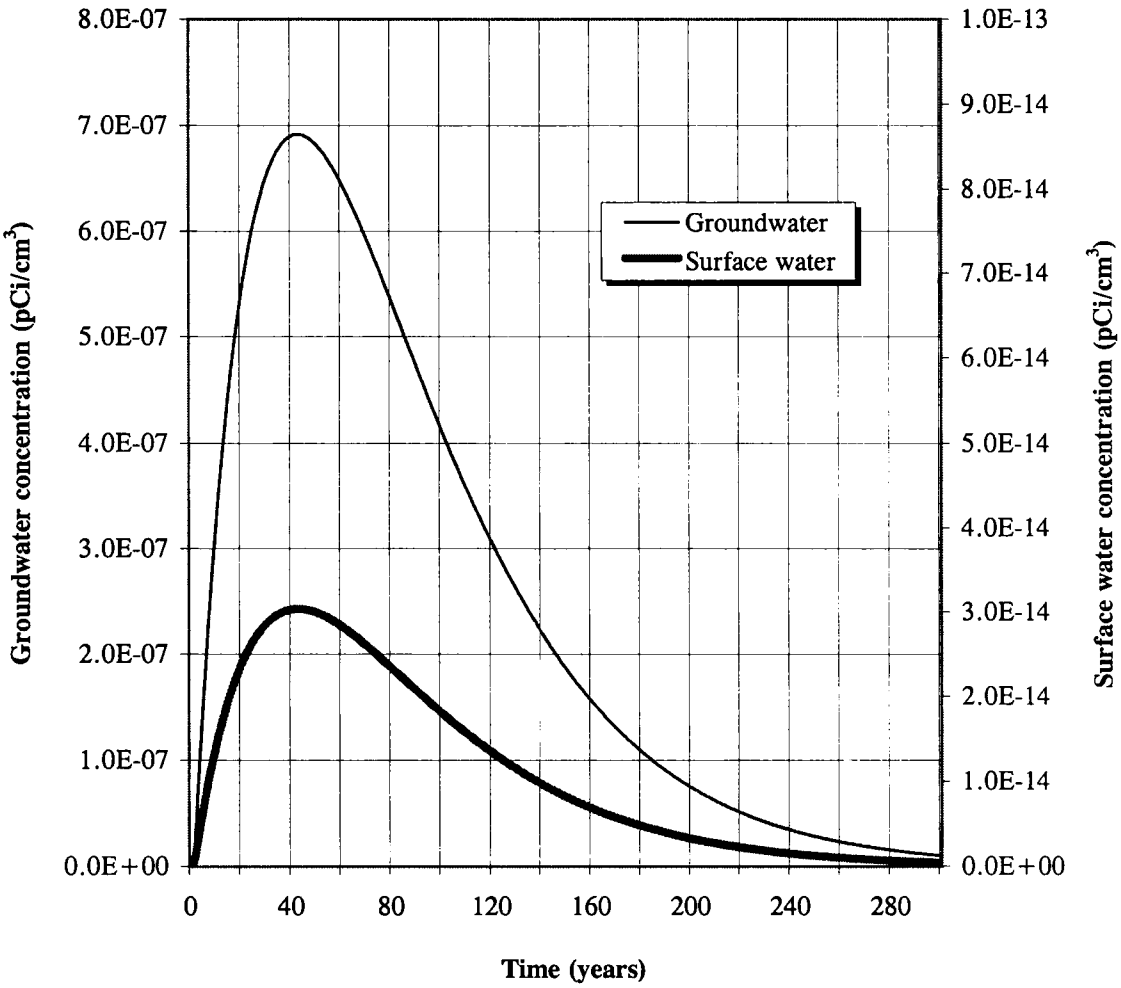


Figure 5.15 Groundwater and surface water predictions on two different scales versus time for the same release scenario

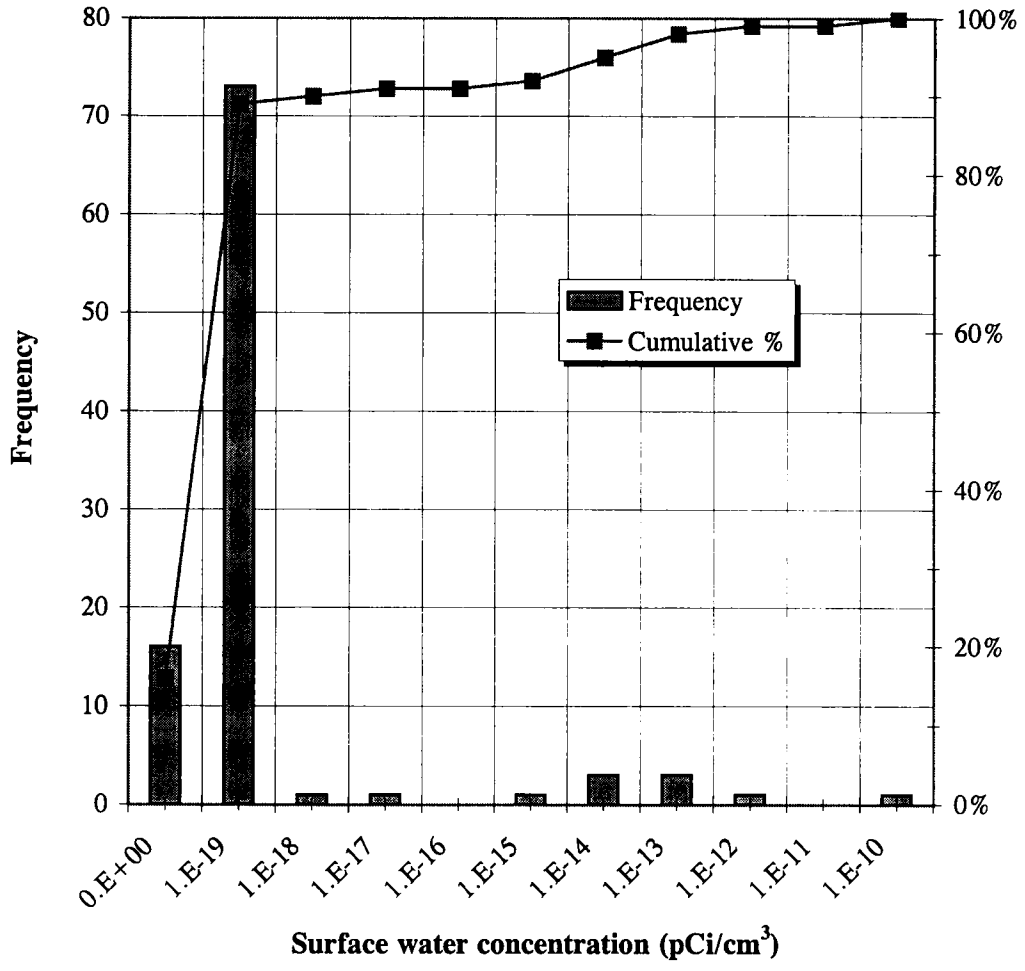


Figure 5.16 Frequency and cumulative distributions of the Multiple Convolution Integral of the DUST, FTWORK, and surface water responses after 30 years from the release time

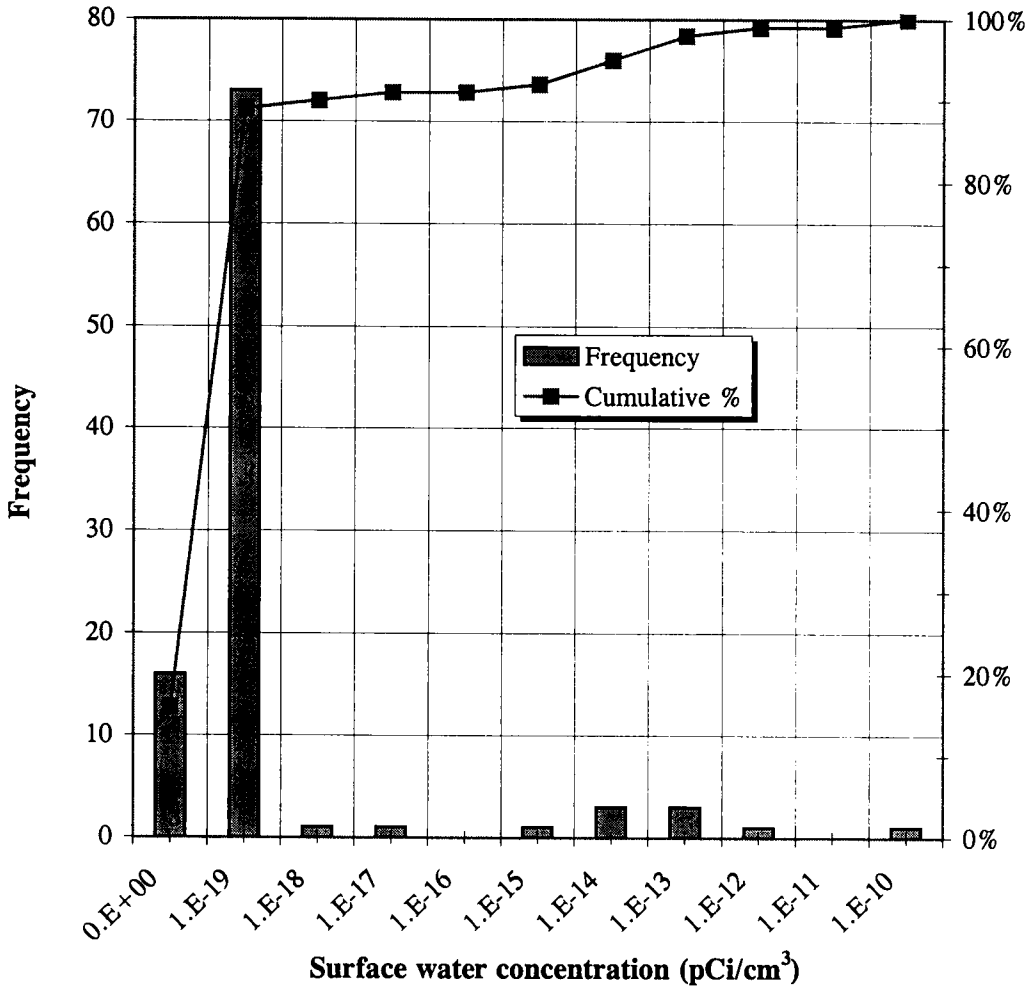


Figure 5.17 Frequency and cumulative distributions of the Multiple Convolution Integral of the DUST, FTWORK, and surface water responses after 50 years from the release time

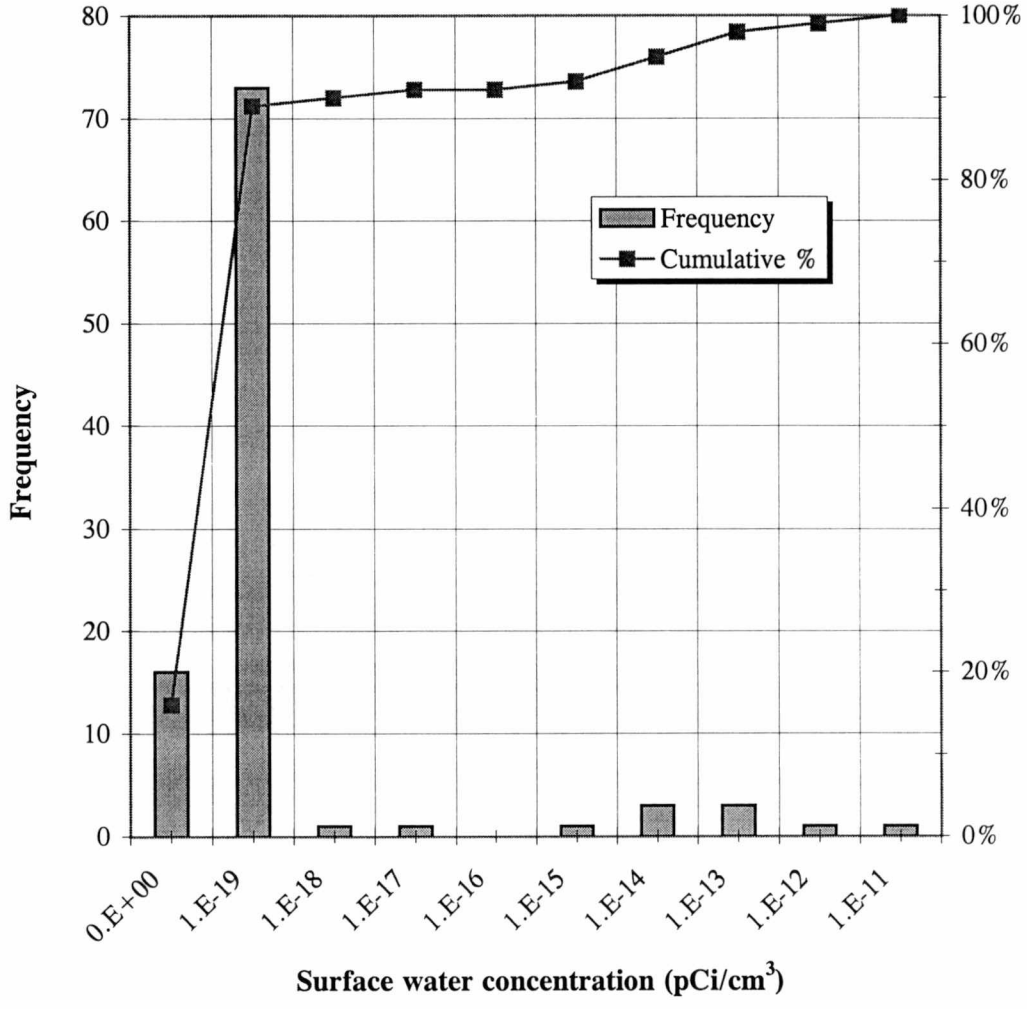


Figure 5.18 Frequency and cumulative distributions of the Multiple Convolution Integral of the DUST, FTWORK, and surface water responses after 100 years from the release time

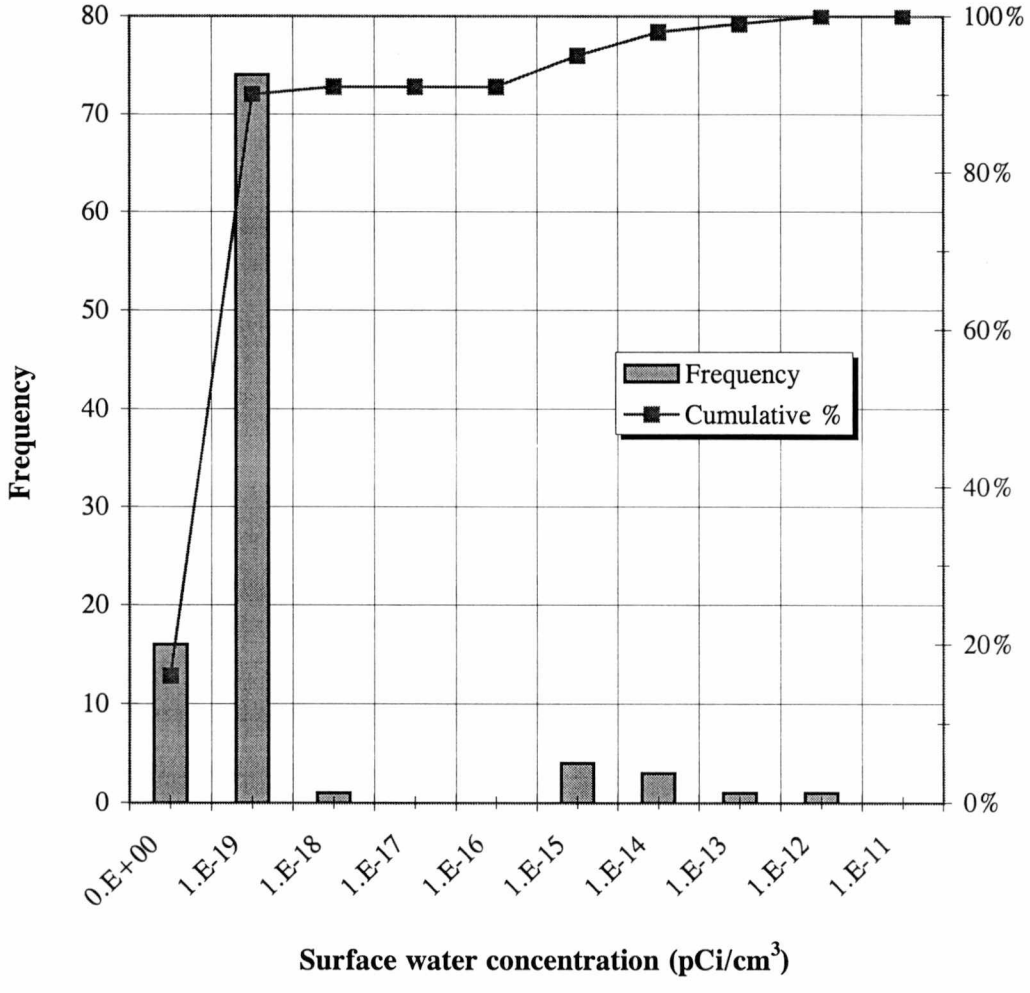


Figure 5.19 Frequency and cumulative distributions of the Multiple Convolution Integral of the DUST, FTWORK, and surface water responses after 200 years from the release time

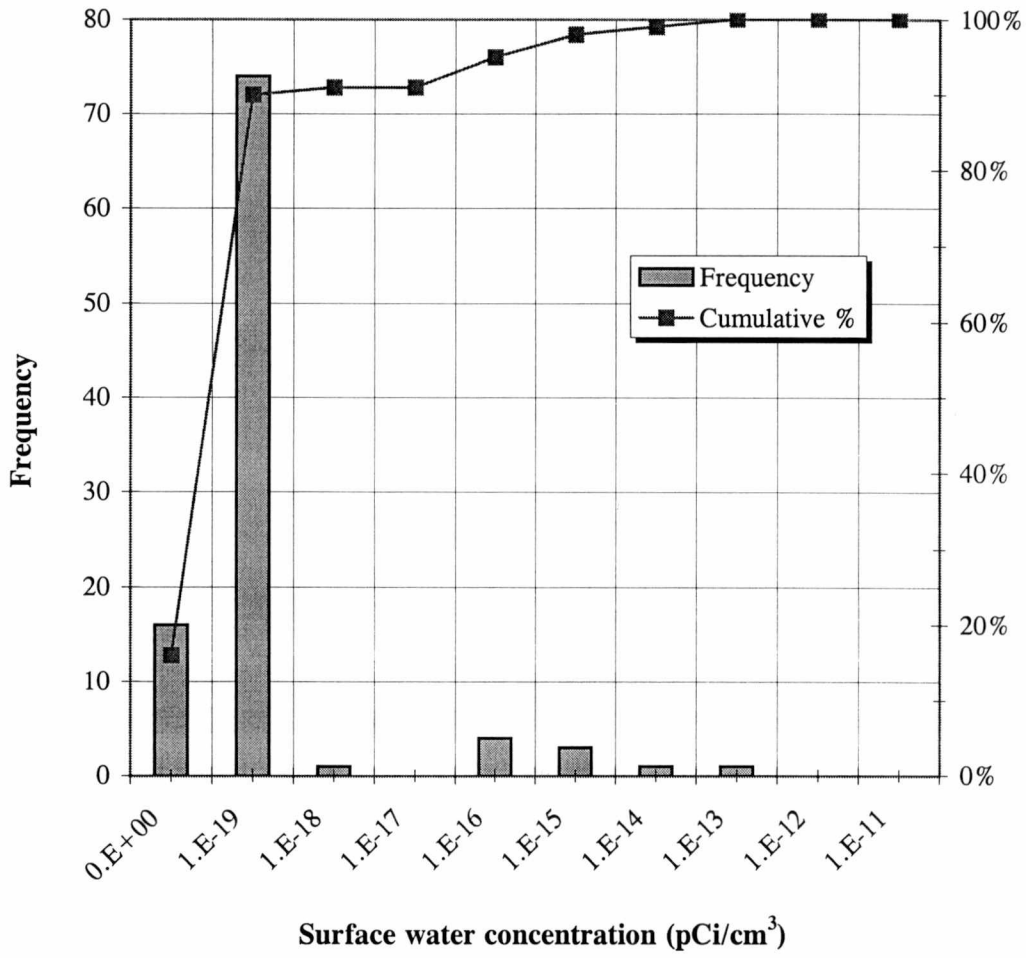


Figure 5.20 Frequency and cumulative distributions of the Multiple Convolution Integral of the DUST, FTWORK, and surface water responses after 300 years from the release time

Table 5.5 Statistical description of the estimated concentrations of ^{90}Sr in surface water (pCi/cm^3) using the Multiple Convolution Integral approach of propagating uncertainty for different time intervals

Time (Years)	*30*	*50*	*100*	*200*	*300*
Mean	1.77E-13	1.68E-13	7.91E-14	8.63E-15	7.26E-16
Median	0.00E+00	0.00E+00	0.00E+00	0.00E+00	0.00E+00
Standard Deviation	1.71E-12	1.63E-12	7.62E-13	8.24E-14	6.84E-15
Variance	2.93E-24	2.64E-24	5.81E-25	6.78E-27	4.68E-29
Kurtosis	9.99E+01	9.99E+01	9.99E+01	9.98E+01	9.98E+01
Skewness	9.99E+00	9.99E+00	9.99E+00	9.99E+00	9.98E+00
Minimum	0.00E+00	0.00E+00	0.00E+00	0.00E+00	0.00E+00
Maximum	1.71E-11	1.63E-11	7.62E-12	8.24E-13	6.84E-14
90.0%-tile	6.38E-18	6.72E-18	2.76E-19	5.01E-20	6.80E-21
95.0%-tile	2.85E-14	2.99E-14	2.48E-15	4.48E-16	6.03E-17
97.5%-tile	6.39E-14	6.61E-14	3.76E-14	6.43E-15	8.21E-16
99.0%-tile	3.93E-13	3.79E-13	1.86E-13	2.18E-14	1.96E-15

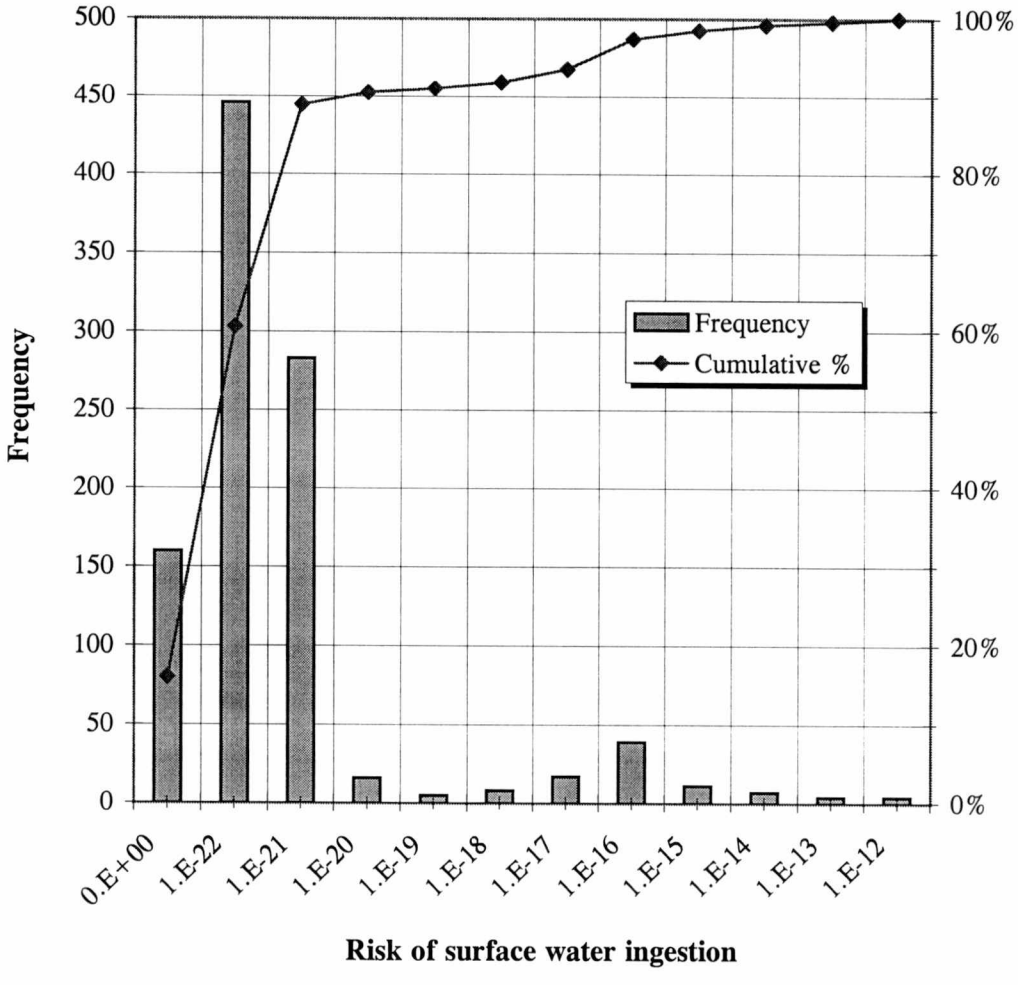


Figure 5.21 Frequency and cumulative distributions of the estimated risk from the ingestion of the modeled surface water concentrations after 30 years from the release time

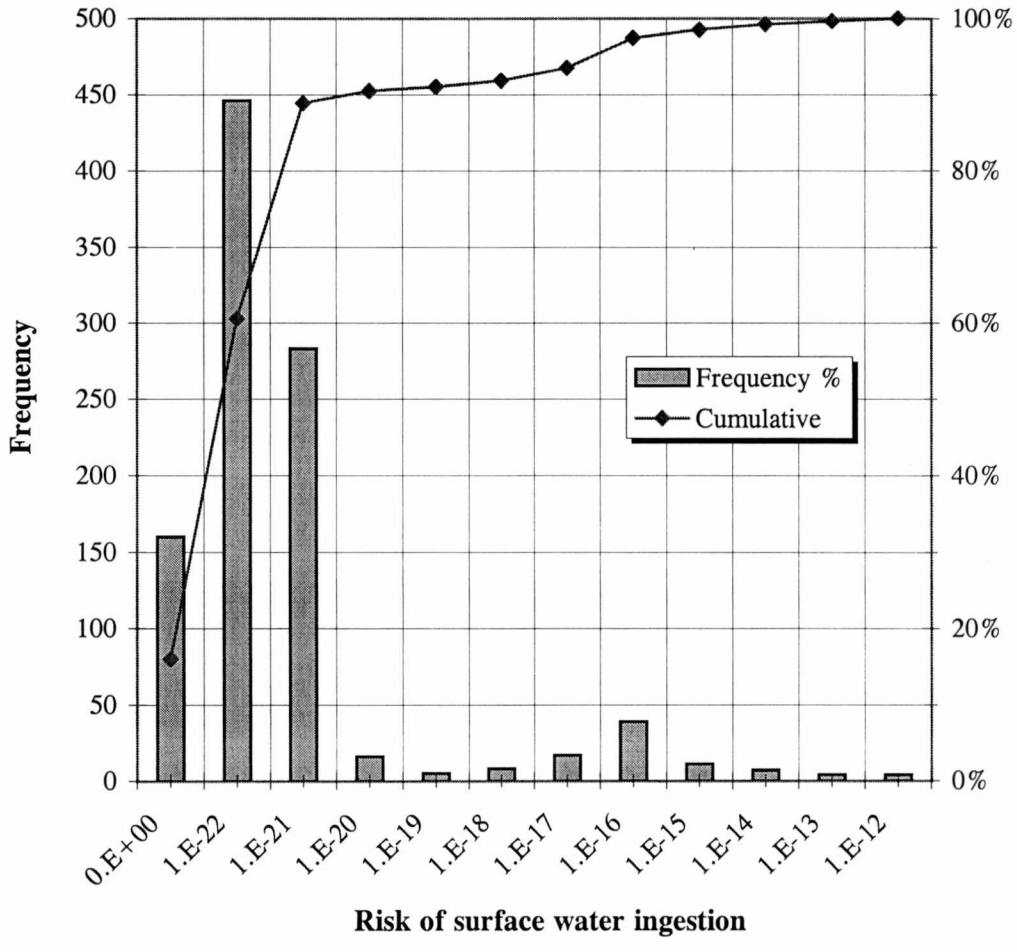


Figure 5.22 Frequency and cumulative distributions of the estimated risk from the ingestion of the modeled surface water concentrations after 50 years from the release time

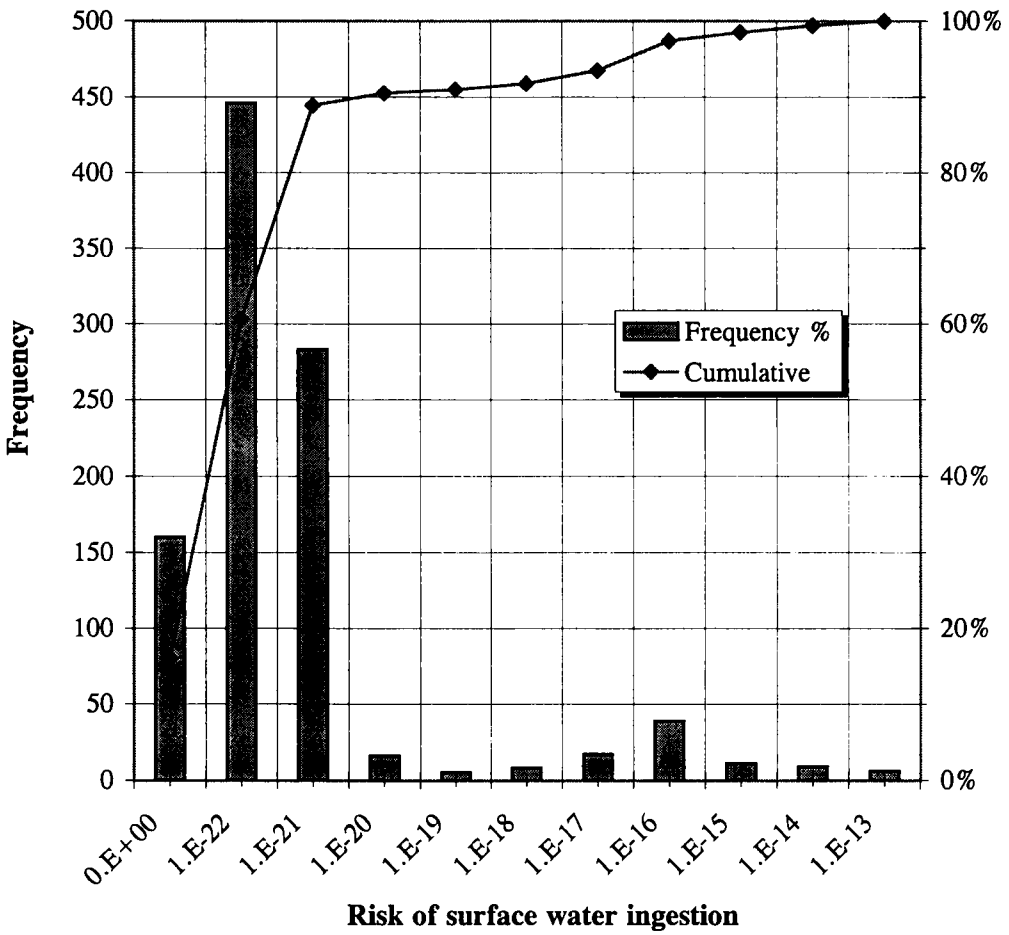


Figure 5.23 Frequency and cumulative distributions of the estimated risk from the ingestion of the modeled surface water concentrations after 100 years from the release time

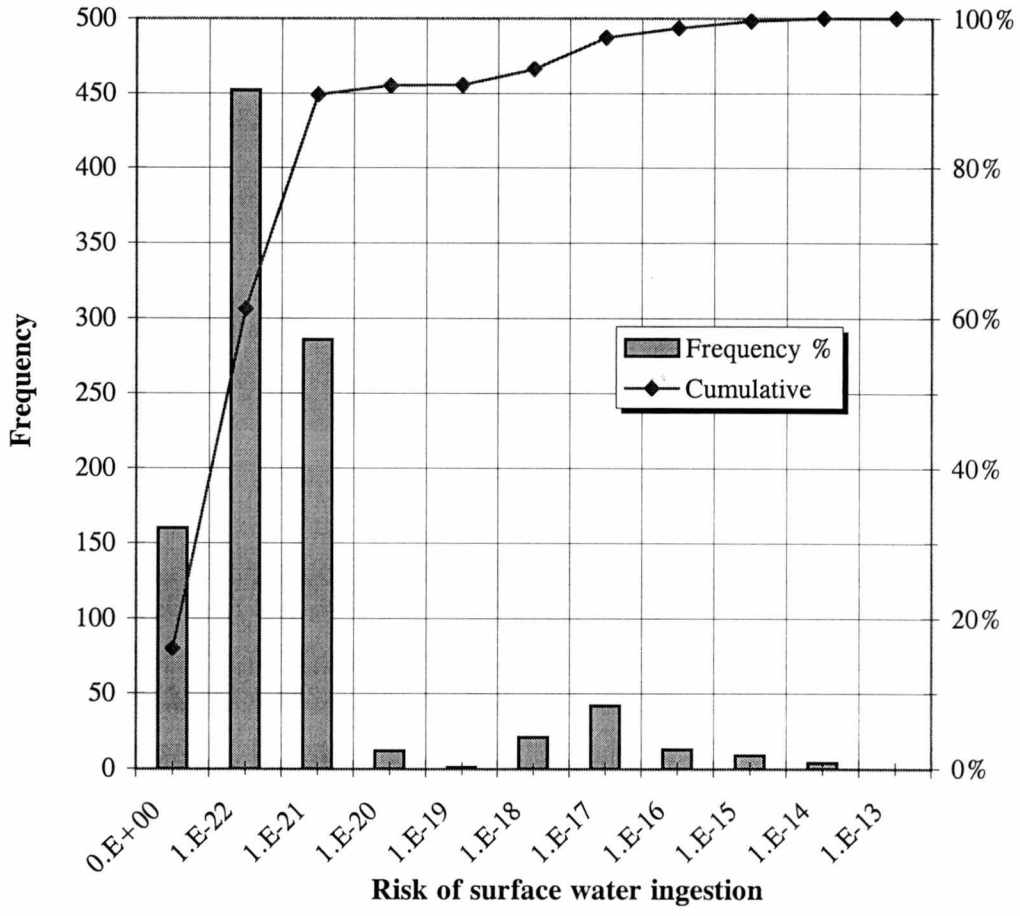


Figure 5.24 Frequency and cumulative distributions of the estimated risk from the ingestion of the modeled surface water concentrations after 200 years from the release time

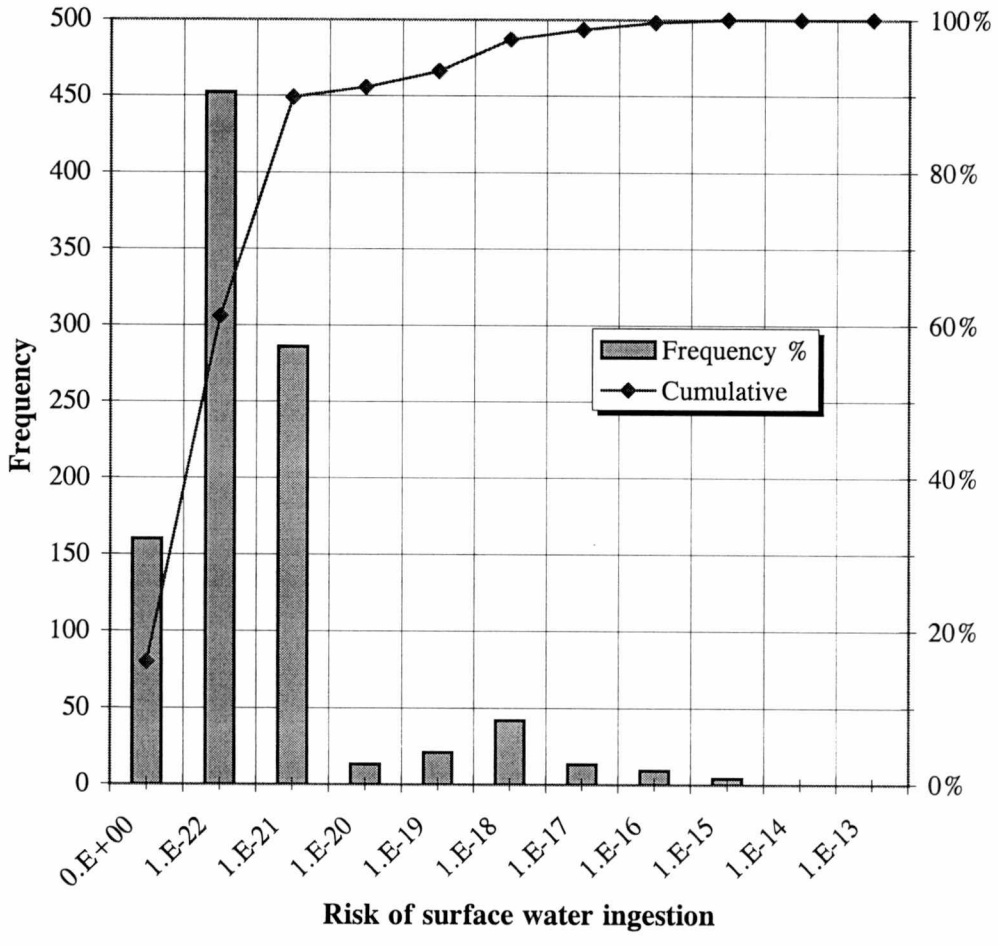


Figure 5.25 Frequency and cumulative distributions of the estimated risk from the ingestion of the modeled surface water concentrations after 300 years from the release time

Table 5.6 Statistical description of the estimated risks from the ingestion of ^{90}Sr in surface water using the Multiple Convolution Integral approach estimates of the concentration for different time intervals

Time (Years)	*30*	*50*	*100*	*200*	*300*
Statistics					
Mean	8.76E-16	8.76E-16	1.04E-16	1.04E-17	1.04E-18
Median	6.46E-23	6.46E-23	6.46E-23	6.38E-23	6.38E-23
Standard Deviation	1.08E-14	1.08E-14	1.10E-15	1.10E-16	1.10E-17
Variance	1.17E-28	1.17E-28	1.21E-30	1.21E-32	1.21E-34
Kurtosis	2.11E+02	2.11E+02	1.96E+02	1.96E+02	1.97E+02
Skewness	1.42E+01	1.42E+01	1.35E+01	1.35E+01	1.35E+01
Minimum	0.00E+00	0.00E+00	0.00E+00	0.00E+00	0.00E+00
Maximum	1.75E-13	1.75E-13	1.75E-14	1.75E-15	1.75E-16
90.0%-tile	2.46E-21	2.46E-21	2.46E-21	1.10E-21	1.10E-21
95.0%-tile	2.56E-17	2.56E-17	2.56E-17	2.56E-18	2.56E-19
97.5%-tile	1.04E-16	1.04E-16	1.04E-16	1.04E-17	1.04E-18
99.0%-tile	4.30E-15	2.92E-15	1.11E-15	1.11E-16	1.11E-17
Risk Sensitive Parameters					
Csw	57.0%	57.0%	57.0%	55.0%	55.0%
ED	46.0%	46.0%	46.0%	47.0%	47.0%
EF	18.0%	18.0%	18.0%	19.0%	19.0%
IR	6.0%	6.0%	6.0%	6.0%	6.0%

5.9 DISCUSSION

The results presented in Fig. 5.4 show that the convolution of the impulse responses of the DUST predictions with the FTWORK predictions are within ±5% of the standard step-by-step solution. Therefore, the propagation of uncertainties of the randomly distributed parameters through the coupled system using the MCI approach (i.e., Algorithm 2) are expected to yield similar model predictions to those obtained by the traditional propagation of uncertainty through the coupled model (i.e., Algorithm 1).

Although the predictions of the two approaches are in agreement, it is observed in this work, that on a Pentuim-200 PC the processor time used by the MCI approach was at least half (subject to the constraints inherent in the combinations of the random sample sets of the uncertain parameters) of the processor time used by the standard step-by-step approach. This is because the later approach requires the solution of a transient groundwater model, in which the solution takes longer to converge compared to the steady state solution used in the former approach. In this application(i.e, for the 16x100-tuples sample sets), the processor time used by the MCI propagation process is 5.7 hours and the corresponding time used by the traditional approach is 13.5 hours.

Comparisons of Figures. 5.5 though 5.9 and 5.10 through 5.14 for the different time intervals show that the propagated uncertainties through the standard step-by-step solution of the coupled system are in agreement with those of the MCI Approach for all time intervals. The statistical results presented in Tables 5.3 and 5.4 show an agreement range of ±1 to ±12% for all descriptive statistical values(i.e., mean, median, standard deviation, Kurtosis, skewness, minimum, maximum, and all right tail fractiles). Also, the results show a wide range of variation between the minimum and maximum predictions indicating highly uncertain predictions. However, since regulatory decisions are based on a comparison of specific right tail fractiles (to maintain highly conservative estimates of risk), special attention is given to the right tail predictions (i.e., , 90, 95, 97.5, and 99%-tiles). It can be seen from the results that even right tail predictions are varying over two orders of magnitude for the first 100 years of simulation time, and over 1 order of magnitude after 200 years. This result is expected since probabilities of higher concentrations are reduced with time due to retardation, dispersion, and radioactive decay effects.

Comparison of the groundwater predictions at the first point of interest with the surface water predictions at the second point of interest (see Fig. 5.15)show that the two peaks occur at the same time, as expected, with a reduction of more than seven orders of magnitude in surface water

concentration due to the transport and dispersion effects of the running stream.

Figures 5.16 through 5.20 show uncertainty in the final predicted concentration at the second point of interest with a range of variation of at least five orders of magnitude over the right tail fractiles. For example, the 90, 95, 97, and 99-tiles of the surface water concentrations after 30 years of simulation are 6.38E-18, 2.85E-14, 6.39E-14, and 3.93E-13, respectively. Refer to Table 5.5 for concentration fractile information of all other time intervals.

Figures 5.21 through 5.25 show uncertainties in the final risk estimates resulting from the ingestion of surface water at the second point of interest. The range of variation of the right tail fractiles are over six orders of magnitude, also. For example the 90, 95, 97, and 99-tiles of the surface water risk estimates after 30 years are 2.46E-21, 2.56E-17, 1.04E-16, and 4.30E-15, respectively (refer to Table 5.6 for risk fractile information of all other time intervals).

In addition, Table 5.6 shows that uncertainties in the final risk predictions are attributed to the uncertainties of the modeled concentrations(55-57%)and exposure duration(46-47%)at all times. The sensitivity of the ingestion rate is found to be 18-19%. The sensitivity of the exposure frequency did not exceed 6% at any simulation time. Therefore, uncertainty in the final risk prediction are mainly attributed to uncertainties inherent in the modeling parameters of the

propagated concentration, and the exposure duration yielding several orders of magnitude of variation over the right tail fractile estimates.

Note that the risk estimates presented in Table 5.6 are independent of time for the first 100 years. The risk-time relationship becomes apparent at 200 and 300 years with one and two orders of magnitude reduction in the risk estimates over the last 200 years. Therefore, if regulatory decision is based on a particular risk-fractile estimate (say the 95%-tile), the clean up goal will be the same for the first 100 years. However, if decision is based on risk estimates after 200 and 300 years contributions, the clean up goal will increase by one and two orders of magnitude, respectively. Therefore, a combination of a time-dependent risk estimate with the use of the actual fractile (say the 95%) estimate will reflect several orders of magnitude in the clean up action level.

The above findings demonstrates that while the above time-dependent risk estimates are highly uncertain, the resulting level of confidence that human health has been protected is only slightly increased (4 to 9% between the 90 and 99, and 95 and 99 fractiles, respectively). In terms of cost, this slight increase in protection will yield huge remediation costs, and will reflect poor management decisions.

CHAPTER 6

CONCLUSIONS

Probabilistic risk analysis are usually avoided in the assessment of human risk from exposure to time-dependent releases of radioactive contamination through sequentially coupled transport submodels. This is because of the limitations of the traditional approach of propagating uncertainty through inter-dependent submodels and the lack of a practical tool for linking fate and transport components together in a fashion that easily facilitates uncertainty analysis.

In this research, we have demonstrated the importance of propagating uncertainty analysis through sequentially coupled fate and transport systems to estimate uncertainty in the final risk predictions. We also demonstrated the significance of the MCI approach in facilitating an independent propagation of uncertainties through the decoupled submodels. In addition, we demonstrated the decoupling of the fate and transport process and the applicability of the approach on a conceptual model extracted from the Inactive Tanks project at the Oak Ridge National Laboratory at the Oak Ridge National Laboratory.

The presented application of using the MCI approach versus the traditional approach (Chapter 5) demonstrated that

compatibility, configuration, and reproduction limitations are eliminated using the MCI approach. Therefore, in spite of the complexity of the subject application, the MCI proved to be very practical, flexible and convenient tool to use for uncertainty analysis of inter-dependent models. Also, the MCI approach used at most half of the processor time needed by the traditional approach to yield equivalent results.

Comparisons of the results of the two approaches shows that the MCI approach is tractable, accurate, and more efficient than the traditional approach. The computational time savings of using the MCI approach are at least two times more than the traditional approach with the flexibility of repeating the simulations of the decoupled responses that are being altered, as needed, without the need to repeat the whole modeling scheme. Therefore, ultimately the MCI facilitated a decoupled propagation of uncertainty through the individual transport submodels with the minimum involvement level of the professional modeling personnel.

The PDFs of risk resulting from the ingestion of surface water at the second point of interest shows that these risk estimates are highly uncertain. The range of variation of the right tail fractiles, commonly used in regulatory decisions, are over several orders of magnitude. The sensitivity results also, showed that uncertainties in the final risk predictions are mainly attributed to uncertainties inherent in the modeling parameters of the propagated concentration (55-57%

for all times) and the exposure duration parameter (46-47%). The sensitivity of the risk model to uncertainties in the , ingestion rate and exposure frequency are found to be 18-19% and 6%, respectively.

In general, the application presented in this study demonstrates that, uncertainty analysis is a very vital tool in decision analysis. As we said earlier, environmental remediation activities across the DOE complex are generally based on a combination of the Human Health Risk Assessment findings and costs of remediation. Costs of remediation are directly related and often very sensitive to the findings in the risk assessment phase. Protecting human health using conservative estimates of the uncertainty prediction of risk can significantly drive up the cost of the project.

The above results demonstrate that while the variation in the tail of time-dependent risk PDF(the region of interest to regulatory decisions) are large, the resulting confidence level that human health has been protected is only slightly increased (e.g., about 4 to 9% between the 95 and 99, and 90 and 99 fractiles, respectively). In terms of remediation cost, this slight increase yields huge costs, and might reflect poor management decisions. Such finding stresses the importance of uncertainty analysis, particularly, when armed with the MCI approach, it becomes an essential and effective decision tool.

REFERENCES

REFERENCES

Ashwood, T.L. et al. 1986. "An Experimental Approach to Determine Subsurface Leakage from a Surface Impoundment Using a Radioactive Tracer". *Proceedings of the Focus Conference on Southeastern Groundwater Issues, October 6-8, 1986, Tampa, Florida*. National Water Well Association. Dublin, Ohio.

Baes, C.F.III, R.D. Sharp, A.L.Sjoreen, R.W. Shor, 1984. *A Review and Analysis of Parameters for Assessing Transport for Environmentally Released Radionuclides Through Agriculture*, ORNL-5786, Oak Ridge National Laboratory, Oak Ridge, TN.

Binford, F.T. and S.D. Orfi. 1979. *The Intermediate-Level Liquid Waste System at the Oak Ridge National Laboratory - Description and Safety Analysis*. ORNL/TM-6959. Oak Ridge National Laboratory, Oak Ridge, Tennessee.

BNI 1991, *RCRA Facility Investigation Report for Waste Area Grouping 6 at Oak Ridge National Laboratory, Tennessee*, ES/ER-22/V1&D1, ORNL/ER/Sub-87/99053/5/V1, Oak Ridge National Laboratory, Oak Ridge, TN.

Borders, D.M. 1992. D.M. Borders (Oak Ridge National Laboratory), personal communication with Vefa Yucel (Bechtel National, Inc.). Oak Ridge, Tennessee.

Codell R.B., K.T.Key and G. Whelan, 1982. *A Collection of Mathematical Models for Dispersion In Surface Water and Groundwater*. NUREG-0868, U.S. Nuclear Regulatory Commission, Washington, D.C.

Cowgill M.G. and T.M. Sullivan, 1992. *Source Term Evaluation for Low-Level Radioactive Waste Disposal Performance*, NUREG/CR-5911, BNL-NUREG-52334, Brookhaven National Laboratory.

Cowgill M.G. and T.M. Sullivan, 1992a. *Source Term Evaluation for Performance Assessment of LLW Disposal*, WM '92, ed.R.G. Post, Tucson, AZ, 1993.

DOE (Department of Energy) 1992. *Site Characterization Summary Report for Waste Area Grouping 1 at Oak Ridge National Laboratory, Oak Ridge, Tennessee.* DOE/OR-1043/V1&D1. ORNL/ER-131/V1&D1. ORNL/ER/Sub/87-99053/59/V1.

DOE (Department of Energy) 1993. *Waste Characterization Data Manual for the Inactive Liquid Low-Level Waste Tank Systems at Oak Ridge National Laboratory, Oak Ridge, Tennessee.* DOE/OR/01-1159&D1).

DOE (Department of Energy) 1994. *Addendum to the East Fork Poplar Creek–Sewer Line Beltway Remedial Investigation Report*, DOE/OR/02-1119&D2/A1/R1. 1994.

DOE (Department of Energy) 1997. *Performance Assessment for Continuing and Future Operations at Solid Waste Storage Area 6*, Oak Ridge National Laboratory, Oak Ridge, TN.

Faust, C. R., P. N. Sims, C. P. Spalding, and P. F. Anderson. 1990. *FTWORK: Groundwater Flow and Contaminant Transport in Three Dimensions, Version 2.4*, Geotrans, Inc., 250 Exchange Place, Suite A, Herndon, Virginia 22070, June.

Freeze, R. A. and J. A. Cherry. 1979. *Groundwater*, Prentice Hall, Englewood Cliffs, New Jersey.

Gorelick, S. M., R. A. Freeze, D. Donohue, and J. F. Keely. 1993. *Groundwater Contamination: Optimal Capture and Containment*, Lewis Publishers, Boca Raton, Florida.

Gardner, R. H., B. Rojder, and U.Berstrom 1983. PRISM, *A systematic Method for Determining the Effect of Parameter Uncertainties on Model Predictions*, Report NW-83-555, Studsvik Energiteknik AB, Nykoping, Sweden.

Geochemical Parameters for Assessing Subsurface Transport at the Savannah River Plant, DSPT-88-904, DE87-013051, E.I. duPont de Nemours& Co..

Huff, D.D. 1985. *Dry-weather Dye Tracing Investigation - Groundwater Flow Pathways from Line Break.* RAP-85-6. Oak Ridge National Laboratory, Oak Ridge, Tennessee.

ICRP (International Commission on Radiological Protection. 1991. *Recommendations of the International Commission on Radiation Protection.* ICRP Pub. 60. Pergamon Press, Inc. New York, New York.

Israeli, M. and C. B. Nelson. 1992. Distribution and expected time of residence for U.S. Households, *Risk Analysis* 12:65.

Kocher, D.C. 1981. *Radioactive Decay Data Tables.* DOE/TIC-11026. Technical Information Center. U.S. Dept. of Energy.

Lee, R.R., et al. 1989. *Calibration of a Groundwazter Flow and Contaminant Transport Model: Progress Toward Model Validation*, ORNL/TM-11294, Oak Ridge National Laboratory, Oak Ridge, TN.

Logan, K.H., 1939. *Engineering Significance of National Bureau of Standards Soil-Corrosion Data*, Journal of Research of the National Bureau of Standards, Vol.22.

Looney B.B., M.W. Grant, and C.M. King, 1987. *Estimation of* Romanoff, M., 1957. Underground Corrosion, National Bureau of Standards Circular 579.

McKay, M.D, R.J. Beckman and W.J. Conover, 1979. *A comparison of Three Methods for Selecting Values of Input Variables in the Analysis of Output from a Computer Code*, Technometrics, Vol. 68, pp. 322-337

McMaster, W.M. 1967. "Hydrologic Data for the Oak Ridge Area, Tennessee". U.S. Geological Survey Water-Supply Paper 1893-N. Nashville, Tennessee.

Melroy, L. 1986. *3019/3074 Wet Weather Dye Tracer Study.* RAP 86-42. Oak Ridge National Laboratory, Oak Ridge, Tennessee.

Moore, G.K. 1988. *Concepts of Groundwater Occurrence and Flow near Oak Ridge National Laboratory,* Tennessee, ORNL/TM-10969, Oak Ridge National Laboratory, Oak Ridge, TN.

Moore, G.K. 1989. *Groundwater Parameters and Flow Systems near Oak Ridge National Laboratory,* Tennessee, ORNL/TM-11368, Oak Ridge National Laboratory, Oak Ridge, TN.

ORNL 1994, Toxicity Values for Use in Hazardous Waste Risk Assessment and Remediation. Vol. I. ES/ER/TM-76. Biomedical and Environmental Analysis Section, Health Sciences Research Division, Oak Ridge National Laboratory, Oak Ridge, TN.

Robinson, S.M. et al. 1991. *Federal Facility Agreement Contingency, Upgrade and Replacement Plans for the ORNL Active Low-Level Radioactive Waste Tank System.* ORNL/TM-11795. Oak Ridge National Laboratory, Oak Ridge, Tennessee.

Sanders, C.L. 1986. *Toxicological Aspects of Energy Production.* Macmillan Publishing Co. New York, New York.
Smith, roy. 1994. *Use of Monte Carlo Simulation fro Human Exposure Assessment at a Superfund Site,* Risk Analysis, Vol.14, No.4.

Stockdale, P.B. 1951. *Geological Conditions at the ORNL (X-10) Area Relevant to the Disposal of Radioactive Waste.* ORO-58. Oak Ridge, Tennessee.

Stueber, A.M. et al. 1981. *An Investigation of Radioactive Release from Solid Waste Disposal Area 3, Oak Ridge National Laboratory.* ORNL/TM-7323. Oak Ridge National Laboratory, Oak Ridge, Tennessee.

Sullivan T.M. and C.J.Suen, 1988. *Low-Level Waste Source Term Evaluation Quarterly Progress Report*, WM-3276-7, Brookhaven National Laboratory, 1988

Sullivan T.M., 1993. *Disposal Unit Source Term* code, prepared for the U.S. Nuclear Regulatory Commission, NUREG/CR-6041, BNL-NUREG-52375, Brookhaven National Laboratory, 1993.

Sullivan T.M. and C.J.Suen, 1991. *Low-Level Waste Source Term Model Development and Testing*, prepared for the U.S. Nuclear Regulatory Commission, NUREG/CR-5681, BNL-NUREG-52280, Brookhaven National Laboratory, 1991

Turner, J.E. 1986. *Atoms, Radiation, and Radiation Protection*. Pergamon Press, Inc. New York, New York.

United States Environmental Protection Agency (EPA). 1991. *Risk Assessment Guidance for Superfund Volume I: Human Health Evaluation Manual Supplemental Guidance Standard Default Exposure Factors*. OSWER Directive 9285.6-03. Office of Emergency and Remedial Response. Toxics Integration Branch.

Van Genuchten M. T., and W. J. Alves, 1982. *Analytical Solutions of the One-dimensional Convective-Dispersive Solute Transport Equation*. Technical Bulletin No. 1661, U. S. Department of Agriculture.

Whelan G., S. M. Brown, D. L. Strenge, A. P. Schwab and P. J. Mitchel, 1987. *Contaminant Assessment Modeling Under the Resource Conservation and Recovery Act*. EA-5342. Electric Power Research Institute, Palo Alto, California.

APPENDICES

APPENDIX 1

A Matlab Program Propagating The DUST Estimates

Through to The FTWORK

```
%=================================================================
% Executable Matlab File Name: "bfdiss.m" is the standard step-by-step analysis
% This main subroutine will execute DUST, propagate results to FTWORK, then execute
% FTWORK, propagate results to surface water model for the sample size of the
% uncertain parameters and will create a design matrix for the size of the sample
%=================================================================
samplesize=100;
initialtime=365.00;
finaltime=109500.00;
stepsnumber=finaltime/initialtime;
dt=1.0;
n=1:stepsnumber+1;
x1=[1 0 1 0];
x0=[1 0 0 0 1.0];
settime=[initialtime initialtime];
%=================================================
% Read sampled data of the uncertain parameters
%=================================================
fid=fopen('c:\diss\main\pardata.txt','r');
fgetl(fid);
for I=1:samplesize
    kd(I) = str2num(fscanf(fid,'%s',1));
    rho(I) = str2num(fscanf(fid,'%s',1));
    vd(I) = str2num(fscanf(fid,'%s',1));
    theta(I) = str2num(fscanf(fid,'%s',1));
    n1eff(I) = str2num(fscanf(fid,'%s',1));
```

```
    n2eff(I) = str2num(fscanf(fid,'%s',1));
    rr(I) = str2num(fscanf(fid,'%s',1));
    alfal(I) = str2num(fscanf(fid,'%s',1));
    alfat(I) = str2num(fscanf(fid,'%s',1));
end
fclose(fid);
%=========================================================
% Open and load the DUST input file for each random selection of a sample set
%=========================================================
 for I=1:samplesize
    fid=fopen('c:\diss\dusty\dustdiss.inp','r+');
    fseek(fid,0,0);
  for j = 1:12
    fgetl(fid);
  end
  fseek(fid,10,0);
  fprintf(fid,'%10.3E %9.2E',kd(I),rho(I));
  fseek(fid,0,0);
  for j = 1:31
     fgetl(fid);
  end
  fseek(fid,10,0);
  fprintf(fid,'%10.2E %9.2E',vd(I),vd(I));
  fseek(fid,0,0);
  fgetl(fid);
  fseek(fid,31,0);
  fprintf(fid,'%9.2E',theta(I));
  fclose(fid);
%=========================================================
```

```
% Execute the Dust code for sample set I.
%=================================================
cd c:\diss\dusty;
 delete dustest.dat;
 eval('dos dustybat.bat');
 y=0;
 while y==0
   y=exist('dustest.dat');
 end
 DUSTExecutionNumber = I
%=================================================
% Read the time and concentration of the DUST output
% create an array of the DUST predicted concentrations
%=================================================
 fid=fopen('c:\diss\dusty\tracecnd.dat','r');
 cd c:\diss\main;
 fdust(i,n)=readg2(fid,stepsnumber);
 for k=1:stepsnumber
     cs(i,k)=1e12*(fdust(i,k)+fdust(i,k+1))/2;
 end
 fclose(fid);
%=================================================
% Open and load  the FTWORK input file of each  sample set
%=================================================
 fid=fopen('c:\diss\ftwork\var20.dat','r+');
 for j = 1:174
     fgetl(fid);
 end
 fseek(fid,0,0);
```

```
fprintf(fid,'%4.3f %2.1f',n1eff(I),0.0);
fseek(fid,0,0);
fgetl(fid);
fseek(fid,0,0);
fprintf(fid,'%4.3f %2.1f',n2eff(I),0.0);
fseek(fid,0,0);
for j = 1:3
    fgetl(fid);
end
fseek(fid,0,0);
fprintf(fid,'%8.3e %2.1f',rr(I),0.00);
fseek(fid,0,0);
for j = 1:3
    fgetl(fid);
end
fseek(fid,0,0);
fprintf(fid,'%4.3f %4.3f %2.1f',alfal(I),alfat(I),0.00);
fseek(fid,0,0);
for j = 1:2
    fgetl(fid);
end
fseek(fid,0,0);
fprintf(fid,'%10.3e %2.1f %3.2f',kd(I),1.0,rho(I));
fseek(fid,0,0);
for j = 1:1601
 fgetl(fid);
end
cmax=1.0e-1;
if kd(I)>200 cmax= 1e-2;end
```

```
 if kd(I)>700 cmax=1e-3;end
 if kd(I)>1000 cmax=1e-4;end
 fseek(fid,0,0);
 fprintf(fid,'%3.1f\t %3.1f\n', 0,0);
 fprintf(fid,'%9.3e\t %9.3e\n', rr(i),1.0E-10);
 fprintf(fid,'%5.1e\t %5.1e\t %5.1f\t %2.1f\t %9.1f\t',1e-2,1e-2,365.0,1.5,365.0);
 fprintf(fid,'%2d %2d %2d %d %9.1e\n',x1,1.0E+000);
 fprintf(fid,'%3.1f\t %3.1f\n', 0,0);
 fprintf(fid,'%9.3e\t %9.3e\n', rr(i),cs(i,1));
 for k=2:stepsnumber
                    fprintf(fid,'%5.1f\t %5.1f\t %5.1f\t %2.1f\t
%9.1f\t',initialtime*(k-1),365.0,365.0,1,initialtime*(k));
  fprintf(fid,'%2d %2d %2d %d %9.1e\n',x1,1.0E+000);
  fprintf(fid,'%3.1f\t %3.1f\n', 0,0);
%   fprintf(fid,'%9.3e\t %3.1f\n', rr(i),0);
  fprintf(fid,'%9.3e\t %9.3e\n', rr(i),cs(i,k));
 end
 fprintf(fid,'%5.1f\t %5.1f\t %5.1f\t %2.1f\t %9.1f\t',initialtime,settime,1,0);
 fprintf(fid,'%2d %2d %2d %d %3.1f\n',x0);
 for l=1:500
  fprintf(fid,'%200s ', ' ');
 end
 fclose(fid);
%=========================================================
% Execute the FTWORK code for sample i.
%=========================================================
 cd c:\diss\ftwork;
 delete test.obs;
 eval('dos var2bat.bat&');
```

```
 x=0;
 while x==0
     x=exist('test.obs');
 end
 FTWORKExecutionNumber = i
%=========================================================
% Read the time and concentration of the FTWORK output
% Create an array for the FTWORK predicted concentration
%=========================================================
 fid=fopen('c:\diss\ftwork\var20.obs','r');
 cd c:\diss\main;
 [fftwork(i,n),wakat(n)]=readg30(fid,initialtime,finaltime,stepsnumber);
 fclose(fid);
end
%=========================================================
% Open and write to  an output  text file
%=========================================================
fid=fopen('c:\diss\main\bfdiss.txt','w');
for l=1:stepsnumber+1
  fprintf(fid,'%9.3E',time(l));
  fprintf(fid,' ');
  for i=1:samplesize
   fprintf(fid,'%9.3E',fftwork(i,l));
   fprintf(fid,' ');
  end
  fprintf(fid,'\n');
end
fclose(fid);
%=========================================================
```

APPENDIX 2

A Matlab Program Convolving the DUST Estimates

With the FTWORK Estimates

```
%=================================================================
% Executable Matlab File Name: "convdiss.m" is the convolution approach
% This main subroutine will execute DUST, FTWRK, and the analytical Surface water
% models independently for the sample size
% And will create and store 3 design matrices of concentration as a function of time
% The three matrices are convolved using the MCI approach to estimate the final
% concentration
%=================================================================
initialclock=clock;
samplesize=100;
initialtime=365.00;
finaltime=109500.00;
stepsnumber=finaltime/initialtime;
dt=1.0;
n=1:stepsnumber+1;
x1=[1 0 1 0];
x0=[1 0 0 0 1.0];
settime=[initialtime initialtime];

%=================================================================
% Read sampled data of the uncertain parameters
%=================================================================
fid=fopen('c:\diss\main\parameters.txt','r');
fgetl(fid);
```

```
for i=1:samplesize
        kd(i) = str2num(fscanf(fid,'%s',1));
        rho(i) = str2num(fscanf(fid,'%s',1));
        vd(i) = str2num(fscanf(fid,'%s',1));
        theta(i) = str2num(fscanf(fid,'%s',1));
        n1eff(i) = str2num(fscanf(fid,'%s',1));
        n2eff(i) = str2num(fscanf(fid,'%s',1));
        rr(i) = str2num(fscanf(fid,'%s',1));
        alfal(i) = str2num(fscanf(fid,'%s',1));
        alfat(i) = str2num(fscanf(fid,'%s',1));
end
fclose(fid);
%=================================================================
% Open and load the DUST input file for each random selection of a sample set
%=================================================================
for i= 1:samplesize
        fid=fopen('c:\diss\dusty\dustdiss.inp','r+');
        fseek(fid,0,0);
        for j = 1:12
          fgetl(fid);
        end
        fseek(fid,10,0);
        fprintf(fid,'%10.3E %9.2E',kd(i),rho(i));
        fseek(fid,0,0);
        for j = 1:31
          fgetl(fid);
        end
```

```
    fseek(fid,10,0);
    fprintf(fid,'%10.2E %9.2E',vd(i),vd(i));
    fseek(fid,0,0);
    fgetl(fid);
    fseek(fid,31,0);
    fprintf(fid,'%9.2E',theta(i));
    fclose(fid);
%=================================================================
% Execute the Dust code for sample i.
%=================================================================
    cd c:\diss\dusty;
    delete dustest.dat;
    eval('dos dustybat.bat');
    y=0;
    while y==0
        y=exist('dustest.dat');
    end
%=================================================================
% Read the time and concentration of the DUST output and create a design
% matrix of gdust as a function of time
%=================================================================
    fid=fopen('c:\diss\dusty\tracecnd.dat','r');
    cd c:\diss\main;
    [gdust(i,n),time]=readg2(fid,stepsnumber);
    fclose(fid);
end
fid=fopen('c:\diss\main\g1conc.txt','w');
```

```
for l=1:stepsnumber+1
    fprintf(fid,'%8.2E',time(l));
    fprintf(fid,' ');
    for i=1:samplesize
    fprintf(fid,'%9.3E',gdust(i,l));
    fprintf(fid,' ');
end
fprintf(fid,'\n');
end
fclose(fid);
%=========================================================
% Open and load the FTWORK input file for each sample set
%=========================================================
for i=1:samplesize
    fid=fopen('c:\diss\ftwork\unit20.dat','r+');
    for j = 1:174
        fgetl(fid);
    end
    fseek(fid,0,0);
    fprintf(fid,'%4.3f %2.1f',n1eff(i),0.0);
    fseek(fid,0,0);
    fgetl(fid);
    fseek(fid,0,0);
    fprintf(fid,'%4.3f %2.1f',n2eff(i),0.0);
    fseek(fid,0,0);
    for j = 1:3
        fgetl(fid);
    end
```

```
fseek(fid,0,0);
fprintf(fid,'%8.3e %2.1f',rr(i),0.00);
fseek(fid,0,0);
for j = 1:3
    fgetl(fid);
end
fseek(fid,0,0);
fprintf(fid,'%4.3f %4.3f %3.2f',alfal(i),alfat(i),0.00);
fseek(fid,0,0);
for j = 1:2
    fgetl(fid);
end
fseek(fid,0,0);
fprintf(fid,'%10.3e %2.1f %3.2f',kd(i),1.0,rho(i));
fseek(fid,0,0);
for j = 1:1601
    fgetl(fid);
end
cmax=2E+8;
if kd(i)>200 cmax= 1e+8;end
if kd(i)>700 cmax=5e+7;end
if kd(i)>1000 cmax=1e+6;end
fseek(fid,0,0);
fprintf(fid,'%3.1f\t %3.1f\n', 0,0);
fprintf(fid,'%9.3e\t %9.3e\n', rr(i),1.0E-10);
fprintf(fid,'%5.1e\t %5.1e\t %5.1f\t %2.1f\t %9.1f\t',1e-2,1e-2,365.0,1.5,365.0);
fprintf(fid,'%2d %2d %2d %d %9.1e\n',x1,cmax);
fprintf(fid,'%3.1f\t %3.1f\n', 0,0);
```

```
    fprintf(fid,'%9.3e\t %9.3e\n', rr(i),1.00E+12);
    fprintf(fid,'%5.1f\t %5.1f\t %5.1f\t %2.1f\t
%9.1f\t',initialtime,365.0,365.0,1,finaltime);
    fprintf(fid,'%2d %2d %2d %d %9.1e\n',x1,cmax);
    fprintf(fid,'%3.1f\t %3.1f\n', 0,0);
    fprintf(fid,'%9.3e\t %9.3e\n', rr(i),0.0);
    fprintf(fid,'%5.1f\t %5.1f\t %5.1f\t %2.1f\t %9.1f\t',initialtime,settime,1,0);
    fprintf(fid,'%2d %2d %2d %d %3.1f\n',x0);
    for l=1:300
        fprintf(fid,'%200s ', ' ');
    end
    fclose(fid);
%=================================================================
% Excecute the FTWORK code for sample i.
%=================================================================
    cd c:\diss\ftwork;
    delete test.obs;
    dos('unit2bat.bat &');
    x=0;
    while x==0
        x=exist('test.obs');
    end;
    FTWORKExectionNumber = i
%=================================================================
% Read the time and concentration of the FTWORK and create the design matrix
% of gftwork as a function of time.
%=================================================================
    fid=fopen('c:\diss\ftwork\unit20.obs','r');
```

```
    cd c:\diss\main;
    [gftwork(i,n),time]=readg30(fid,initialtime,finaltime,stepsnumber);
    fclose(fid);
end
fid=fopen('c:\diss\main\g2conc.txt','w');
for l=1:stepsnumber+1
    fprintf(fid,'%8.2E',time(l));
    fprintf(fid,' ');
    for i=1:samplesize
        fprintf(fid,'%9.3E',gftwork(i,l));
        fprintf(fid,' ');
    end
    fprintf(fid,'\n');
end
fclose(fid);

%=========================================================
% Convolve gftwork and gdust in sx
for i=1:samplesize
 sx(i,n)=convolve(gdust(i,n),gftwork(i,n),dt,stepsnumber);
end
%=========================================================
% Open an write the first convolution results in an output file
%=========================================================
fid=fopen('c:\diss\main\convout.txt','w');
for l=1:stepsnumber+1
    fprintf(fid,'%9.3E',time(l));
    fprintf(fid,' ');
```

```
    for i=1:samplesize
        fprintf(fid,'%9.3E',sx(i,l));
        fprintf(fid,' ');
    end
    fprintf(fid,'\n');
end
fclose(fid);
%=========================================================================
```

APPENDIX 3

A Matlab Program Convolving the Analytical Surface Water Model Estimates with the DUST-FTWORK Convolved Estimates

```
%=========================================================
% The Function name is "sw3.m"
% This matlab functions calculates the instantaneous solution of a surface model
% and then convolves the result with a time dependent input for the sample size
%=========================================================
samplesize=100;
tf=300;
x=250;      %Downstream distance from the release point(m)
m0=1;       %Initial Inventory(Ci);
thalf=28.6;  %Half Life(y)
lamda=0.693/thalf; % Radioactivity coefficient (1/d)
t(1)=1e-10;
t(2:tf+1)=1:tf;
dr=5.34e4; % discharge rate= dr(m/y) x A(m2)
fid=fopen('c:\diss\sw\swdata3.txt','r');
fgetl(fid);
for i=1:samplesize
    w(i) = str2num(fscanf(fid,'%s',1));          %Width of river(ft)
    h(i) = str2num(fscanf(fid,'%s',1));          %Depth of water(ft)
    s(i) = str2num(fscanf(fid,'%s',1));          %Channel slope(unitless)
    qr(i)= str2num(fscanf(fid,'%s',1));          %River Flow rate(ft3/y)
end
fclose(fid);
for I=1:samplesize
ushear=(60*60*24*365)*sqrt(9.81*h(i)*s(i));      %Shear velocity(m/d)
u=qr(i)/(w(i)*h(i));                             %River velocity((m/y)
```

```
kl=.18*((ushear/u)^1.5)*qr(i)^2/(ushear*h(i)^3);% longitudinal dispersion coefficient(m2/y)
for j=1:tf+1
    swout3(i,j)=(dr*m0/sqrt(4*3.14*kl*t(j)))* exp(-((x-u*t(j))^2/(4*kl*t(j))) - (lamda*t(j)));
end
end
t(1)=0;
fid=fopen('c:\diss\main\swout3.txt','w');
for j=1:tf+1
    fprintf(fid,'%9.3E',t(j));
    fprintf(fid,' ');
    for i=1:samplesize
        fprintf(fid,'%9.3E',swout3(i,j));
        fprintf(fid,' ');
    end
    fprintf(fid,'\n');
end
fclose(fid);
%=========================================================
% Convolves the surface water output with the time-dependent input
%=========================================================
for i=1:samplesize
 ssx(i,n)=convolve(swout(i,n),convout(i,n),dt,stepsnumber);
end
%=========================================================
% Creates a design matrix and writes the results to an output file
%=========================================================
fid=fopen('c:\diss\main\convconv.txt','w');
for l=1:stepsnumber+1
    fprintf(fid,'%9.3E',time(l));
```

```
        fprintf(fid,' ');
        for i=1:samplesize
            fprintf(fid,'%9.3E',ssx(i,l));
            fprintf(fid,' ');
        end
        fprintf(fid,'\n');
    end
    fclose(fid);
%=========================================================================
```

APPENDIX 4

Matlab Functions Called by Main Programs

```
%=================================================================
%                  General functions used in the Main Programs
%=================================================================
%=================================================================
% This Function name is "readg2.m"
% This function reads modeled concentrations from an observation
% file identified by the fid parameter, and then
% returns the read concentrations (g2) to the main program
%=================================================================
function [g2,time]=readg2(fid,timesteps);
for j = 1:6
    fgetl(fid);
end
for l= 1:timesteps+1
    time(l)=str2num(fscanf(fid,'%s',1));
    g2(l)=str2num(fscanf(fid,'%s',1));
end
return;
%=================================================================
%=================================================================
% This fuction Name is " readg3.m"
% This function reads modeled concentrations from an FTWORK observation file
% Then returns the read concentrations to the main program
%=================================================================
function [g3,time]=readg3(fid,initialtime,finaltime,stepsnumber);
for j = 1:16
   fgetl(fid);
```

```
end
fseek(fid,0,0);
fscanf(fid,'%s',3);
x = str2num(fscanf(fid,'%s',1));
while x < initialtime
    fscanf(fid,'%s',1);
    str2num(fscanf(fid,'%s',1));
    position1=ftell(fid);
    fscanf(fid,'%s',3);
    x = str2num(fscanf(fid,'%s',1));
    position2=ftell(fid);
end
position=-(position2-position1);
fseek(fid,position,0);
g3(1)=0.0;
time(1)=0.0;
for n=1:stepsnumber
     fscanf(fid,'%s',3);
    time(n+1)=str2num(fscanf(fid,'%s',1))/initialtime;
    fscanf(fid,'%s',1);
    g3(n+1) = 1e-12*str2num(fscanf(fid,'%s',1));
end
return
%==========================================================
%==========================================================
% This Function name is "convolve.m"
% Calculate outputs using the convolution Integral
% between any two components (e.g. DUST and FTWORK modeled results)
%==========================================================
```

```
function [sx]=convolve(g1,g3,dt,tf) sx(1)=0;
for j=1:tf/dt
    n=j/dt;
    fxx=conv(g1(1:n+1),g3(1:n+1));
    sx(j+1)= fxx(n+1);
    clear fxx;
 end
%=============================================================
```

APPENDIX 5

A Mathematical Demonstration of The Accuracy Of the MCI Approach

Assume that H(s) = 1/(s+ a) and G(s) = 1/(s+b) are the Laplace transforms of h(t) and g(t), respectively, where a and b are two randomly varying parameters with known statistical distributions. Now, the outputs: y(t) = h(t) and z(t) = g(t) are the impulse response solutions of the decoupled components. For a general input x(t), the solution of the coupled system can be determined by finding the Laplace inverse of the of the following equation:

$$Z(s) = \frac{X(s)}{(s+a)(s+b)}$$

For an impulse input, x(t) = δ(t), the analytical impulse response of the coupled system is easily calculated:

$$z(t) = \frac{1}{a - b}\left(e^{-bt} - e^{-at}\right)$$

Which is equivalent to the convolution of the impulse responses of the decoupled components. For a decaying input function $x(t) = e^{-\lambda t}$, the analytical solution of the coupled system can be written as follows:

$$z(t) = \frac{1}{a - b}\left(\frac{e^{-\lambda t} - e^{-bt}}{b - \lambda} - \frac{e^{-\lambda t} - e^{-at}}{a - \lambda} \right)$$

For the above case study, the multiple convolution integral method can be used by decoupling the two components with the same input function for each sample set. The time dependent impulse output of each sample component are then convolved using Eqs. 5 or 9 with the actual input function, x(t), to determine the final output, z(t), of the coupled system for that particular sample. The convolution of the decoupled components with the actual input function will be repeated for the size of the sample to determine the uncertainty in the model prediction as a function of time. Further, uncertainties in the model output (i.e., the predicted concentration) and exposure parameters can then be propagated in the risk model to determine the uncertainty in the final risk prediction.

Table A5.1 summarizes the statistical results obtained using the Multiple Convolution Integral versus the traditional approaches of propagating uncertainties of the input parameter through the components of the above sequentially coupled systems.

Table A5.1 Comparion of the Statistical descriptions of the MCI approach versus the Traditional approach predictions

Time(years)	*50*		*100*		*150*		*200*		*250*		*300*	
	MCI	Traditional	MCI	Traditional	MCI	Traditional	MCI	Traditional	MCI	Traditional	MCI	Traditional
Mean	2.162E-13	2.166E-13	2.249E-13	2.254E-13	1.286E-13	1.288E-13	5.816E-14	5.817E-14	2.318E-14	2.324E-14	8.597E-15	8.561E-15
Standard Error	7.496E-14	7.510E-14	7.089E-14	7.112E-14	3.720E-14	3.728E-14	1.550E-14	1.550E-14	5.717E-15	5.739E-15	1.976E-15	1.963E-15
Median	7.610E-15	7.678E-15	1.045E-14	1.045E-14	7.205E-15	7.219E-15	3.840E-15	3.842E-15	1.779E-15	1.780E-15	7.555E-16	7.555E-16
Standard Deviation	8.481E-13	8.497E-13	8.020E-13	8.047E-13	4.209E-13	4.218E-13	1.754E-13	1.754E-13	6.468E-14	6.493E-14	2.235E-14	2.220E-14
Sample Variance	7.193E-25	7.220E-25	6.432E-25	6.475E-25	1.772E-25	1.779E-25	3.076E-26	3.077E-26	4.184E-27	4.217E-27	4.997E-28	4.930E-28
Kurtosis	7.407E+01	7.407E+01	6.362E+01	6.373E+01	5.367E+01	5.354E+01	4.375E+01	4.372E+01	3.474E+01	3.494E+01	2.725E+01	2.689E+01
Skewness	7.924E+00	7.924E+00	7.238E+00	7.245E+00	6.565E+00	6.557E+00	5.871E+00	5.869E+00	5.209E+00	5.224E+00	4.625E+00	4.597E+00
Range	8.530E-12	8.546E-12	7.790E-12	7.819E-12	3.930E-12	3.936E-12	1.560E-12	1.560E-12	5.441E-13	5.470E-13	1.770E-13	1.752E-13
Minimum	1.460E-19	1.545E-19	6.540E-19	6.734E-19	8.270E-19	8.421E-19	6.310E-19	6.391E-19	3.726E-19	3.690E-19	1.850E-19	1.860E-19
Maximum	8.530E-12	8.546E-12	7.790E-12	7.819E-12	3.930E-12	3.936E-12	1.560E-12	1.560E-12	5.441E-13	5.470E-13	1.770E-13	1.752E-13
Sum	2.768E-11	2.773E-11	2.879E-11	2.885E-11	1.646E-11	1.649E-11	7.445E-12	7.445E-12	2.967E-12	2.974E-12	1.100E-12	1.096E-12
95%-tile	3.395E-13	3.402E-13	3.415E-13	3.424E-13	1.898E-13	1.902E-13	8.366E-14	8.367E-14	3.259E-14	3.268E-14	1.185E-14	1.179E-14

VITA

Emran Dawoud was born on March 2, 1964 in Qalquilia, Palestine. He graduated from High School in 1981 from Hawalli, Kuwait. In 1981 he enrolled in Al-Yarmouk University in Jordan. In 1982 he transferred to the Physics Department at Kuwait University. In May 1985 , he received a B.S. degree in Physics and immediately enrolled in the graduate program of Physics at the same university. As a graduate Teaching Assistant, he acquired teaching skills for three years while worked in the field of Solid State Physics. After receiving his masters in 1988, he worked as a Physics and Mathematics teacher at Al-Bayan bilingual School in Al-Jabria, Kuwait. In January, 1990, He worked as a science instructor at a technical school for the ministry of Defense of Kuwait. In January 1991, Emran joined the graduate program of the Nuclear Engineering Department at the University of Tennessee, Knoxville, for his doctorate degree in Nuclear Engineering. During his study, in 1994 he was employed by the Risk Analysis Section, of the Life Sciences Division at Oak Ridge National laboratory (ORNL), Oak Ridge, Tennessee. He worked as a Human Health Risk Assessor, and fate and transport modeler. Currently, he is working for the Toxicology and Risk Analysis Section at ORNL, Oak Ridge, Tennessee.